

RMZ

**MATERIALS and
GEOENVIRONMENT**

MATERIALI in GEOOKOLJE



RMZ – M&G, **Vol. 61**, No. 1
pp. 1–74 (2014)

Ljubljana, September 2014

RMZ – Materials and Geoenvironment

RMZ – Materiali in geokolje

ISSN 1408-7073

Old title/Star naslov

Mining and Metallurgy Quarterly/Rudarsko-metalurški zbornik

ISSN 0035-9645, 1952–1997

Copyright © 2014 RMZ – Materials and Geoenvironment

Published by/Izdajatelj

Faculty of Natural Sciences and Engineering, University of Ljubljana/

Naravoslovnotehniška fakulteta, Univerza v Ljubljani

Associated Publisher/Soizdajatelj

Institute for Mining, Geotechnology and Environment, Ljubljana/

Inštitut za rudarstvo, geotehnologijo in okolje

Velenje Coal Mine/Premogovnik Velenje

Editor-in-Chief/Glavni urednik

Peter Fajfar

Editorial Manager/Odgovorni urednik

Jakob Likar

Editorial Board/Uredniški odbor

Vlasta Čosović, Sveučilište u Zagrebu

Evgen Dervarič, Univerza v Ljubljani

Meta Dobnikar, Ministrstvo za izobraževanje, znanost in šport

Jan Falkus, Akademia Górniczo-Hutnicza im. S. Staszica w Krakowie

Aleksandar Ganić, Univerzitet u Beogradu

Borut Kosec, Univerza v Ljubljani

Jakob Likar, Univerza v Ljubljani

David John Lowe, British Geological Survey

Ilija Mamuzić, Sveučilište u Zagrebu

Milan Medved, Premogovnik Velenje

Peter Moser, Montanuniversität Leoben

Primož Mrvar, Univerza v Ljubljani

Heinz Palkowski, Technische Universität Clausthal

Daniele Peila, Politecnico di Torino

Sebastiano Pelizza, Politecnico di Torino

Jože Ratej, Inštitut za rudarstvo, geotehnologijo in okolje v Ljubljani

Andrej Šmuc, Univerza v Ljubljani

Milan Terčelj, Univerza v Ljubljani

Milivoj Vulić, Univerza v Ljubljani

Nina Zupančič, Univerza v Ljubljani

Franc Zupanič, Univerza v Mariboru

Editorial Office/Uredništvo

Secretary/Tajnica Ines Langerholc

Technical Editor/Tehnična urednica Helena Buh

Editor of website/Urednik spletne strani Timotej Verbovšek

Editorial Address/Naslov uredništva

RMZ – Materials and Geoenvironment

Aškerčeva cesta 12, p. p. 312

1001 Ljubljana, Slovenija

Tel.: +386 (0)1 470 45 00

Fax.: +386 (0)1 470 45 60

E-mail: rmz-mg@ntf.uni-lj.si

Linguistic Advisor/Lektor

Jože Gasperič

Design and DTP/Oblikovanje, prelom in priprava za tisk

IDEJA za ITGTO

Print/Tisk

Birografika BORI, d. o. o.

Printed in 200 copies./Naklada 200 izvodov.

Published/Izhajanje

4 issues per year/4 številke letno

Partly funded by Ministry of Education, Science and Sport of Republic of Slovenia./Pri financiranju revije sodeluje Ministrstvo za izobraževanje, znanost in šport Republike Slovenije.

Articles published in Journal "RMZ M&G" are indexed in international secondary periodicals and databases:/Članki, objavljeni v periodični publikaciji „RMZ M&G“, so indeksirani v mednarodnih sekundarnih virih: Civil Engineering Abstracts, CA SEARCH® – Chemical Abstracts® (1967–present), Materials Business File, Inside Conferences, ANTE: Abstract in New Technologies and Engineering, METADEX®, GeoRef, CSA Aerospace & High Technology Database, Aluminium Industry Abstracts, Computer and Information Systems, Mechanical & Transportation Engineering Abstracts, Corrosion Abstracts, Earthquake Engineering Abstracts, Solid State and Superconductivity Abstracts, Electronics and Communications Abstracts.

The authors themselves are liable for the contents of the papers./Za mnenja in podatke v posameznih sestavkih so odgovorni avtorji.

Annual subscription for individuals in Slovenia: 16.69 EUR, for institutions: 22.38 EUR. Annual subscription for the rest of the world: 20 EUR, for institutions: 40 EUR/Letna naročnina za posameznike v Sloveniji: 16,69 EUR, za inštitucije: 33,38 EUR. Letna naročnina za tujino: 20 EUR, inštitucije: 40 EUR.

Current account/Tekoči račun

Nova ljubljanska banka, d. d., Ljubljana: UJP 01100-6030708186

VAT identification number/Davčna številka

24405388

Online Journal/Elektronska revija

www.rmz-mg.com

Table of Contents

Kazalo

Original scientific papers

Izvirni znanstveni članki

- Thermodynamical analysis of Al-Cu-Mn system using RKM model** 3
Termodinamična analiza sistema Al-Cu-Mn z uporabo modela RKM
Lidija Gomidželovič, Jožef Medved, Tamara Holjevac Grgurič, Mirko Gojič, Dragana Živković
- Modelling surface degradation in hot rolling work rolls** 11
Modeliranje degradacije površine valjev za vroče valjanje
Milan Terčelj, Matevž Fazarinc, Primož Mrvar, Borut Žužek, Peter Fajfar
- Assessment of heavy metals in wastewater obtained from an industrial area in Ibadan, Nigeria** 19
Ocena težkih kovin v odpadnih vodah industrijske cone v Ibadanu v Nigeriji
Omotayo Ayeni
- Basic parameters of small underground nuclear power stations** 25
Osnovni parametri majhnih podzemnih nukleark
Jakob Likar, Eivind Grøv, Tina Marolt

Review papers

Pregledni članki

- Analysis of risk assessment and law basis for construction of underground structures** 39
Analiza ocene tveganja in pravni okvirji gradnje podzemnih objektov
Mario Mazurek, Peter Grilc, Jakob Likar

Professional papers

Strokovni članki

- A review of stratigraphic surfaces generated from multiple electrical sounding and profiling** 49
Prikaz sekvenčnih stratigrafskih površin, pridobljenih z geoelektričnim sondiranjem in profiliranjem
Kamaldeen Omosanya, Akinwale Akinmosin, Jonathan Balogun

In memorium

In memorium

- Jakob Mostar** 71
Jakob Mostar
Primož Mrvar, Jurij Smole

Historical Review

More than 90 years have passed since the University Ljubljana in Slovenia was founded in 1919. Technical fields were united in the School of Engineering that included the Geologic and Mining Division, while the Metallurgy Division was established only in 1939. Today, the Departments of Geology, Mining and Geotechnology, Materials and Metallurgy are all part of the Faculty of Natural Sciences and Engineering, University of Ljubljana.

Before World War II, the members of the Mining Section together with the Association of Yugoslav Mining and Metallurgy Engineers began to publish the summaries of their research and studies in their technical periodical Rudarski zbornik (Mining Proceedings). Three volumes of Rudarski zbornik (1937, 1938 and 1939) were published. The War interrupted the publication and it was not until 1952 that the first issue of the new journal Rudarsko-metalurški zbornik – RMZ (Mining and Metallurgy Quarterly) was published by the Division of Mining and Metallurgy, University of Ljubljana. Today, the journal is regularly published quarterly. RMZ – M&G is co-issued and co-financed by the Faculty of Natural Sciences and Engineering Ljubljana, the Institute for Mining, Geotechnology and Environment Ljubljana, and the Velenje Coal Mine. In addition, it is partly funded by the Ministry of Education, Science and Sport of Slovenia.

During the meeting of the Advisory and the Editorial Board on May 22, 1998, Rudarsko-metalurški zbornik was renamed into “RMZ – Materials and Geoenvironment (RMZ – Materials in Geokolje)” or shortly RMZ – M&G. RMZ – M&G is managed by an advisory and international editorial board and is exchanged with other world-known periodicals. All the papers submitted to the RMZ – M&G undergoes the course of the peer-review process.

RMZ – M&G is the only scientific and professional periodical in Slovenia which has been published in the same form for 60 years. It incorporates the scientific and professional topics on geology, mining, geotechnology, materials and metallurgy. In the year 2013, the Editorial Board decided to modernize the journal’s format.

A wide range of topics on geosciences are welcome to be published in the RMZ – Materials and Geoenvironment. Research results in geology, hydrogeology, mining, geotechnology, materials, metallurgy, natural and anthropogenic pollution of environment, biogeochemistry are the proposed fields of work which the journal will handle.

Editor-in-Chief

Zgodovinski pregled

Že več kot 90 let je minilo od ustanovitve Univerze v Ljubljani leta 1919. Tehnične stroke so se združile v tehniški visoki šoli, ki sta jo sestavljala oddelka za geologijo in rudarstvo, medtem ko je bil oddelek za metalurgijo ustanovljen leta 1939. Danes oddelki za geologijo, rudarstvo in geotehnologijo ter materiale in metalurgijo delujejo v sklopu Naravoslovnotehniške fakultete Univerze v Ljubljani.

Pred 2. svetovno vojno so člani rudarske sekcije skupaj z Združenjem jugoslovanskih inženirjev rudarstva in metalurgije začeli izdajanje povzetkov njihovega raziskovalnega dela v Rudarskem zborniku. Izšli so trije letniki zbornika (1937, 1938 in 1939). Vojna je prekinila izdajanje zbornika vse do leta 1952, ko je izšel prvi letnik nove revije Rudarsko-metalurški zbornik – RMZ v izdaji odsekov za rudarstvo in metalurgijo Univerze v Ljubljani. Danes revija izhaja štirikrat letno. RMZ – M&G izdajajo in financirajo Naravoslovnotehniška fakulteta v Ljubljani, Inštitut za rudarstvo, geotehnologijo in okolje ter Premogovnik Velenje. Prav tako izdajo revije financira Ministrstvo za izobraževanje, znanost in šport.

Na seji izdajateljskega sveta in uredniškega odbora je bilo 22. maja 1998 sklenjeno, da se Rudarsko-metalurški zbornik preimenuje v RMZ – Materials in geokolje (RMZ – Materials and Geoenvironment) ali skrajšano RMZ – M&G. Revija RMZ – M&G upravljata izdajateljski svet in mednarodni uredniški odbor. Revija je vključena v mednarodno izmenjavo svetovno znanih publikacij. Vsi članki so podvrženi recenzijskemu postopku.

RMZ – M&G je edina strokovno-znanstvena revija v Sloveniji, ki izhaja v nespremenjeni obliki že 60 let. Združuje področja geologije, rudarstva, geotehnologije, materialov in metalurgije. Uredniški odbor je leta 2013 sklenil, da posodobi obliko revije.

Za objavo v reviji RMZ – Materials in geokolje so dobrodošli tudi prispevki s širokega področja geoznanosti, kot so: geologija, hidrologija, rudarstvo, geotehnologija, materiali, metalurgija, onesnaževanje okolja in biokemija.

Glavni urednik

Thermodynamical analysis of Al-Cu-Mn system using RKM model

Termodinamična analiza sistema Al-Cu-Mn z uporabo modela RKM

Lidija Gomidželović^{1,*}, Jožef Medved², Tamara Holjevac Grgurić³, Mirko Gojić³, Dragana Živković⁴

¹Mining and Metallurgy Institute, Zelenci bulevar 35, 19210 Bor, Serbia

²University in Ljubljana, Faculty of Natural Sciences and Engineering, Lepi pot 11, 1000 Ljubljana, Slovenia

³Faculty of Metallurgy, University of Zagreb, Aleja narodnih heroja 3, Sisak, Croatia

⁴University of Belgrade, Technical faculty Bor, VJ12, 19210 Bor, Serbia

*Corresponding author. E-mail: lgomidzelovic@yahoo.com

Abstract

The results of thermodynamic analysis of alloys in ternary system Al-Cu-Mn are presented in this work. Thermodynamic analysis was carried out by applying Redlich-Kister-Muggianu (RKM) method in selected sections from aluminum, copper and manganese corner, in the temperature interval from 1 073 K to 1 873 K. Thermodynamic properties (excess integral Gibbs energy and activity of components) have been calculated using Redlich-Kister parameters of constituent binary systems and presented in form of graphics. Analyzing calculated data it can be concluded that high content of manganese in alloy can significantly lower miscibility of alloy.

Key words: thermodynamics, RKM model, Al-Cu-Mn system

Izveček

V delu so predstavljeni rezultati termodinamične analize zlitin iz ternarnega sistema Al-Cu-Mn. Termodinamična analiza je bila opravljena z uporabo Redlich-Kister-Muggianujeve (RKM) metode v izbranih področjih aluminijevega, bakrovega in manganovega kota, v temperaturnem območju od 1 073 K do 1 873 K. Termodinamske lastnosti (presežne intergralne Gibbsove energije in aktivnosti komponent) so bile izračunane z uporabo Redlich-Kisterjevih parametrov za komponente binarnih sistemov in so predstavljene v grafični obliki. Iz analize izračunanih podatkov je mogoče sklepati, da lahko visoka vsebnost mangana v zlitini bistveno zmanjša sposobnost mešanja zlitine.

Ključne besede: termodinamika, RKM-model, sistem Al-Cu-Mn

Introduction

Shape memory materials are able to recover their original shape, after being distorted, at the presence of right stimulus. These materials include: a) Shape memory alloys, b) shape memory polymers, c) shape memory composites and newly developed d) shape memory hybrids^[1].

Shape memory alloys (SMAs) are characterized by unique properties (pseudo-elasticity and shape memory effect), which enables them to “remember” their original shapes. These alloys are used as activators which change their shape, position and other mechanical characteristics in response to variation in temperature and electromagnetic field^[2].

Alloys from ternary system Cu-Al-Mn belongs to wide group of Cu-Al-based shape memory alloys (SMAs)^[3, 4].

Thermodynamic data related to ternary Cu-Al-Mn system is, at best, scarce. Thermodynamic description of Cu-Al-Mn System in the Cu-rich corner (Al contents up to $w = 18\%$ and Mn contents up to $w = 50\%$), using available data for binary systems (Cu-Al, Cu-Mn and Al-Mn) was given by Miettinen^[5]. Kainuma et al.^[6] studied phase equilibria between α , β and γ phase in Cu-rich portion of Cu-Al-Mn system, by means of TEM-EDS, DSC and X-ray diffraction.

Main area of use for alloys which belong to Cu-Al-Mn system is connected to martensitic transformation and shape memory effect, so these properties and possible applications have been primary focus of researchers^[7-24].

Additional research have been done on influence of composition and maximum cycling temperature on Cu-Al-Mn shape memory alloys microstructure^[25], seismic application of Cu-Al-Mn alloy bars^[26, 27], damping capacity of Cu-Al-Mn alloys^[28-30] and magnetic properties of chosen Cu-Al-Mn alloys^[31, 32].

Objective of this work is to give some information about thermodynamic properties of ternary Al-Cu-Mn system, taking into account current lack of such data in literature.

Theoretical basis

Many different methods for predicting thermodynamic properties of ternary systems based on information about binary systems included in their composition are available in the literature. In this paper, Redlich-Kister-Muggianu model^[33] is used for calculation of thermodynamic properties of the investigated ternary system.

$$\begin{aligned} \Delta G^E = & x_1 x_2 [L_{12}^0 + (x_1 - x_2) L_{12}^1 + (x_1 - x_2)^2 L_{12}^2 + \dots] \\ & + x_2 x_3 [L_{23}^0 + (x_2 - x_3) L_{23}^1 + (x_2 - x_3)^2 L_{23}^2 + \dots] \\ & + x_1 x_3 [L_{13}^0 + (x_1 - x_3) L_{13}^1 + (x_1 - x_3)^2 L_{13}^2 + \dots] \\ & + L_{23}^1 x_1 x_2 x_3 \dots \end{aligned} \quad (1)$$

The basic equation of Redlich-Kister-Muggianu^[33] model for ternary system is:

For the calculation it is adopted that the value of ternary interaction parameter L_{123} is zero and all the ternary interatomic reactions are ignored due to the lack of experimental data for ternary systems.

In the equation (1), DG^E and DG_{ij}^E correspond to the integral molar excess Gibbs energies for ternary and binary systems, respectively, while x_1, x_2, x_3 correspond to the mole fraction of components in investigated ternary system. Partial thermodynamic quantities of aluminum, copper and manganese are calculated according to the equations:

$$G_i^E = G^E + (1-x_i)(\partial G^E / \partial x_i) = RT \ln \gamma_i \quad (2)$$

and

$$a_i = x_i \gamma_i \quad (3)$$

Results and discussion

From the concentration area of ternary system Al-Cu-Mn sections shown in Figure 1. were selected and thermodynamic prediction was carried out using RKM model^[33], with content of the third component $x_i = 0, 0.1-0.9, 1$ in temperature interval 1 073–1 873 K. Redlich-Kister

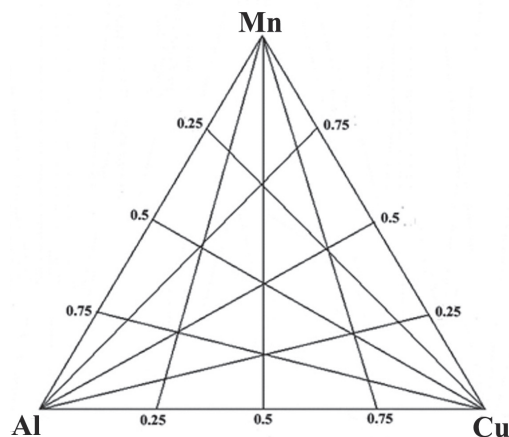
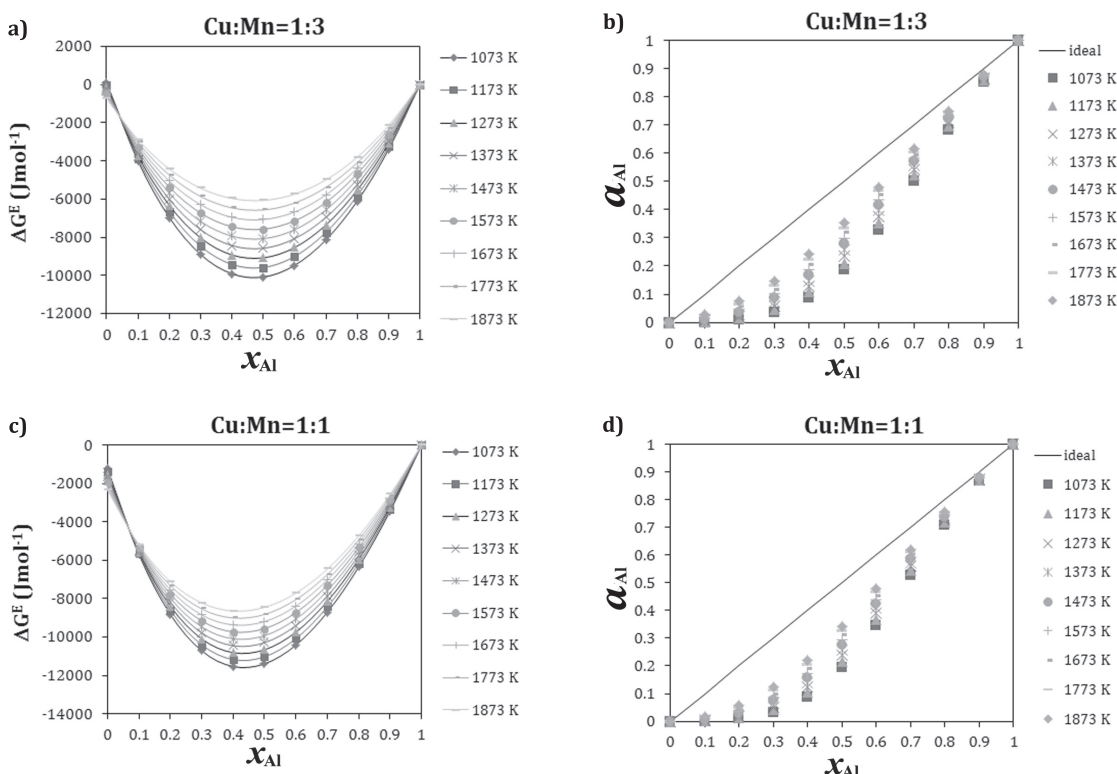
Table 1: Redlich-Kister parameters for the constituent binary systems

System ij	$L^0_{ij} (T)$	$L^1_{ij} (T)$	$L^2_{ij} (T)$	$L^3_{ij} (T)$
Al-Cu ^[34]	$-67\,094 + 8.555 \cdot T$	$32\,148 - 7.118 \cdot T$	$5\,915 - 5.889 \cdot T$	$-8\,175 + 6.049 \cdot T$
Cu-Mn ^[35]	$1118.55 - 5.622 \cdot T$	$-10\,915.375$	0	0
Al-Mn ^[36]	$-66\,174 + 27.098 \cdot T$	$-7\,509 + 5.483 \cdot T$	$-2\,639$	0

parameters of constituent binary systems presented in Table 1, were used for the calculation.

Values of excess integral Gibbs energy and activity for all components, in sections from aluminum, copper and manganese corner of ternary Al-Cu-Mn system, calculated using RKM method and equations (2) and (3) are shown in Figures 2-4.

As can be seen in figures 2-4., values for excess integral Gibbs energy of investigated sections from the corner of aluminum and copper are negative, with minimum values up to -14 kJ/mol, while for the investigated section from the corner of copper Gibbs energy goes up to -15 kJ/mol.

**Figure 1:** Schematic diagram of the investigated cross-sections of ternary Al-Cu-Mn system.**Figure 2:** Results of thermodynamic predicting according to RKM model in temperature range 1 073-1 873 K for cross-sections from aluminum corner (part 1).

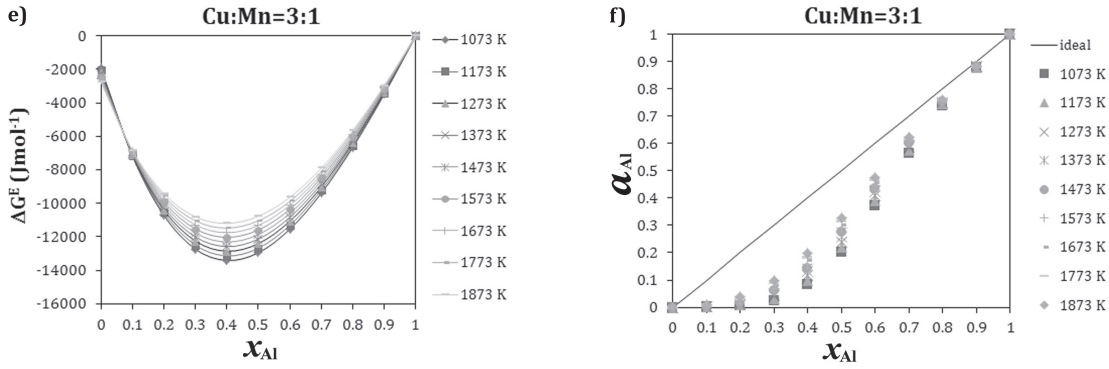


Figure 2: Results of thermodynamic predicting according to RKM model in temperature range 1 073-1 873 K for cross-sections from aluminum corner (part 2).

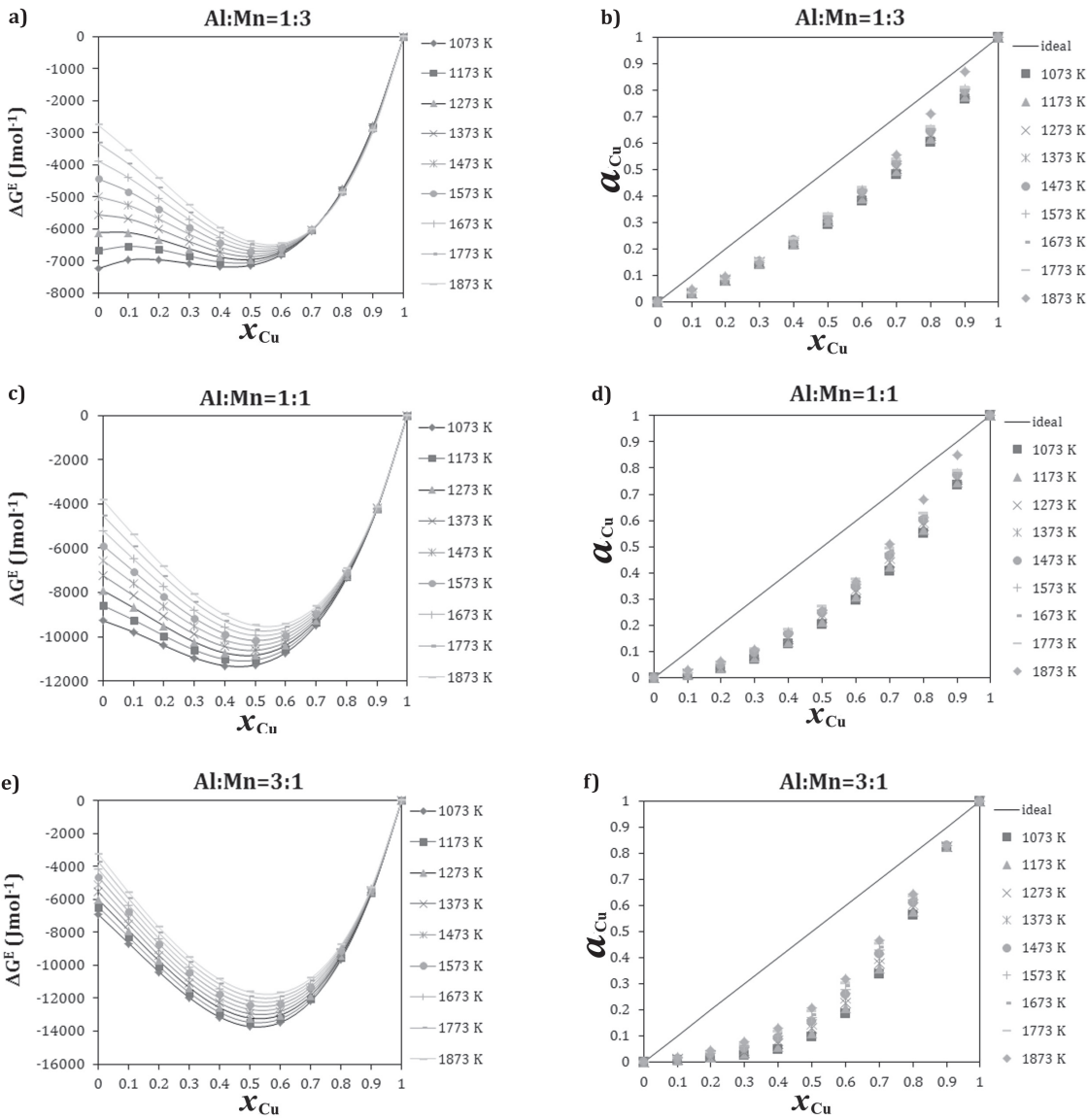


Figure 3: Results of thermodynamic predicting according to RKM model in temperature range 1 073-1 873 K for cross-sections from copper corner.

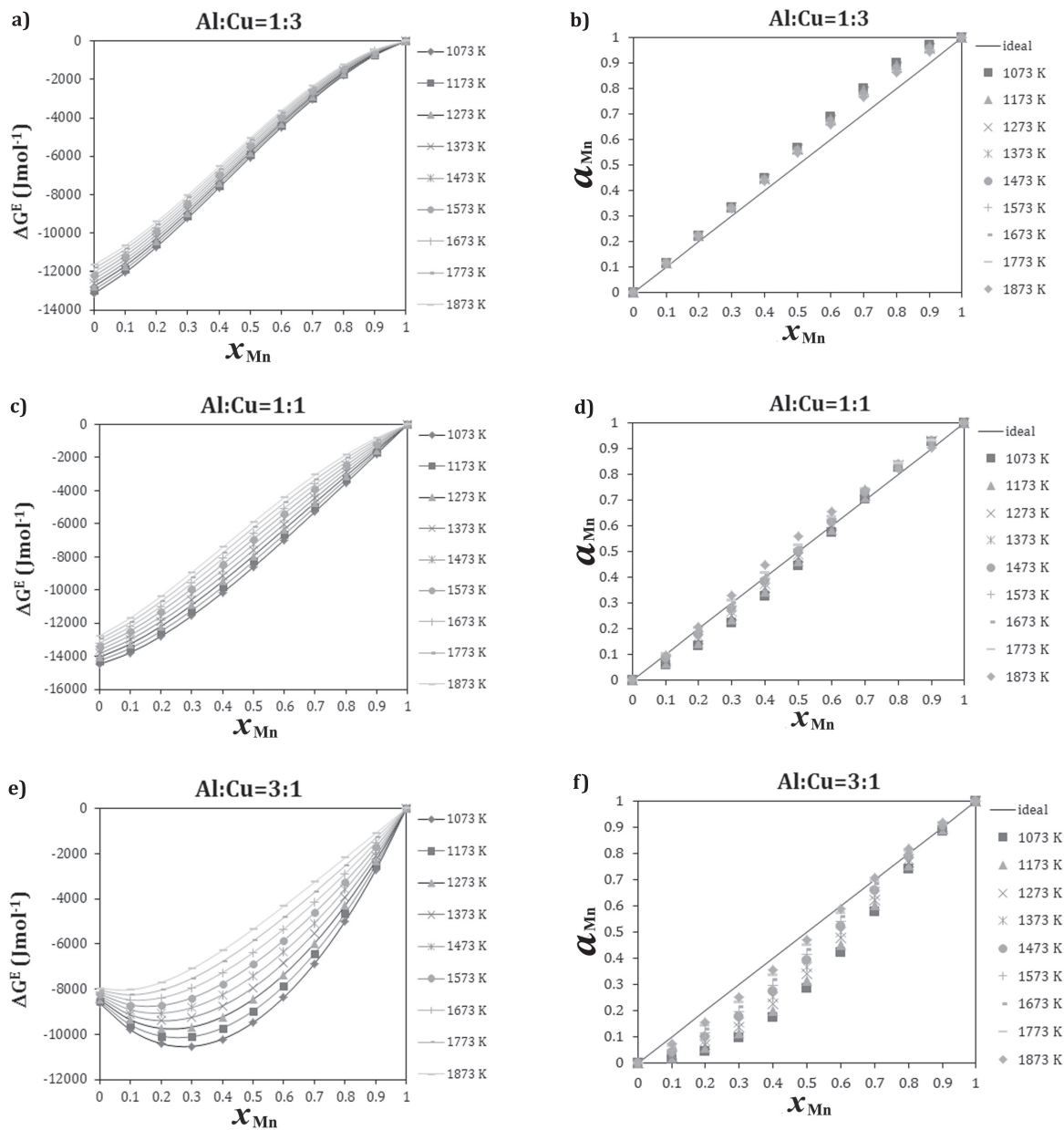


Figure 4: Results of thermodynamic predicting according to RKM model in temperature range 1073–1873 K for cross-sections from manganese corner.

Aluminum and copper activity shows pronouncedly negative deviation from Rault's law for all investigated sections. Different situation can be observed for activity of manganese, where in section Al : Cu = 1 : 3 positive deviation from line of ideal condition is present. For cross section Al : Cu = 1 : 1 manganese activity is near to ideal solution line, while for cross section Al : Cu = 3 : 1 negative deviation can be seen. From all this data it can be concluded that high content of manganese in alloy significantly lowers miscibility of alloy, which can lead to occurrence of layering between different metals. Also it can be noticed that with increasing aluminum content in alloy with simultaneously lowering content of copper, previously positive deviation of manganese activity from Rault's law, gradually changes to negative deviation, as seen in cross section Al : Cu = 3 : 1.

Conclusion

Thermodynamic analysis of alloys in ternary Al-Cu-Mn system has been conducted using the Redlich-Kister-Muggianu model. Thermodynamic properties (excess integral Gibbs energy and activity of components) has been calculated using Redlich-Kister parameters of constituent binary systems and presented in form of graphics. Calculation has been carried out in temperature interval 1 073–1 873 K.

Considering current lack of thermodynamic data about Al-Cu-Mn alloys in literature, thermodynamic data presented in this work could be useful for the further assessment of this system and its phase diagram as well as for completing thermodynamic description of these alloys.

Acknowledgement

The authors are grateful to Basileus IV project (Erasmus Mundus Partnerships), Ministry of Science and Environmental Protection of the Republic of Serbia (Projects N^o142043 and 34005) and Program WORLD (Project title: Development of Shape Memory Alloys, University of Zagreb) for financial support.

References

- [1] Huang, W.M., Ding, Z., Wang, C.C., Wei, J., Zhao, Y., Purnawali, H. (2010): Shape memory materials. *MaterialsToday*, 13, pp. 54–61.
- [2] Achitei, D., Vizureanu, P., Cimpoesu, N., Dana, D. (2012): Thermo-mechanical fatigue of Cu-Al-Zn shape memory alloys, 44th International October Conference on Mining and Metallurgy, Bor, Serbia, Proceedings, pp. 401–404.
- [3] Milosavljević, A. Kostov, A. Todorović, R., (2011): Smart materials: Shape memory alloys. *Bakar*, 36, pp. 39–44. (in Serbian)
- [4] P. Vizureanu, P., Achitei, D., Cimpoesu, N., Dana, D. (2012): Studies concerning thermal conductivity for shape memory alloy alike CuAlMn, 44th International October Conference on Mining and Metallurgy, Bor, Serbia, Proceedings, pp. 405–408.
- [5] Miettinen, J., (2003): Thermodynamic Description of the Cu-Al-Mn System in the Copper-Rich Corner. *Calphad*, 27, pp. 103–114.
- [6] R. Kainuma, N. Satoh, X.J. Liu, I. Ohnuma, K. Ishida, (1998): Phase equilibria and Heusler phase stability in the Cu-rich portion of the Cu-Al-Mn system. *Journal of Alloys and Compounds*, 266, pp. 191–200.
- [7] Mallik, U. S., Sampath, V. (2008): Effect of alloying on microstructure and shape memory characteristics of Cu–Al–Mn shape memory alloys. *Materials Science and Engineering A*, 481–482, pp. 680–683.
- [8] U.S. Mallik, V. Sampath, (2008): Influence of aluminum and manganese concentration on the shape memory characteristics of Cu–Al–Mn shape memory alloys. *Journal of Alloys and Compounds*, 459, pp. 142–147.
- [9] S. Ignacova, T. Cernoch, V. Novak, P. Sittner, (2008): The reorientation of the 2H martensite phase in Cu–Al–Mn shape memory single crystal alloy. *Materials Science and Engineering A*, 481–482, pp. 526–531.
- [10] Y. Zheng, C. Li, F. Wan, Y. Long, (2007): Cu–Al–Mn alloy with shape memory effect at low temperature. *Journal of Alloys and Compounds*, 441, pp. 317–322.
- [11] Egorov, S. A. (2007): Heat of the Martensitic Transformation in CuAlMn Alloy Subjected to Thermal Cycling under Constrained Deformation Conditions. *Technical Physics*, 52, pp. 1462–1465.
- [12] F.-J. Perez-Reche, M. Stipcich, E. Vives, L. Manosa, A. Planes, (2004): Kinetics of martensitic transitions in Cu-Al-Mn under thermal cycling: Analysis at multiple length scales. *Physical Review B*, 69, pp. 1–7.

- [13] Zárubová, N. Novák, V. (2004): Phase stability of CuAlMn shape memory alloys. *Materials Science and Engineering A*, 378, pp. 216–221.
- [14] T. Omori, J. Wang, Y. Sutou, R. Kainuma, K. Ishida, (2002): Two-way shape memory effect induced by bending deformation in ductile Cu-Al-Mn alloys. *Materials Transactions*, 43, pp. 1676–1683.
- [15] R. Wang, J. Gui, X. Chen, S. Tan, (2002): EBSD and TEM study of self-accommodating martensites in Cu75.7Al15.4Mn8.9 shape memory alloy. *Acta Materialia*, 50, pp. 1835–1847.
- [16] J. Marcos, A. Planes, L.I. Manosa, A. Labarta, B. J. Hattink, (2001): Effect of a magnetic field on the martensitic transition of Cu-Al-Mn alloys. *Journal de Physique IV*, 11, pp. 257–262.
- [17] Prado, M. O. (2001): Martensitic transformation in mictomagnetic Cu-Al-Mn alloy. *Scripta materialia*. 44, pp. 2431–2436.
- [18] E. Obrado, L.I. Manosa, A. Planes, R. Romero, A. Sommoza, (1999): Quenching effects in Cu–Al–Mn shape memory alloy. *Materials Science and Engineering A*, 273–275, pp. 586–589.
- [19] E. Obrado, L.I. Manosa, A. Planes, (1997): Stability of the bcc phase of Cu-Al-Mn shape-memory alloys. *Physical Review B*, 56, pp.20–23.
- [20] E. Obrado, L.I. Manosa, A. Planes, (1997): Influence of Composition and Thermal Treatments on the Martensitic Transition of Cu-Al-Mn Alloys. *Journal de Physique IV*, 7, pp. 233–238.
- [21] Zak, G., Kneissl, A. C., Zatulskij, G. (1996): Shape memory effect in cryogenic Cu-Al-Mn alloys. *Scripta Materialia*, 34, pp. 363–367,
- [22] J. Dutkiewicz, E. Cesari, C. Segui, J. Pons, (1991): Response of Cu-Al-Mn alloys to ageing in β phase. *Journal de Physique IV*, 1, pp. 229–234.
- [23] B.G. Mellor, J.M. Guilemany, J. Fernandez, (1991): Two way shape memory effect obtained by stabilized stress induced martensite in Cu-Zn-Al-Co and Cu-Al-Mn alloys. *Journal de Physique IV*, 1, pp. 457–462.
- [24] H. Kubo, A. Miyake, K. Shimizu, (1983): Electron Microscopy Observation and X-ray Microanalysis of Cu-12.9mas%Al-2.5mas%Mn Shape Memory Alloy. *Transactions of the Japan Institute of Metals*, 24, pp. 603–612.
- [25] M. L. Blazquez, C. Lopez del Castillo, C. Gomez, (1989) Influence of the Composition and Maximum Cycling Temperature on the Microstructure of Cu-Al-Mn Shape Memory Alloys. *Metallography*, 23, pp. 119–133.
- [26] Y. Araki, N. Maekawa, T. Omori, Y. Sutou, R. Kainuma, K. Ishida, (2012): Rate-dependent response of superelastic Cu–Al–Mn alloy rods to tensile cyclic loads. *Smart Materials and Structures*, 21, pp. 1–7.
- [27] Y. Araki, T. Endo, T. Omori, Y. Sutou, Y. Koetaka, R. Kainuma, K. Ishida, (2011): Potential of superelastic Cu–Al–Mn alloy bars for seismic applications. *Earthquake Engineering and Structural Dynamics*, 40, pp. 107–115.
- [28] J. Yu-qin, W. Yu-hua, L. Ning, H. Jia-qiang, T. Jin, (2009): Effect of environmental temperature on damping capacity of Cu-Al-Mn alloy. *Transactions of the Nonferrous Metals Society of China*, 19, pp. 616–619.
- [29] Mallik, U. S., Sampath, V. (2008): Effect of composition and ageing on damping characteristics of Cu–Al–Mn shape memory alloys. *Materials Science and Engineering A*, 478, pp. 48–55.
- [30] N. Koeda, T. Omori, Y. Sutou, H. Suzuki, M. Wakita, R. Kainuma, K. Ishida, (2005): Damping Properties of Ductile Cu-Al-Mn-Based Shape Memory Alloys. *Materials Transactions*, 46, pp. 118–122.
- [31] Canbay, C. A. Aydogdu, A., Aydogdu, Y. (2011): The Investigation of Thermal and Magnetic Properties and Microstructure Analysis of Cu–Al–Mn Shape Memory Alloys. *Journal of Superconductivity and Novel Magnetism*, 24, pp. 871–877.
- [32] Sasmaz, M., Bayri, A., Aydogdu, Y., (2011): The Magnetic Behavior and Physical Characterization of Cu–Mn–Al Ferromagnetic Shape Memory Alloy. *Journal of Superconductivity and Novel Magnetism*, 24, pp. 757–762.
- [33] Redlich, O., Kister, A.T. (1948): Algebraic representation of thermodynamic properties and the classification of solutions. *Industrial & Engineering Chemistry*, 24, pp. 345–348.
- [34] Witusiewicz, V.T., Hecht, U., Fries, S. G., Rex, S., (2004): The Ag-Al-Cu system Part I: reassessment of the constituent binaries on the basis of new experimental data. *Journal of Alloys and Compounds*, 385, pp. 133–143.
- [35] He, C., Du, Y., Chen, H. L., Liu, S., Xu, H., Quyang, Y., Liu, Z-K. (2008): Thermodynamic modeling of the Cu-Mn system supported by key experiments. *Journal of Alloys and Compounds*, 457, pp. 233–238.
- [36] Liu, X. J., Ohnuma, I., Kainuma, R., Ishida, K. (1999): Thermodynamic assessment of the Aluminum-Manganese (Al-Mn) Binary Phase Diagram. *Journal of Phase Equilibria*, 20, pp. 45–56.

Modelling surface degradation in hot rolling work rolls

Modeliranje degradacije površine valjev za vroče valjanje

Milan Terčelj¹, Matevž Fazarinc², Primož Mrvar¹, Borut Žužek³, Peter Fajfar^{1,*}

¹Department of Material Science and Metallurgy, Faculty of Natural Sciences and Engineering, University of Ljubljana, Aškerčeva cesta 12, 1000 Ljubljana, Slovenia

²RCJ, d.o.o., Cesta Franceta Prešerna 61, 4270 Jesenice, Slovenia

³IMT, Lepi pot 11, 1000 Ljubljana, Slovenia

*Corresponding author: E-mail: peter.fajfar@omm.ntf.uni-lj.si

Abstract

For better understanding of materials behaviour subjected to thermal fatigue of work rolls used in hot rolling mill, two thermal fatigue tests were developed. Tests were performed using Gleeble 1500D thermo-mechanical simulator. The first test was applied for the testing of thermal fatigue resistance of work rolls used in common rolling conditions. The average cracks length and the crack density of the specimens were established at varying test temperatures and the number of thermal fatigue cycles. The second test enabled the simulation of the thermal loading of the work rolls during a rolling mill stall. The growth of stall band firecracks after different cooling condition of the work rolls is presented.

Key words: hot rolling, work roll, thermal fatigue, fire cracks

Izvleček

Za boljše razumevanje vedenja materiala izpostavljene ga termičnemu utrujanju delovnih valjev, ki se uporabljajo za vroče valjanje, sta bila razvita dva preizkusa za termično utrujanje valjev. Preizkusi so bili izvedeni z uporabo termomehanskega simulatorja Gleeble 1500D. Prvi preizkus je bil uporabljen za preizkušanje odpornosti proti termičnemu utrujanju delovnih valjev v normalnih razmerah valjanja. Za določitev povprečne dolžine in gostote razpok so bili preizkusi izvedeni pri različnih temperaturah in številu ciklov termičnega utrujanja. Drugi preizkus omogoča simulacijo toplotne obremenitve delovnih valjev med zastojem valjalnega stroja. Prikazana je rast razpok v vročem glede na različne razmere pri ohlajanju delovnih valjev.

Ključne besede: vroče valjanje, delovni valj, termično utrujanje, razpoke v vročem

Introduction

Work rolls represent an important segment in the operating cost of a modern rolling mill. They are expensive and a large number of work rolls must be in stock to assure the continuous operating of the mill. During hot rolling work, rolls are subjected to successive heating and cooling conditions. Their surface is exposed to rapid temperature changes due to the contact with hot rolled material and due to cold water used for work rolls cooling. This cyclic heating/cooling conditions cause thermal fatigue which is one of the most important factors affecting the rate of surface deterioration as well as mechanical fatigue and abrasion. Thermal fatigue is a low-cycle failure mechanism that occurs due to the cyclic thermal loading of the work rolls surfaces.

Cooling process of the work rolls is one of the most important tasks during hot rolling. Their surface is exposed to rapid temperature change due to the contact with hot rolled material and cooling with water sprays. If cooling is not intensive enough, wear of rolls and fire cracks appear. Fire cracks can appear after only a few turns of rolls, starting on the surface and growing perpendicular to the surface of the rolls. The intensity of the growth and the depth of the cracks mostly depends on the temperature gradient during alternating heating and cooling^[1-3].

The evolution of work roll surface temperature during one revolution is presented in Figure 1^[4]. The work roll is divided into angular sections. In the section 1, a high increase of the roll surface temperature is noticed. The reason is in the heat transfer from the hot slab to the roll. The contact time between the slab and the roll is very short, only the skin of the roll is subject to the very high thermal gradients. In section 2, the work roll slowly cools down due to radiation and convection. In section 3, the surface temperature decreases during water cooling. In sections 4 and 5, the surface temperature rises slightly due to the heat transfer from the roll centre. A drop of the surface temperature due to the contact with the back-up roll occurs. In section 6, the temperature decreases due to the water cooling and in section 7, the surface temperature rises due to the radiation of the slab surface.

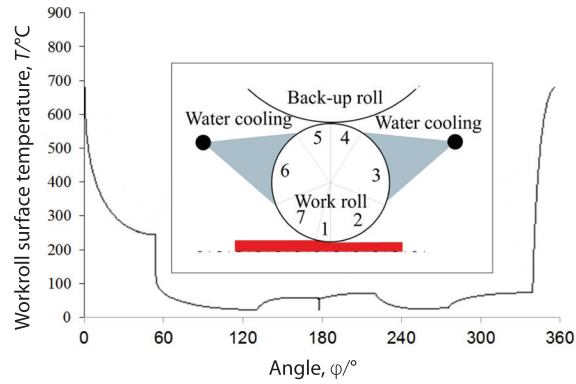


Figure 1: Evolution of work roll surface temperature.

In this paper, two different tests for the laboratory assessments of the thermal fatigue resistance of work rolls are presented. The first test enables a simulation of the thermal fatigue of work rolls during hot rolling of flat products at common condition^[5-7]. Furthermore, with the second test, the thermal fatigue resistance of work rolls in the case of the rolling mill stalls can be investigated. Both tests were implemented in a thermo-mechanical simulator of metallurgical states, the Gleeble 1500D. The resistance heating and the water cooling of the samples as well as air blowing (water emptying process) were computer-controlled. The samples were freely spanned in the working jaws of the Gleeble loading system, keeping the outer force on the samples at 0 N.

Experimental

Specimen

Specimens were machined from the work rolls. They were cylindrically shaped with a borehole in the longitudinal axis that enabled the cooling of the specimens with a stream of water and air (Figure 2). The reduction of the diameter in the central part of the specimen intensified the temperature gradient during the heating and the cooling stage of the experiment. The temperature was controlled with the thermocouple that was spot-welded in the middle of the reduced part of the specimen (Figures 2, 3).

The thermal fatigue tests were performed on thermal-mechanical simulator Gleeble 1500D.

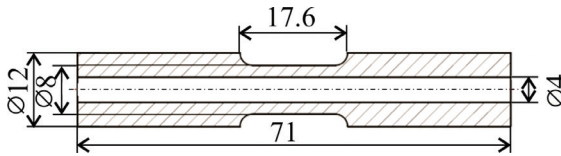


Figure 2: Specimen.

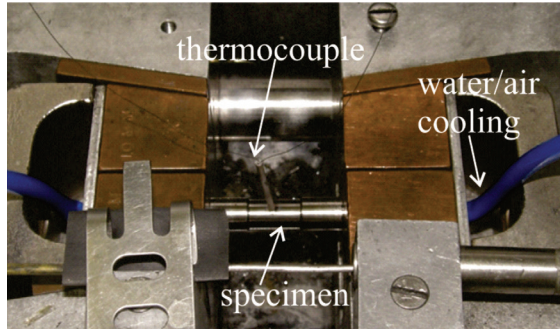


Figure 3: Test cell with specimen, Gleeble 1500D.

Thermal fatigue of work rolls

Specimens were tested at similar conditions found on the surface of rolls during hot rolling. Specimens were heated to four different temperatures, 400 °C, 500 °C, 600 °C and 700 °C and then rapidly cooled with water and air. Two series of experiments with 500 and 1 000 thermal fatigue cycles were carried out. Each cycle was composed of three phases: resistance heating, water cooling and cooling of the specimen with air, all in duration of 4.8 s.

Material

The specimens were electric-discharge machined from an indefinite chill roll. All these rolls were cast as a double layer. The hard working surface consisted of matrix of dendrite grains from bainite and martensite, ledeburite and some free graphite. The core of the roll can be made either out of the alloyed grey cast iron or out of the alloyed nodular cast iron. These types of rolls are used for roughing and finish rolling mills. The typical chemical composition is listed in Table 1.

Table 1: Typical chemical composition of the indefinite chill roll in mass fractions, w/%

	C	Si	Mn	Cr	Ni	Mo
min.	3.0	0.8	0.2	1.4	4.0	0.2
max.	3.4	1.1	0.5	2.0	4.6	0.5

Stall band firecracks

For the investigation of the formation of stall band firecracks on the work roll surface, five tests were performed.

For the first test, the specimen was heated up to 600 °C for each thermal fatigue cycle and then cooled down with a stream of water and air. This was a base test condition for all other tests. After 500 cycles, the specimens were held at the testing temperature for 15 s or 60 s and then cooled down to the room temperature with water or air (Figure 4).

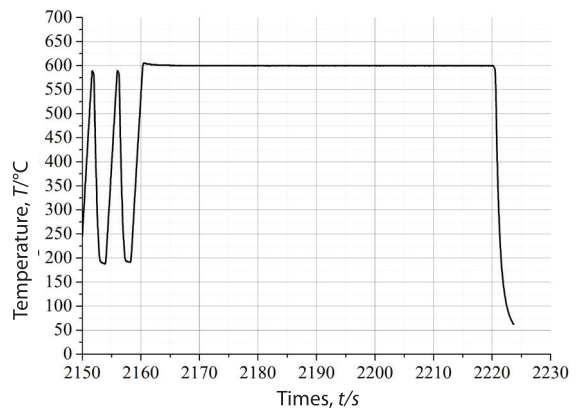
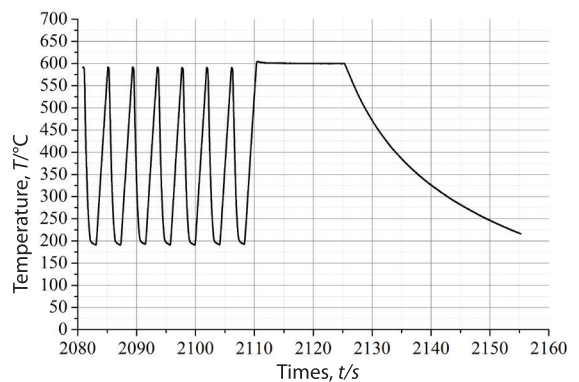


Figure 4: Measured temperature a) holding time $t = 15$ s, free air cooling; b) holding time $t = 60$ s, forced water cooling.

Material

The specimens were machined from high chromium iron rolls. These are double layer centrifugal cast compound rolls: with the cast iron outer layer with high chromium content and the core made either of a grey or a nodular cast iron. Work surface contains very hard chromium carbides, fine grained and equally distributed within the matrix which is made mainly from pearlite as well as the tempered martensite. High chromium rolls are used for hot rolling of flat products. The typical chemical composition is listed in Table 2.

Table 2: Typical chemical composition of the high chromium iron roll in mass fractions, w/%

	C	Si	Mn	Cr	Ni	Mo	V
min.	1.0	0.5	0.6	10.0	1.0	1.0	0.2
max.	2.0	1.0	1.2	13.0	2.0	2.0	0.5

Results and discussion

Temperature measurement

Temperature was measured at the centre of the exterior surface of the specimen. The wall thickness of the specimen was 2.0 mm. This is one of the reasons why the measured cooling temperature is not in accordance with the programmed one (Figure 4). The Figure 4 represents the course of the programmed temperature (black curve), the measured temperature (red curve) and the rate of the change of the temperature during testing.

The cooling rate increased with the increasing test temperature. At the test temperature 400 °C, the cooling rate was 300 °C/s and at the test temperature 700 °C, the cooling rate was 550 °C/s.

The entire time for one thermal fatigue cycle was composed of 2.2 s of resistance heating to the test temperature, 1.8 s of water quenching, and 0.8 s of forced air cooling. During the water cooling, the cooling rate was at 136 °C/s, and during the air cooling it decreased to 13 °C/s.

Thermal fatigue of work rolls

During the testing thermal fatigue, cracks appeared on all of the specimens. Cracks start to

grow on the cooled surface of the specimen on the phase boundaries between grains of bainite and martensite and grains of ledeburite. Cracks propagate in depth of specimen mostly through the ledeburitic phase, (Figure 6).

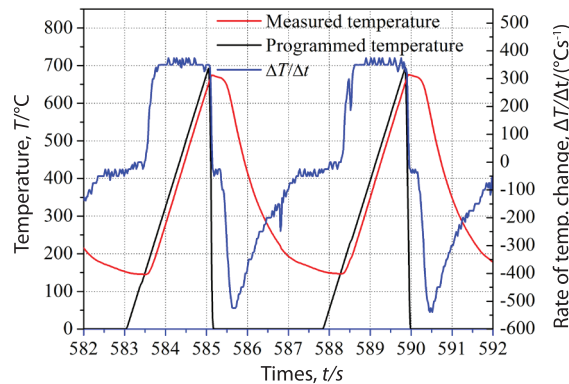


Figure 5: Testing conditions: A – resisting heating, B – water quenching, C – air cooling.

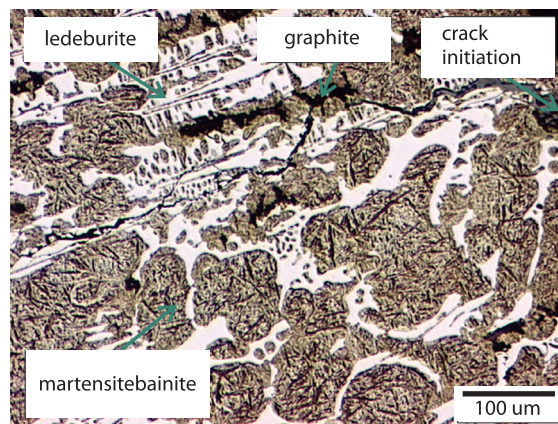


Figure 6: Crack propagation, $T = 700\text{ }^{\circ}\text{C}$, 500 cycles.

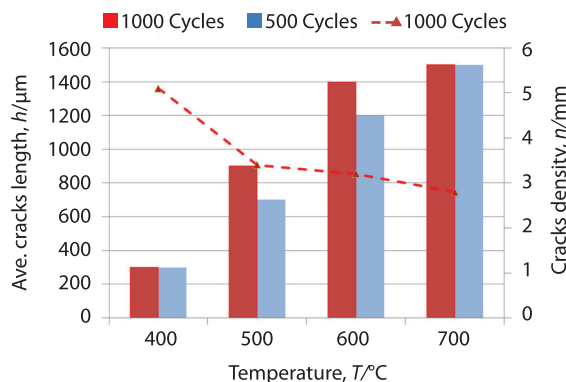


Figure 7: Average cracks length and crack density.

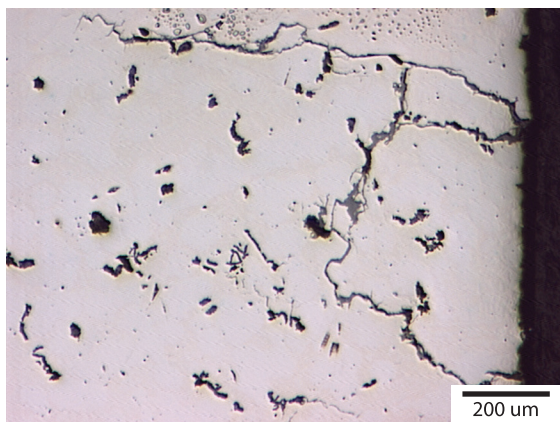


Figure 8: Linking of cracks.

With a higher test temperature during a single cycle and a higher number of cycles, cracks become wider and deeper, but lower in density. At the temperature of 400 °C, 5.1 cracks/mm were formed on average. At the temperature of 700 °C, the density of cracks was reduced to 2.8 cracks/mm. In the 2.0 mm thick wall of specimens, cracks reached a length between 300 µm and 1 500 µm (Figure 7).

At higher temperature, the cracks can link together and subsequent spalling of roll surface fragments may occur (Figure 8).

Stall band firecracks

During a mill stall or a sudden stop of the rolling mill, the hot rolled strip is in contact with the work roll surface for an extended period of time. Due to extended (lasting up to several minutes) holding of rolls at high temperatures (850 °C–1 250 °C), the local overheating of work rolls appears. During that, the overheated surface expands in radial direction and contracts in axial and tangential direction. When the remaining stresses exceed the yield strength of the material, the stall band firecracks form with net-like shape (Figure 9).



Figure 9: Stall band firecracks at the work roll surface.

The main task after this type of incident is to minimize the severity of the cracking that will result. There are several procedures at our disposal:

- to remove the rolls from the rolling mill,
- to rotate the rolls for about half an hour without water cooling or
- to cool down rolls with the water cooling system.

In the present work, the simulation of stall band firecracks growth of the work rolls after different cooling condition is presented. The mill stall was simulated with 500 thermal fatigue cycles followed by 15 s or 60 s holding time at the test temperature of 600 °C and then finished with forced water cooling or free air cooling.

In general, the lengths of firecracks were in the range of 5 mm to 422 mm. The largest average crack length and the lowest crack density were obtained in specimens, which were free cooled on air (Figures 10, 11, 12). The crack density and the average cracks length obtained at the holding time of 15 s are similar to the base test (Figures 11, 12).

From these results we can draw the conclusion that the best procedure to reduce firecracking of the work rolls after the rolled material is removed from the roll gap is forced cooling of the work rolls with water. In this case the density of firecracks is higher, but the lengths of the cracks are shorter. The growth of the cracks is accelerated by the cracks oxidation while the oxides have bigger volume than the base material and they act as the wedge to the crack. The oxide thickening is accelerated by the increase in temperature^[1].

The SEM micrograph of the oxidated firecrack is shown in Figure 13a and the related EDS spectra in Figure 13b. These results are contradict the findings found in the literature^[6]. It is suggested that after the rolled material is removed from the roll, the water cooling should be turned off. Extended contact times with rapid water cooling will result in a larger cell size and deeper cracks. Once the rolled material has been removed from the roll gap, the rolls should be rotated for a minimum of 20 min to allow equalization of the roll surface temperature. Further testing will be carried out to optimize the cooling time of the rolls, which would contribute to decrease in down-time of the rolling mill after such an event.

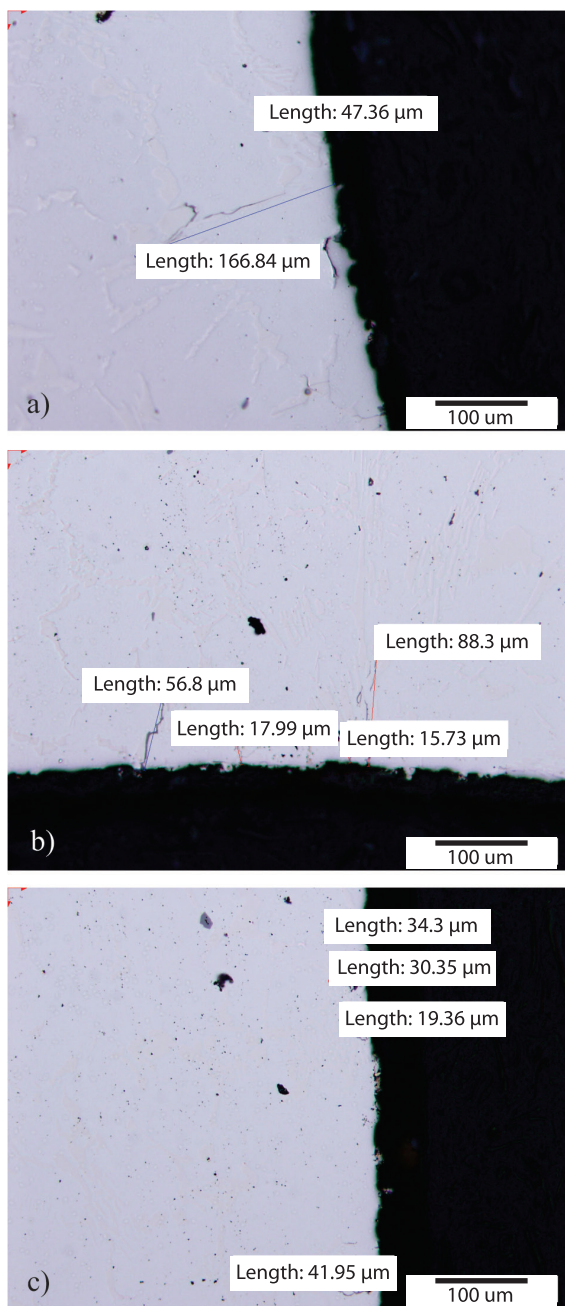


Figure 10: Crack lengths: $t = 15$ s, air cooling (a), $t = 60$ s, air cooling (b), $t = 60$ s, water cooling (a).

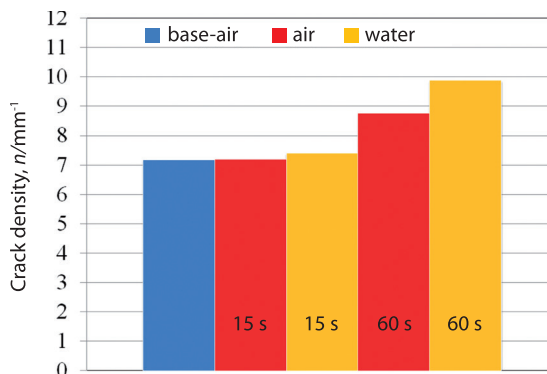


Figure 11: Crack density.

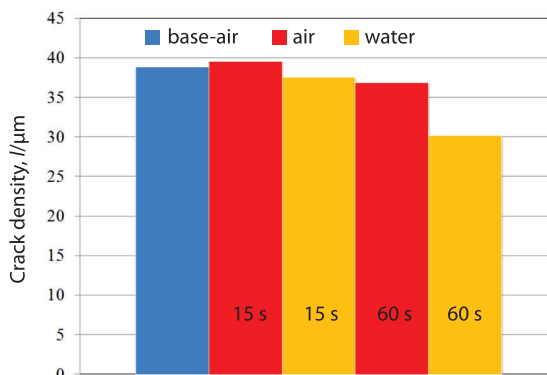


Figure 12: Average cracks length.

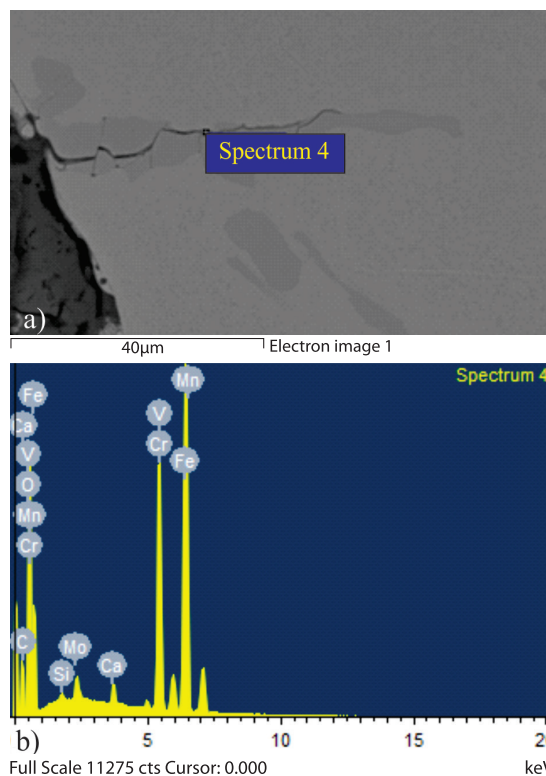


Figure 13: SEM micrographs of the investigated crack (a), and the related EDS spectra (b).

Conclusion

Two thermal fatigue tests for the estimation of thermal fatigue resistance of work rolls were developed. They are based on computer guided heating and cooling of the specimen using Gleeble 1500D thermo-mechanical simulator. The specimen geometry enables the achievement of high temperature gradients. These tests will contribute to better understanding of crack nucleation and their growth during the usual hot rolling conditions, as well as for the case of rolling mill stalls.

References

- [1] Colás, R., Ramírez J., Sandoval, I., Morales, J. C., Leduc, L.A. (1999): Damage in hot rolling work rolls. *Wear*, 230, pp. 56–60.
- [2] Fischer, F.D., Schreiner, W.E., Werner, E.A., Sun, C.G. (2004): The temperature and stress fields developing in rolls during hot rolling. *Journal of Materials Processing Technology*, 150, pp. 263–269.
- [3] CAEF - The European Foundry Association - Roll section (2002): *Roll Failures Manual-Hot Mill Cast Work Rolls*. 27 p.
- [4] Guerrero, M.P., Flores, C. R., Pérez, A., Colás, R. (1999): Modelling heat transfer in hot rolling work rolls. *Journal of Materials Processing Technology*, 94, pp. 52–59.
- [5] Fazarinc, M., Turk, R., Kugler, G., Mrvar, P. and Terčelj, M. (2008): Development of test rig for thermal fatigue testing - preliminary results. *RMZ-M&G*, 55, pp. 31–40.
- [6] Turk, R., Fazarinc, M. (2008): Newly developed test for assesment of thermal fatigue resistance. Sixteenth annual international conference on composites/nano engineering, Kunming, Yunnan Province, China : ICCE 16, pp. 721–722.
- [7] Fajfar, P., Fazarinc, M., Žužek, B., Kugler, G., Terčelj, M. (2013): New progress in laboratory testing of thermal fatigue resistance. V: 45th International October Conference on Mining and Metallurgy - IOC 2013, Bor, Serbia, Proceedings. Bor: Technical Faculty, pp. 329–332.

Assessment of heavy metals in wastewater obtained from an industrial area in Ibadan, Nigeria

Ocena težkih kovin v odpadnih vodah industrijske cone v Ibadanu v Nigeriji

Omotayo Ayeni

Department of Geography and Environmental Sciences, University of Hertfordshire, Hatfield, AL10 9AB, United Kingdom

Corresponding author. E-mail: omotayoayeni@yahoo.com

Abstract

The distribution of heavy metals, namely, Copper (Cu), Chromium (Cr), Lead (Pb), Cadmium (Cd) and Nickel (Ni) in wastewater samples from an industrial area in Ibadan, South-western Nigeria have been evaluated. Wastewater samples were collected from the discharge points of six manufacturing industries and conveyed to the laboratory for chemical analysis. The concentration of heavy metal constituents was determined using Inductively Coupled Plasma (ICP) and Optical Electro Spectrometer (OES) standard methods. The results obtained reveal average concentration in the order of abundance given as Cu>Cr>Ni>Pb>Cd.

This study reveals that the concentration of toxic heavy metals was significantly higher than the permissible limits of WHO which could pose a huge threat to human health and the natural environment. Therefore, the polluting industries have the duty-of-care to manage their wastewater disposal in order to safeguard the aesthetic integrity of the environment and ensure the safety of public health. It is recommended that the manufacturing companies should pre-treat their wastewaters using appropriate green technology prior to disposal in order to improve environmental sustainability.

Key words: Heavy metals, wastewater, industrial estate, pollution, health hazard

Izveleček

Ocenjena je porazdelitev težkih kovin, in sicer bakra (Cu), kroma (Cr), svinca (Pb), kadmija (Cd) in niklja (Ni) v vzorcih odpadne vode iz industrijske cone v Ibadanu v jugozahodni Nigeriji. Odpadne vode so vzorčili v izlivnih točkah šestih proizvodnih industrijskih družb in jih dostavili v analizo v kemijski laboratorij. Koncentracijo težkih kovin so določili s standardnima metoda induktivno vezane plazemske (ICP) in optične emisijske spektrometrije (OES). Iz analiznih rezultatov sledijo povprečne koncentracije kovin v naslednjem zaporedju: Cu>Cr>Ni>Pb>Cd.

Raziskava je razkrila, da je koncentracija toksičnih težkih kovin značilno višja od vrednosti, ki jih dopušča WHO, kar lahko resno ogrozi človekovo zdravje in naravno okolje. Onesnaževalne industrijske panoge so zato obvezane urediti odstranjevanje svojih odpadnih vod tako, da zagotovijo vzdrževanje estetskega videza okolja in varovanje javnega zdravja. Industrijskim podjetjem priporočajo, da zavoljo zagotovitve trajnostnega stanja okolja svoje odpadne vode ob uporabi primerne zelene tehnologije grobo očistijo preden jih odtočijo.

Ključne besede: težke prvine, odpadna voda, industrijska cona, onesnaženje, nevarnost za zdravje

Introduction

Environmental pollution is one of the major concerns of this century. Soil, water and air pollution have attracted continued interventions at a global level regarding remedial approaches to sustainable development due to alarming rates of the associated potential health risks posed to man and the environment. Rapid industrialization and socio-economic development in the 21st century has led to increased growth of the industrial sector in developing countries. As a result, the quantity of wastewater being discharged into the environment has increased over time and has been creating undue environmental degradation and health hazards.

Many researchers have investigated the effect of the prolonged exposure of humans, animals and plants to toxic heavy metals in industrialized cities. Heavy metals such as Arsenic (As), Mercury (Hg), Iron (Fe), Nickel (Ni), Zinc (Zn), Lead (Pb), Copper (Cu), Chromium (Cr) and Cadmium (Cd) are prominent components of industrial wastewaters^[1,2]. Some biochemical accumulation risks of heavy metals and uptake effects on the biology of *Sitophilus* have been studied^[3].

The industrial revolution of the 21st century has imposed numerous environmental and health problems to humans in all parts of the world. Mehta et al.^[4] reports the effect of industrial growth on the natural environment. Wastewater treatment and disposal problems have increased on a global scale due to increase in production^[5]. Khurshid et al.^[6] reiterate the effect of wastewater on water quality while Moore and Ramamoorthy^[7] report the negative impact of heavy metals on environmental aesthetics. Akinyeye et al.^[8] and Adedeji et al.^[9] evaluate the status of heavy metal pollutants of the Alaro River at Oluyole industrial area in Ibadan South-western Nigeria while Akinyeye et al.^[4] conducted a study on the impact of industrial wastewaters from Oluyole industrial area on Alaro stream and a pond.

An industrial area in Ibadan, south-western Nigeria, was mapped out for geo-environmental assessment as a result of the indiscriminate disposal of untreated wastewater into the environment from point source discharge. The

objective of this study was to investigate the nature of the composition of the untreated wastewater with respect to heavy metals and to highlight the potential environmental damage and health risks that could arise as a result of the disposal of raw wastewater into the environment.

Materials and methods

The study area is located North-east of Ibadan in the South-western part of Nigeria and is underlain by homogeneous resistant rock which is characteristic of a basement complex setting. The Basement complex forms part of the African Crystalline Shield^[11], while^[12] classifies the rocks of the Basement complex of Nigeria into five main groups which are: Migmatite gneiss complex, Charnokitic rocks, Schist, Older granites and Unmetamorphosed dolerite dykes which are presented in Figure 1. The topographical map of Ibadan (sheet 261 N.E.) on a scale of 1:25,000 was utilised as a base map. A mobile Global Positioning System (GPS) was used to determine the coordinates of the study area which lies within Longitude 3°50'E and 3°52'E, and Latitude 7°21'N and 7°23'N as shown in Figure 2.

The wastewater samples were collected from the points of discharge of the pharmaceutical, agrochemical, confectionery, textile, paint and bottling companies in the study area. The pharmaceutical company was producing a wide range of prescription medicines, vaccines and some healthcare products. Some of the chemicals used for production were albumin, phenols, glycine and aluminum gels. The agrochemical company was producing pesticides and herbicides, while the chemicals and materials used were sulphur, epoxiconazole, fenpropidin and dimethylamine salt. The confectionery company was producing chocolates, sweets and biscuits whilst the materials used were mainly cocoa, sugar, wheat and sweeteners. The textile company manufactured clothes and the raw materials used were cotton, dye, polyacrylamide, Na and Ca lignosulphonate, NaOH and anionic polymer. The paint company was producing emulsion and coating for interior usage and the chemicals used were mainly

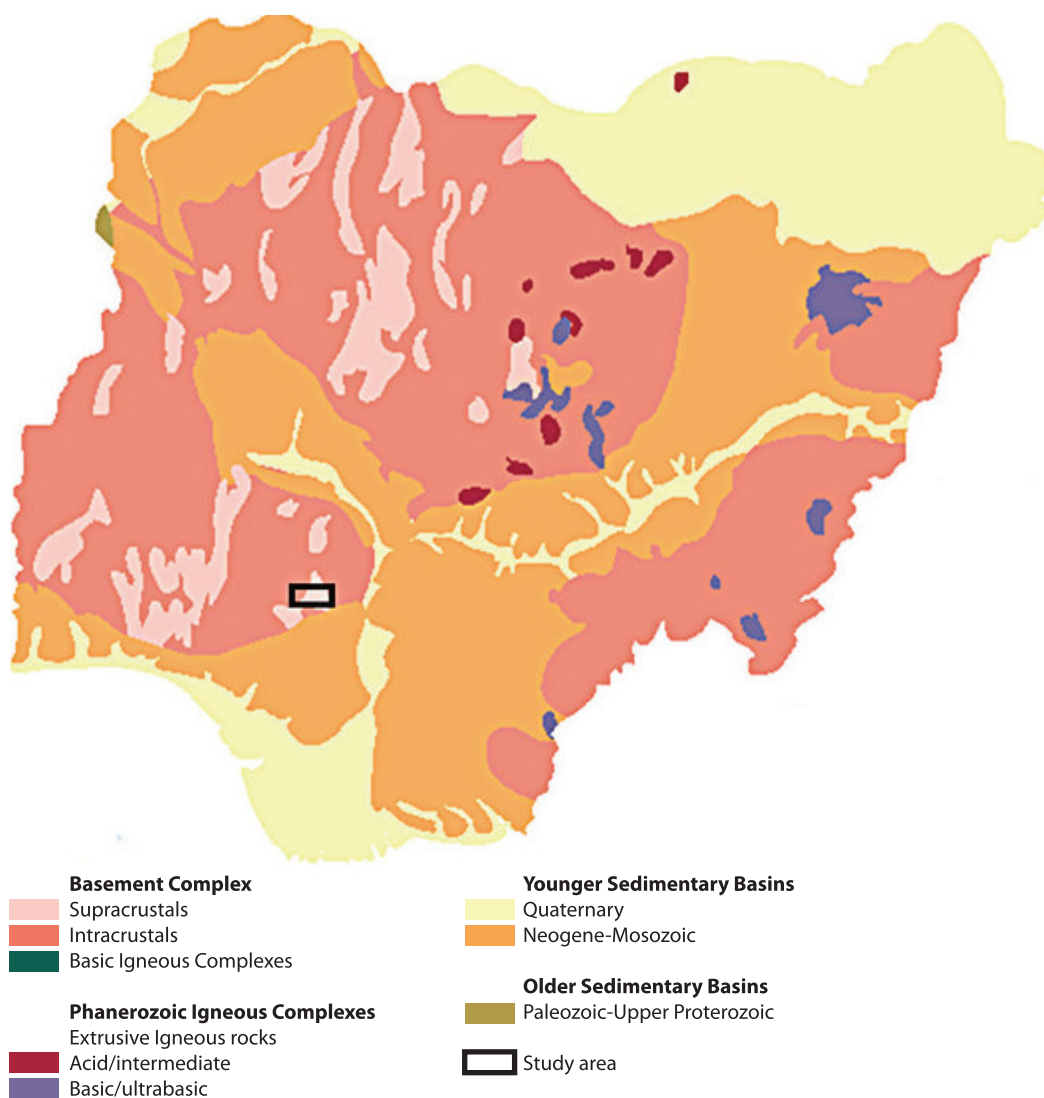


Figure 1: Geological map of Nigeria showing the study area (Adapted from NGSa, 2006)^[13].

Titanium dioxide, Cu monoxide, Al triolyphosphate, Fe oxide and pigment powder whilst the bottling company was producing non-alcoholic drinks and the materials used were mainly water, flavours and sugar.

The sites were denoted with IB-01 to IB-06 as shown in Figure 2 and Table 1 respectively while the concentration of heavy metals in the wastewater samples varied considerably from one site to another. The wastewater samples were collected in plastic containers; these were pre-washed and rinsed with tap water and later soaked in 10 % HNO₃ for 24 h before

they were rinsed with distilled water prior to usage. The wastewater samples were labeled appropriately and conveyed to the laboratory for chemical analysis using the standard ICP and OES chemical procedures proposed by^[14] and the American Environmental Protection Agency EPA^[15]. Accuracy and instrument detection limits for measured heavy metals were estimated by taking replicate measurements of the calibrated blank (1 % nitric acid) in accordance with 85–115 % of EPA^[15] set limit and accuracy of 0.1 for Cd, 1.5 for Pb, 0.5 for Ni and 0.3 for Cr and Cu respectively.

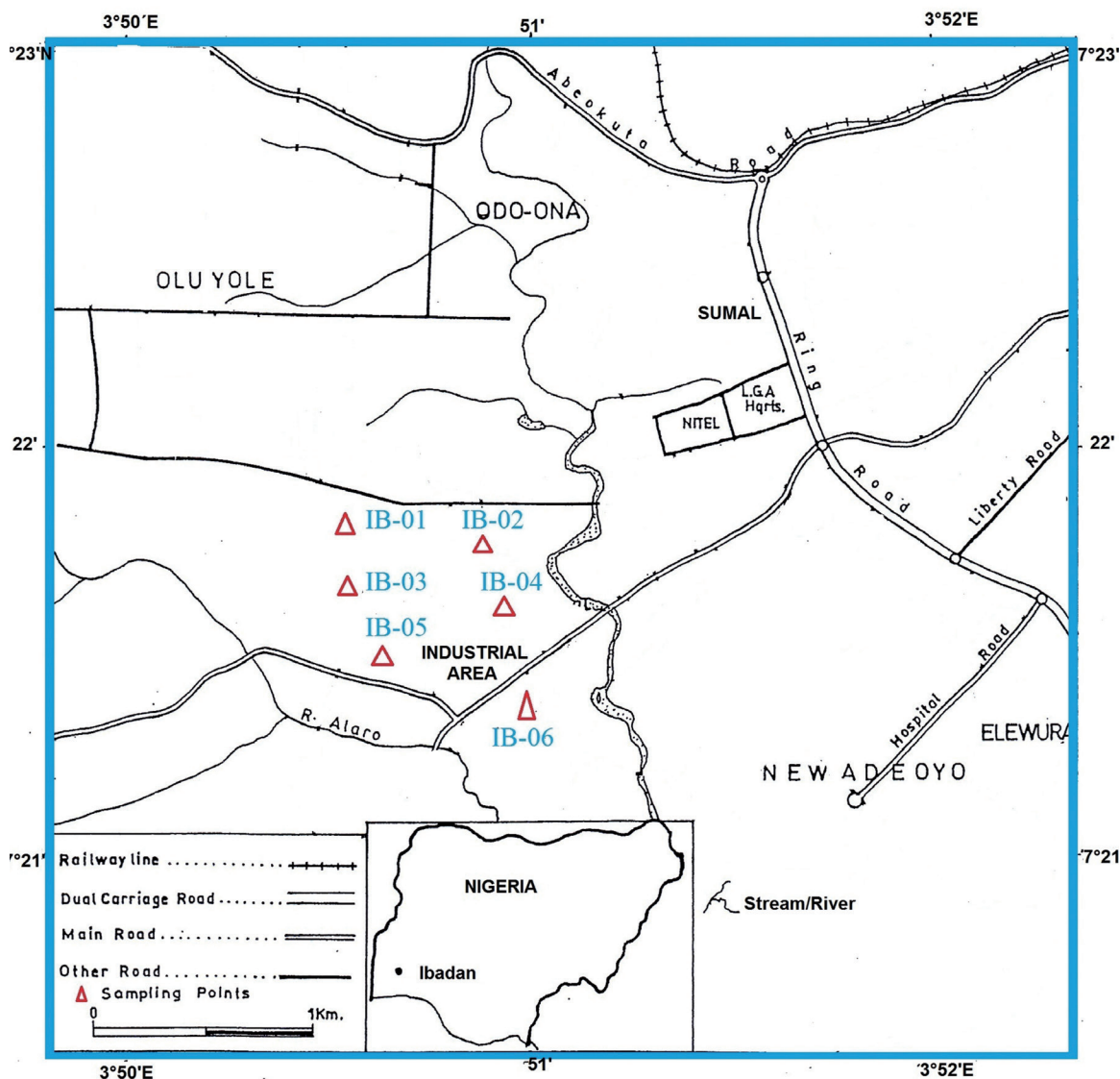


Figure 2: Map of study area showing sampling points.

Results and discussions

The results obtained from the chemical analysis of wastewater samples are reported in Tables 1 and 2 and depicted graphically in Figures 3 and 4 respectively.

Table 2 presents the comparison between the average concentration of heavy metals in wastewater samples and the WHO standards in mg/L. The average concentration of heavy metals is given in the order of abundance as Cu>Cr>Ni>Pb>Cd.

Table 1: Heavy metal concentrations in wastewater samples at various sampling points (mg/L)

Sample points	Cu	Ni	Pb	Cr	Cd
IB-01	5.5	2.3	0.5	2.4	0.6
IB-02	4.1	3.6	0.6	3.2	0.5
IB-03	6.7	4.4	0.9	3.9	0.9
IB-04	3.8	1.7	0.4	2.7	0.4
IB-05	1.9	2.2	0.7	3.8	0.2
IB-06	2.2	1.4	0.3	1.9	0.1

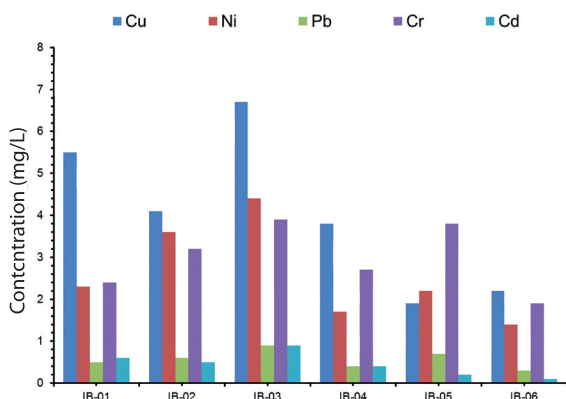


Figure 3: Distribution of heavy metals in wastewater samples.

Table 2: Average concentration of heavy metals in wastewater samples and WHO standards (mg/L)

Parameter	Cu	Ni	Pb	Cr	Cd
Concentration	4.00	2.60	0.60	3.00	0.50
W.H.O. standards	1.20	0.02	0.01	0.05	0.003

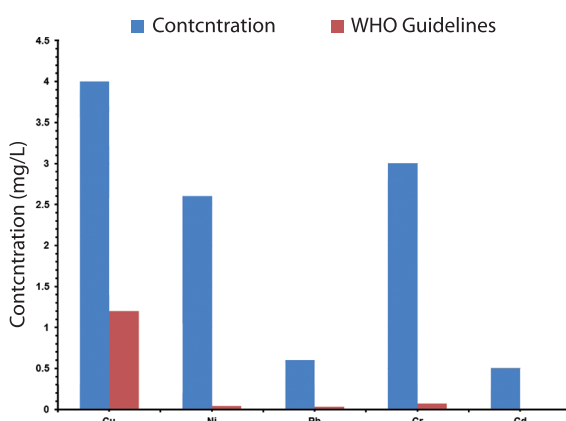


Figure 4: Average concentration of heavy metals in wastewater samples versus WHO Guidelines values (mg/L).

The chemical concentration of heavy metals analysed revealed significant variability across the geographic spread of the sample points in the study area. The order of relative abundance of heavy metals in wastewater samples is given as $Cu > Cr > Ni > Pb > Cd$ indicating a higher concentration of Cu as 6.7 mg/L while Cd has the least value, which is 0.1 mg/L. Higher values obtained for Cu in the wastewater could

have been due to the correspondingly high Cu content of chemical additives used in the production chain. Ayedun et al.^[16] confirms that groundwater pollution by toxic heavy metals has inherent health risks.

This study reveals there is a generally high concentration of toxic heavy metals higher than the permissible contaminant levels established by WHO^[17,18] as shown in Table 2 and Figure 4 respectively. Sharma et al.^[19] confirms that Cu plays an important role in chemical and biological processes in the environment and that excessive exposure could lead to health hazards. In the same vein increased concentration and long term exposure of humans to Ni can lead to decreased body weight, liver and heart damage and skin irritation as reported by James et al.^[20]. Cr has been reported to increase lean body mass and cause a reduction in the percentage of body fat, which may result into weight loss in humans^[21]. Pb can cause acute and chronic symptoms of poisoning depending on the level and duration of exposure^[22] and it can also affect mental development such as impaired intelligence. James et al.^[20] affirms that Cd has been reported to be associated with renal dysfunction and obstructive lung disease which has been linked to lung cancer, skin irritation and ulceration.

Conclusions

The higher concentration of toxic heavy metals in the wastewater samples indicate indiscriminate disposal and negligence of the manufacturing industries towards duty-of-care as a result of untreated wastewater prior to disposal into the environment. The discharge of these raw wastewaters into the natural environment may have also contributed significantly to the bioaccumulation of heavy metals in the ecosystem. Therefore, it is expedient that the polluting industries should endeavour to treat raw wastewaters using state-of-the-art technologies before disposal in order to keep the environment safe and reduce the potential health risks in the area.

Acknowledgements

The author would like to thank the officials of the companies where the sampling programme was carried out for granting the permission to collect wastewater samples from various discharge points.

References

- [1] Nriagu, J.O., Pacyna, J.M. (1988): Quantitative assessment of worldwide contamination of air, water and soils with trace metals. *Nature*, 333, pp. 134–139.
- [2] Schalscha, E., Ahumada, I. (1998): Heavy metals in rivers and soils of central Chile. *Water Sci. Technol.*, 37(8), pp. 251–255.
- [3] Omoloye, A.A. (2009): Field accumulation risks of heavy metals and uptake effects on the biology of *Sitophilus zeamais* (Coleoptera: Curculionidae). *African Science*, 10, pp. 3–10.
- [4] Mehta, G., Prabhu, S.M., Kantawala, D. (1995): Industrial wastewater treatment – The Indian experience. *Journal of Indian Assoc. Environ. Management*, 22, pp. 276–287.
- [5] Kolpin, D.W., Furlong, E.T., Meyer, M.T., Thurman, E.M., Zaugg, S.D., Barber, L.B., Buxton, H.T. (2002): Pharmaceuticals, hormones and other organic wastewater contaminants in U.S. streams - A national reconnaissance. *Environ. Sci. Technol.*, 36, pp. 1202–1211.
- [6] Khurshid, S., Abdul, B., Zaheeruddin, A., Usman, S.M. (1998): Effect of waste disposal on water quality in parts of Cochin, Kerala, *Indian Journal of Environ. Health*, 40(1), pp. 45–50.
- [7] Moore, J.W., Ramamoorthy, S. (1984): *Heavy metals in natural waters: Applied monitoring and impact assessment*, Springer-Verlag, New York; 246 p.
- [8] Akinyeye, A.J., Solanke, E.O., Okorie, T.G. (2011a): Heavy metal composition in industrial effluent on Alaro stream benthos. *Australian Journal of Basic and Applied Sciences*, 5(5), pp. 1184–1188.
- [9] Adedeji, O.B., Adeyemo, O.K., Oyedele, M.O. (2011): Heavy metals in snail and water samples from Alaro river Oluyole industrial area of Ibadan South-western Nigeria. *Journal of Applied Sci. Env. Sanitation*, 6(2), pp. 115–121.
- [10] Akinyeye, A.J., Komolafe, J.I., Okorie, T.G. (2011b): Limnological assessment of effluents on invertebrates from Alaro River in Oluyole industrial area of Ibadan, Oyo State, Nigeria. *Agriculture & Biology Journal of North America*, 27, pp. 1045–1053.
- [11] Jones, H.A., Hockey, R.D. (1964): The geology of parts of South-western Nigeria. *Geol. Survey. Nig. Bull.* 31; 101 p.
- [12] Rahman, M.A. (1976): *Review of basement complex geology of South-western Nigeria*. Elizabeth Publishing Co., Lagos, Nigeria; 182 p.
- [13] NGS (2006): *Geological Map of Nigeria*. Nigerian Geological Survey Agency bulletin, 123 p.
- [14] Thompson, J., Welsh, A.T. (1989): A validated Inductively Coupled Plasma (ICP) and Optical Electro Spectrometer (OES) analytical methods. *American Journal of Analytical Chemistry*, 2, pp. 718–725.
- [15] EPA- Determination of metals and trace metals in water and waste by Inductively Coupled Plasma-Atomic Emission Spectrometry [online]. *Analytical chemistry*, 2007, [Cited 25/12/2013]. Available on: http://www.waterscience/methods/method/files/200_7.pdf.
- [16] Ayedun, H., Taiwo, A.M., Umar, B.F., Oseni, O.A., Oderinde, A.A. (2011): Assessment of groundwater contamination by toxic metals in Ifo, Ogun State, South-western Nigeria. *Indian Journal of Science and Technology*, 4, pp. 7–15.
- [17] WHO (2002): *Water Pollutants: Biological agents, dissolved chemicals, non-dissolved chemicals and sediments*. WHO CEHA, Amman, Jordan; 350 p.
- [18] WHO (2003): *The World Health Report 2003: Shaping the future*. World Health Organization, 1211 Geneva 27, Switzerland; 647 p.
- [19] Sharma, D.K., Jangir, J.P., Chandel, C.P.S., Gupta, C.M. (1988): Studies in quality of water in and around Jaipur- Part I. *Journal of Indian Water Works Association*, pp. 257–260.
- [20] James, O.O., Nwaeze, K., Mesagan, E., Agbojo, M., Saka, K. L. Olabanji, D.J. (2013): Concentration of heavy metals in five pharmaceutical effluents in Ogun State, Nigeria. *Journal of Env. Pharmacol. Life Sci.* 2(8), pp. 84–90.
- [21] Anderson, R. A. (1998): Effects of chromium on body composition and weight loss. *Journal of Nutrition reviews*, 56 (9), pp. 266–270.
- [22] Bulinski, R., Bloniarz, J., Libelt, B. (1993): Presence of some trace elements in Polish food products. XV. Contents of Lead, Copper, Cadmium, Nickel, Chromium, Zinc, Cobalt, Manganese, Copper and Iron in some Milk Products. *Bromatologia i. ChemiaToks*, 26, pp. 23–27.

Basic parameters of small underground nuclear power stations

Osnovni parametri majhnih podzemnih nukleark

Jakob Likar^{1,*}, Eivind Grøv², Tina Marolt¹

¹University of Ljubljana, Faculty of Natural Sciences and Engineering, Aškerčeva cesta 12, 1000 Ljubljana, Slovenia

²SINTEF/University of Science and Technology - (NTNU), Trondheim, Norway

*Corresponding author. E-mail: jakob.likar@ntf.uni-lj.si

Abstract

The use of underground space for various needs has seen a significant growth in recent years. This possibility is also reflected in the concept of construction of underground nuclear facilities. Based on previous experience, success in the future might be bound to such as smaller nuclear facilities by some named as Small Modular Reactors (SMRs). Suitable locations at appropriate depth taking advantage of the natural barrier properties afforded by the good quality bedrock have important influence on providing appropriate natural circumstances for SMRs. Underground siting can provide superior protection compared to that of a surface serviced siting in many critical situations and subsequent devastating consequences for the operation of a nuclear facility. Complicated underground complex needed for a nuclear power system need special attention calling for dedicated investigations and also research on such as issues as earthquake hazard, although the latter seems to be documented being advantageous already. The paper will present a case that clearly shows the obvious advantages of the use of underground space for current available nuclear technologies and assessments of seismic loads influences on nuclear underground structures.

Key words: underground space, underground nuclear station, natural containment, seismic loading, rock mass displacement

Izvleček

Izraba podzemnega prostora v zadnjem času hitro narašča. Prav tako je zaznati povečane aktivnosti pri izdelavi konceptov gradnje podzemnih nuklearnih objektov vključno z majhnimi nuklearkami, ki bi bile opremljene s tako imenovanimi majhnimi modularnimi reaktorji (Small Modular Reactors – SMRs). Primerne lokacije za gradnjo tovrstnih objektov v optimalnih globinah in trdnem hribinskem okolju imajo veliko prednosti pred nuklearnimi objekti na površini, saj zagotavljajo naravni sistem zadrževalnikov in neprimerno višjo varnost tovrstnih občutljivih objektov ter realno možnost namestitve majhnih modularnih reaktorjev (SMRs). Navedene prednosti so v času gradnje, obratovanja in zaprtja predvsem v smislu varnega izvajanja del v različnih naravnih okoljih, ki so izpostavljena različnim spremljajočim tveganjem ob pozitivnem vplivu na trajnostni razvoj širših območij. Glede na zadnje zahteve pristojnih institucij, ki spremljajo varnost obratovanja nuklearnih objektov, je treba posebno pozornost posvetiti raziskavam tveganj, ki so povezana s seizmičnimi vplivi na kompleksen sistem podzemnih nuklearnih objektov. V tem prispevku so podane možnosti in prednosti, ki jih daje podzemni prostor sedanjim tehnologijam na področju gradnje majhnih podzemnih nukleark, ter ocene stabilnosti objektov glede izpostavljenosti različnim seizmičnim obremenitvam.

Ključne besede: podzemni prostor, podzemna nuklearka, naravni zadrževalnik, seizmična obtežba, pomiki hribine

Introduction

The use of underground space for various needs in recent years is also reflected in an increased need of looking at construction of small nuclear power stations underground. The reason is partly related to the events which struck us all causing the tragically accident in certain areas and populations as terrorism showed a new face and partly the devastating consequences of natural catastrophes. To mention only two such incidents, one is of course the attacks in USA on September 11, 2001 when terrorists attacked hit the World Trade Center and other symbolic buildings and the other one is the earthquake that surfaced in the area of Fukushima (March 11, 2011) severely damaging a nuclear power last year. In addition to these incidents terrorist threats take place every day around the world and catastrophic weather events cause incomparable damage and heavy human casualties. In that constellation in the future we can expect an increased need for energy, complying and coinciding with an increase number of people living on the Blue Planet. What will be the correlation relationship is difficult to predict today, hopefully it will not be linear. In the 70's it was experienced that safe and secure solutions to build underground nuclear power plants were too expensive to pay off the investment at that time. Today cost estimates per unite single and four installations,

using drill and blast produce around 90 \$ million to 45 \$ per reactor, but for TBM solution the cost is around 25 \$ to 15 \$ million per reactor^[1]. The construction of multiple reactors in single locations is possible in high quality rock environment, self-supporting, with low seismic motion. That technical solution reduces capital cost with using new technologies and techniques for underground construction and reduces life cycle costs and new concept for waste management. A rough estimate of the cost of construction and operation shown expected goal that underground nuclear park concept with 1 000 MW has about 60 years lifetime, with 10 % saving (Figure 1).

Experiences with the underground space use for nuclear activities

In the past there have been several projects that address technical solutions to the implementation of underground nuclear power plants. As already mentioned, in the 70's the technological and cost barriers were show stoppers for carrying out such projects on a large scale. Practically all the nuclear power plants were built on ground surface with deep cuts and excavations to cope with the technological requirements that were applicable to the construction of nuclear power facilities at that time. In the last three decades there were

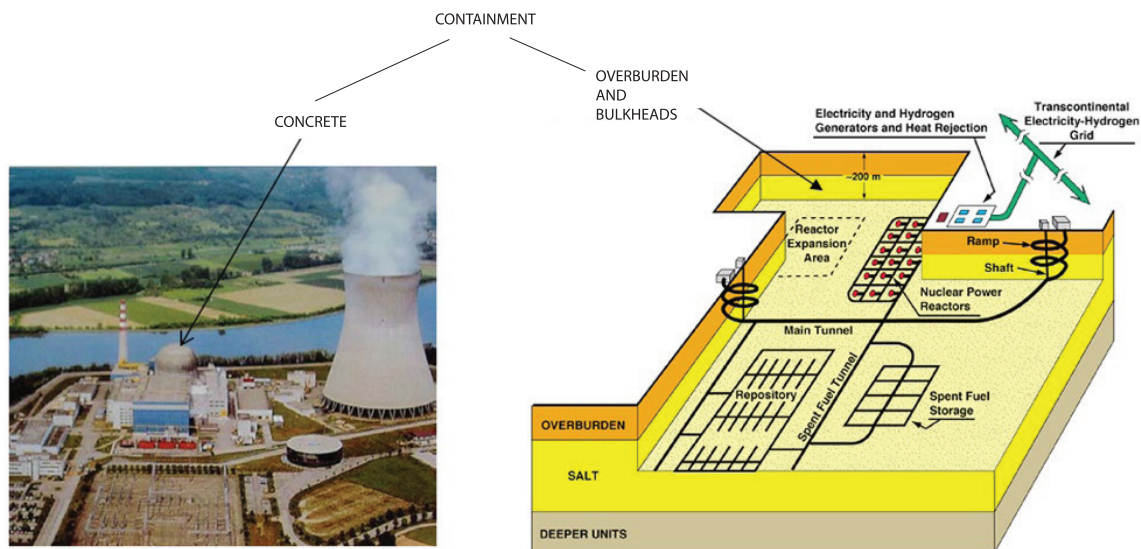


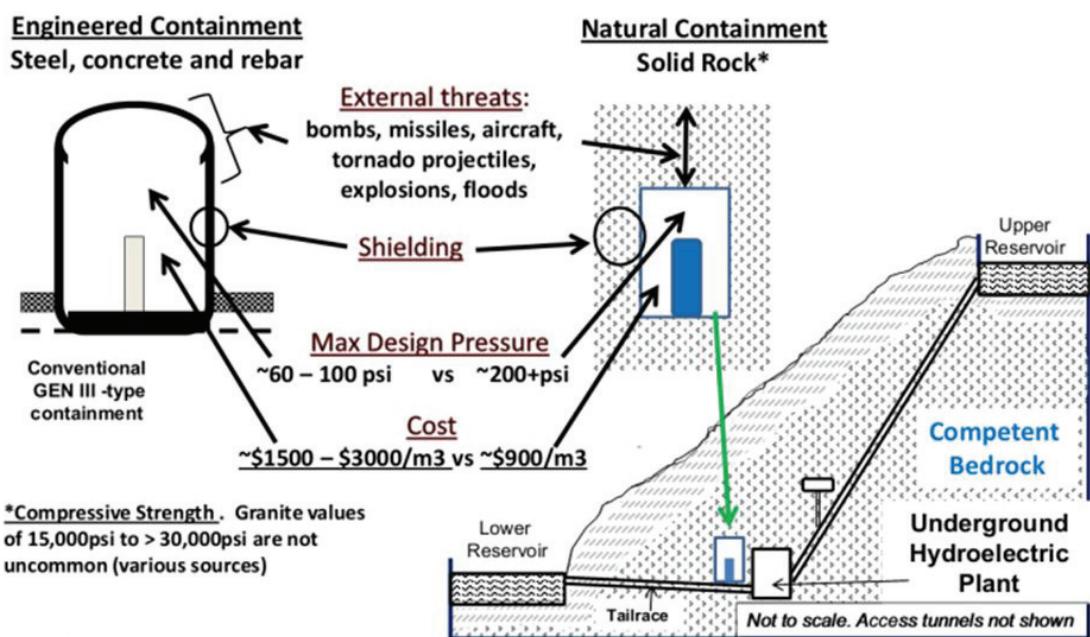
Figure 1: Elimination of need conventional containment structure^[1].

several feasibility studies of underground nuclear power stations undertaken in Canada, USA, Japan, Switzerland and elsewhere. Most of the studies showed positive results in favor of construction of such facilities. It was found that the underground nuclear power plants have many advantages over those that are built on the surface. Specifically highlighted were the aspects of safety and protection against external influences and catastrophic events such as earthquakes, military activities and terrorism and sabotage. The studies prepared in the 70's concluded that there would be an almost certain schedule and cost increase caused by the construction of the underground nuclear facilities and possible cost increase during the operation of the power plants. Underground hydroelectric power plants provides potentially opportunities to exploit the advantages and experiences offered by underground citing in hard rock environment as regards the safety of underground construction and operation of nuclear power plants. Therefore, in the following we will dedicate the paper to aspects of utilizing the capabilities of the rock mass to host underground sittings of nuclear power facilities and the many advantages that accompanies the kind of usage.

Worldwide there are already a number of existing underground structures of various kinds and valuable experience has been gained from the construction and operation of underground hydroelectric power plants. Not so far ago it was shown that it is often a limiting factor in the construction of underground facilities for different purposes due to geological risk because of adverse rock conditions that could potentially cause significantly higher cost of construction. This has a strong influence on final costs of such underground facilities. In the goal to avoid such difficulties in proper time, there is still a need of high quality knowledge of mechanical, thermal, hydrological and geochemical properties of ground.

In the field of underground space applied widely for the development of underground hydro power plant, the experience from Norway is likely one of the best in the world. In explanation the hydropower plant Sima is situated 700 m inside a valley side at Simadalen. It has a static head of water of 1 158 m and is the second largest power station in Norway.

Figure 2 shows the schematic possibility of establishing nuclear facilities combined with hydroelectric power plants.



Conclusion: SMR containment chambers in suitable bedrock at adequate depth could provide increased margins of safety for DBA/Ts, reduced consequences for Beyond-DBA/Ts, and reduced financial risk for future changes to the DBT—all at lower cost.

Figure 2: Potential location of SMRs containment chamber^(1, 2).

Earthquake sensitivity

Underground facilities are an integral part of the infrastructure of modern societies and are used for a wide range of applications, including subways and railways, highways, material storage, and sewage and water transport. A future need exists to look closer at the possibility of developing underground solutions for nuclear facilities also. When the surface area is subject to and also sensitive to earthquake activity and loading, underground utilization should be analyzed on seismic and static loading. Although in the past it has been documented that the underground structures are significantly less prone to seismic risk than those on the surface. The results of professional research works and their conclusions are accessible and confirm the above statement. The currently available risk assessment methods allow analyzing the magnitude of risk for different input parameters of seismic loads in different ground environment. A few authors, like Dowding & Rozen^[3], also proposed a correlation between tunnel damage and peak ground acceleration (PGA) calculated at the free surface immediately above the tunnel through an attenuation law. They suggest that “minor damage” is expected when the value of PGA ranges between 0.19 g and 0.50 g. The corresponding thresholds for peak particle velocity (PGV) range approximately between 20 cm/s and 90 cm/s.

Design analyses of underground structures

Assessing the seismic response of an underground structure is a challenge which is significantly different from that of a corresponding above-ground facility since the overall mass of the structure is usually small compared with the mass of the surrounding soil and the overall confinement acts as a strong damper of the seismic excitation. The development of appropriate ground motion parameters, including peak accelerations and velocities, target response spectra, and ground motion time histories, is briefly described by Hashash^[4].

Based on previous statements the “minor damage” is expected when the value of PGA ranges between 0.19 g and 0.5 g and corresponding thresholds for PGV range approximately between 20 cm/s and 90 cm/s, also Power^[5] proposed a damage classification based on PGA. For ground shaking less than about 0.2 g very little damage occurred in tunnels; in the range of about 0.2 g to 0.5 g, some cases of damage were reported, ranging from slight to heavy (serious damage only occurred in an unlined tunnel and in a tunnel with timber or masonry linings); for PGA exceeding 0.5 g there were a number of instances of slight to heavy damage (serious damage occurred only in a tunnel with unreinforced concrete lining).

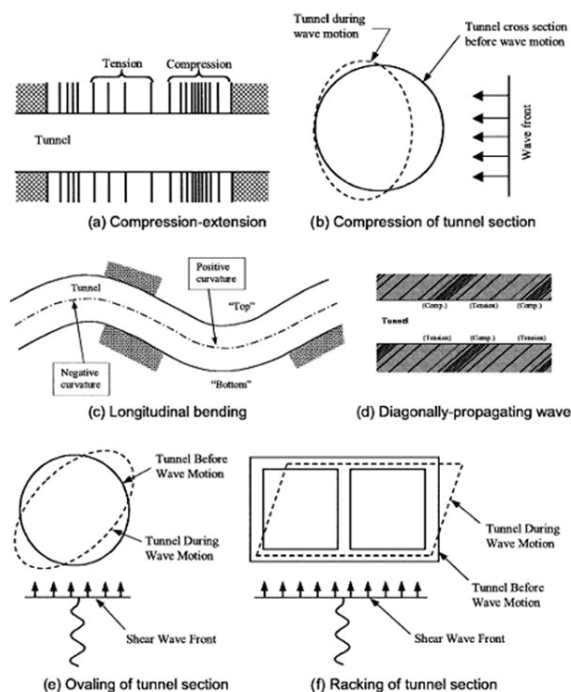


Figure 3: Modes of the tunnels deformation due to seismic waves, (After Owen and Scholl, 1981 cited in Hashash^[4]).

Analysis of seismic loading on underground caverns sited in rock mass

The Phase2 – finite element modeling computer program Rocscience^[6] has a module which allows analysis of seismic loading on underground structures. It is based on pseudo-static

approach, where the additional seismic force is calculated as a product of the specified seismic coefficient, a dimensionless vector and the amplitude of the body force, which is the self-weight of a finite element. In absence of more accurate site-specific depth reduction factor models, the guideline in Hashash et al.^[4] as shown in Table 1 can be used.

Table 1: Ratios of ground motion at depth to motion at ground surface. (After Power et al.1996, cited in Hashash^[4])

Tunnel depth [m]	Ratio of ground motion at tunnel depth to ratio of surface ground motion
≤ 6	1.0
6–15	0.9
15–30	0.8
≥ 30	0.7

For instance, a seismic coefficient of 0.30 used in a model in Phase2, which is the seismic coefficient at tunnel depth of 100 m, corresponds to a seismic coefficient of $0.30/0.70 \approx 0.43$ at ground surface.

A number of numerical analysis on case studies was carried out to investigate the effect of vertical seismic coefficient which is using the pseudo-static seismic loading procedure in Phase2. In the present model a total of five seismic loading scenarios including one case without seismic loading were analyzed. The model which has been applied in the numerical simulation consists of two rock caverns at a depth of 100 m below surface, one big and the other smaller.

The dimensions for the large cavern are: $W_B = 22$ m, $H_B = 46$ m and smaller one has the following dimensions: $W_s = 13$ m and $H_s = 17$ m. The length of each cavern is 170 m. The rock mass quality is proposed by Mohr-Coulomb constitutive model with geotechnical and mechanical parameters which is presented in Table 2. The different cases of seismic loading were included in the model in the third and latest stage when both caverns were stabilized with 10 m long cable bolts with capacity 0.6 MN and 10 cm thick FRS (Fibre Reinforced Shotcrete), as shown in Figure 4a. Results of parametrical investigations used Phase2 code had clear goal to explain what amount of stress-strain changes can be expected related to seismic loading in different directions (Figure 5).

The general assessment was considered being very optimistic because obtained results which are shown on the next figures arrive at the conclusions which were proved in the previous investigations. The model was developed for two underground caverns sited in quite stable rock mass and with a virtually horizontal fault zone of 12 m in thickness. This is located in the central part of the third height of the bigger cavern. This virtual and rather simplified geological base case also has demonstrated the influence of weakness zone on the stability of both the bigger and smaller cavern.

The dimensions of these caverns are in practice quite similar to what can be expected in the future as far as size wise is concerned for underground structures of underground hydro

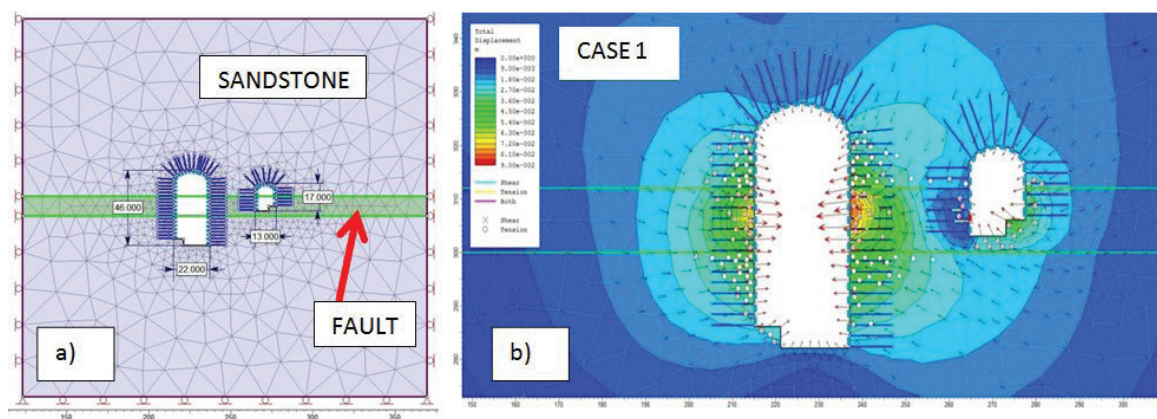


Figure 4: a) Vertical cross section through caverns with dimensions and support elements, b) CASE 1 - maximal calculated displacement without seismic loading.

power plants and future SMRs incorporated in small underground nuclear power plants.

In Figure 5 the changes of maximum displacements are presented for four cases in which different combinations of horizontal and vertical seismic coefficients are included in the FEM numerical analysis. The significant differences in the calculated results have been caused by the adequate responses of rock mass – support system. One of the main consequences of increasing the main stress values is the vertical seismic coefficients K_v , which is directed downward in the same direction as Earth's gravity (CASE 4 and CASE 5). In Figure 4 where the contour plots of the total displacements for the four loading cases are described it can be concluded that the distribution of the total calculated displacement around the caverns periphery generally resembles an ellipse.

The maximum stresses appear along the horizontal axis of the ellipse. At the same time the direction of the horizontal component of the primary stress is bigger than the vertical component and influencing on the stress compensating. This means, if an anisotropic primary stress field exists, the influence of seismic loading in horizontal direction does not have a decisive influence on general stability on the analyzed caverns. Altering the direction of the vertical seismic coefficient does not result in any drastic change in the location of the long-axis of the ellipse. The magnitude of the stresses around the tunnel is greater when the direction of the vertical seismic coefficient is downward (negative), in the same direction as the gravitational force.

Since the CASE 2 is where $K_h = 0.30$ and the vertical seismic coefficient was ignored, the CASE 2 and CASE 3 are compared with CASE 1, but last two cases (4, 5) have distinguished differences compared to first three load cases, which come from the effect of the vertical seismic coefficient.

From the diagrams in Figure 6 it can be concluded that the effect of vertical seismic coefficient is significant in Cases 4 and 5. The similar can be found in these two cases, when a comparison is done on stress fields where main stresses increased.

Table 2: Some important input parameters for FEM analysis

Field stress: gravity	
Using actual ground surface	
Total stress ratio (horizontal/vertical in-plane): 1.5	
Total stress ratio (horizontal/vertical out-of-plane): 1.5	
1. Material: sandstone	
Unit weight	0.027 MN/m ³
Young's modulus	4 500 MPa
Poisson's ratio	0.25
Peak tensile strength	0 MPa
Residual tensile strength	0 MPa
Peak friction angle	45 degrees
Peak cohesion	0.8 MPa
Residual Friction Angle	25 degrees
Residual Cohesion	0.1 MPa
Unit weight of overburden	0.027 MN/m ³
2. Material: fault	
Unit weight	0.027 MN/m ³
Young's modulus	3 000 MPa
Poisson's ratio	0.3
Peak friction angle	35 degrees
Peak cohesion	0.2 MPa
Residual Friction Angle	25 degrees
Residual Cohesion	0.1 MPa
Liner: shotcrete	
Liner Type	Standard
Beam Formulation	Timoshenko
Thickness	0.1 m
Young's modulus	15 000 MPa
Poisson's ratio	0.25
Strength Parameters	
Peak compressive strength	40 MPa
Residual compressive strength	20 MPa
Peak tensile strength	8 MPa
Residual tensile strength	1 MPa
Bolt Properties	
Bolt Type	Fully bonded bolt
Diameter	30 mm
Young's modulus	200 000 MPa
Tensile capacity	0.6 MN
Residual Tensile capacity	0.6 MN
Pre-tensioning	0 MN
Out-of-plane spacing	2 m
Allow Joints to Shear Bolt	Yes

In the analyzed point B in the large cavern it was further identified small damages on the primary shotcrete lining of the smaller cavern. The calculated total displacement in the analyzed points showed similar conclusions, except that

the reductions of displacements due to point A where the compensation between secondary stresses and stresses in the system caused by seismic loads are present.

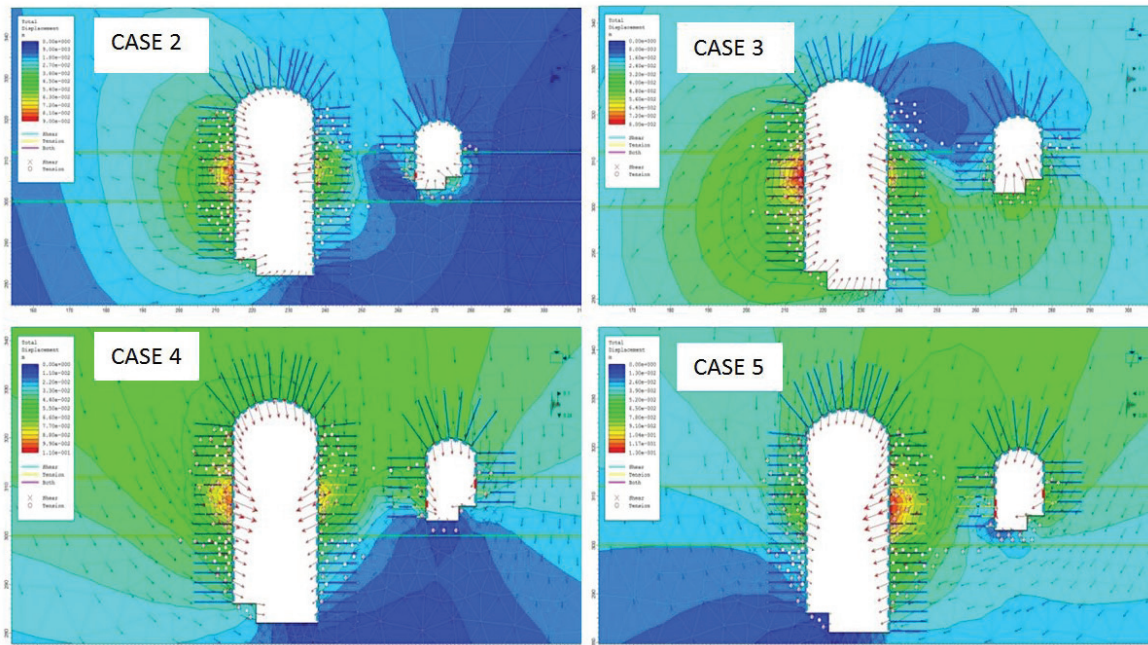
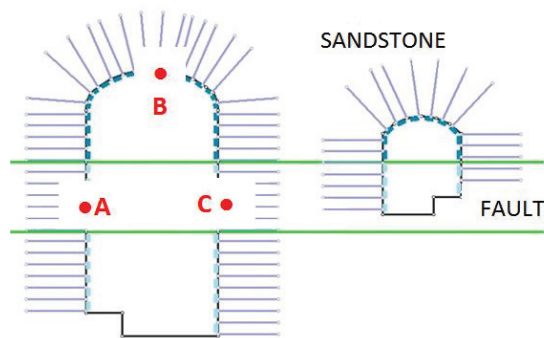


Figure 5: Maximum calculated displacement versus different seismic coefficients combination and their directions for four CASES (2 to 5).



Case number	Seismic coefficient
1.	$K_h = 0.0, K_v = 0.0$
2.	$K_h = 0.30, K_v = 0.0$
3.	$K_h = 0.30, K_v = 0.24$
4.	$K_h = 0.30, K_v = -0.24$
5.	$K_h = -0.30, K_v = -0.24$

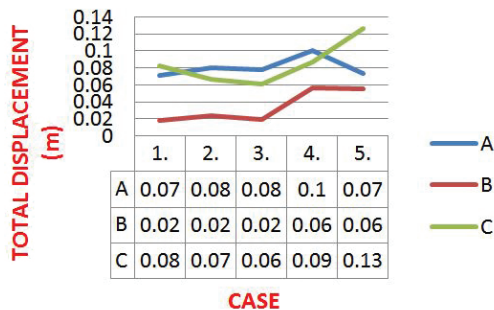
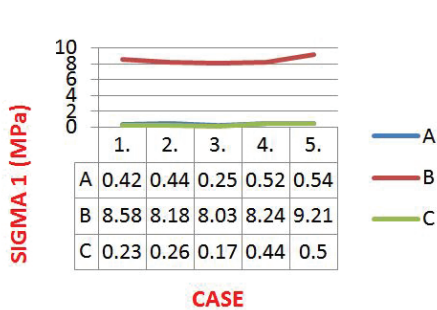


Figure 6: Combination of seismic coefficients and three analyzed points A, B, C.

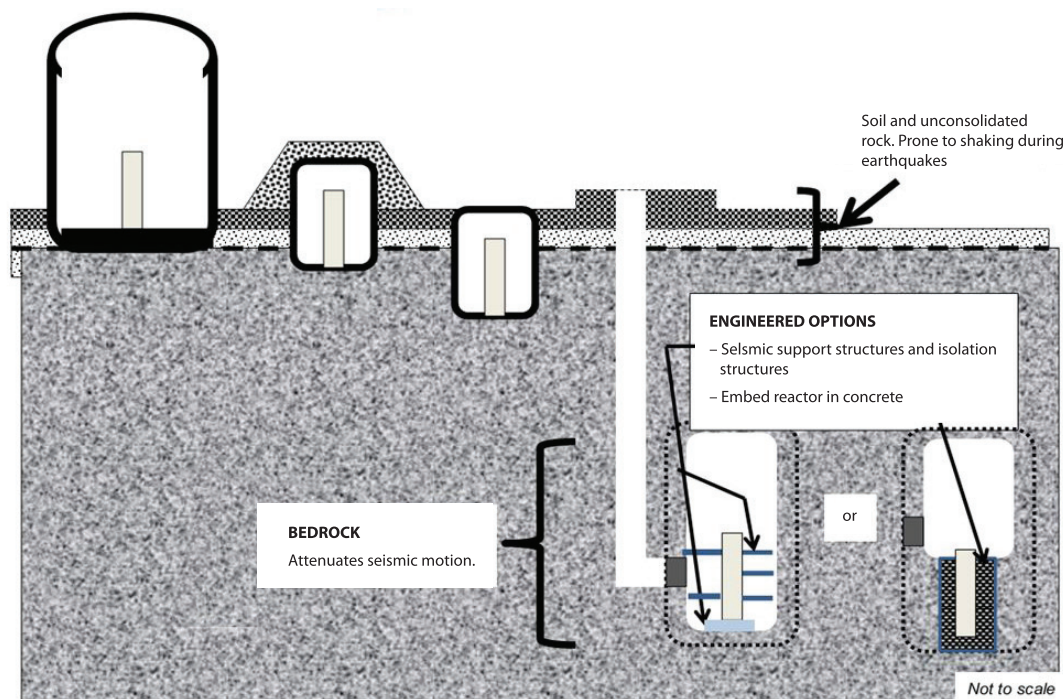
Conclusion from the above findings shows that a vertical seismic coefficient $K_v = 0.5 k_h$ is always applied in downward (negative) direction for all parametric analysis using pseudo-static seismic loading on underground structures. If for example use $K_h = 0.30$, representing a horizontal PGA at tunnel depth of 0.30 g, the $K_v = 0.50/0.30 = 0.15$. Assuming 0.70 as the reduction factor from surface to 100 m depth, surface PGA is ca. $0.30/0.7 = 0.43$ g.

Natural containment

Today many options for designing nuclear power plants are available with the use of underground cavern and tunnel construction. It is evident that in any chosen design for such underground construction, cost savings can be materialized following the reduction of manmade containment structures typically required for an aboveground nuclear power plant. Thus are relying on the natural containment by the rock mass and the ground water. Reactor containment structures for current power plant designs are typically built in one of two ways. One option for a containment structure

is a pre-stressed reinforced concrete shell with an interior steel liner which serves primarily as an impermeable membrane. A second option is a high integrity steel vessel that serves for containment with an independent concrete building around the vessel for shielding purposes^[7]. Containment structures are typically designed to with-stand an interior pressure of four to five bars above atmospheric pressure.

Containment of an underground reactor could be significantly simplified compared to both surface and above ground solutions. Using the underground method of construction, no strong concrete structures are needed because the host rock surrounding a reactor serves the dual roles of shielding and providing the structural integrity of a containment structure as a natural barrier. In this basis of proposed technical solution, a containment structure for an underground nuclear reactor could consist of simply a thin steel liner supported by the host rock^[1]. The steel liner would serve as an impermeable membrane between the reactor and the rock. This approach would eliminate the significant costs associated with construction of high-integrity steel structures which are needed in the above ground cases.



Result: greater safety and lower cost to protect against earthquakes.

Figure 7: Improved earthquake resistance^[1].

Geometrical bases of underground nuclear power plant (unpp)

In the present case all excavation are proposed with use drill and blast. Table 3 gives a preliminary cost estimate. The starting point for the concept shown in Figure 8 is with the dimensions and excavation cost for the shafts and tunnels and chambers for the reactor and turbine-generators for a 1 000 MW PWR in an underground nuclear park in granite^[8]. This was done to arrive at a conservative preliminary estimate of excavation cost.

The main shaft is 24 m in diameter. It is excavated first to provide personnel and equipment access for all subsequent excavation operations.

After construction, the reactor pressure vessel, turbine-generators and other equipment

would be transported down the main shaft to the main cavern. A secondary shaft, 12 m diameter, is constructed at the end of the main cavern opposite the main shaft and used for safety, ventilation and additional personnel and equipment access. The main cavern is 15 m wide × 15 m high × 120 m long, giving it a volume (27 000 m³) approximately one-third the volume of the main cavern (77 000 m³) for a 1 000 MW PWR reactor^[8]. This is considered reasonable because the steam generator for the PWR is a large separate component, but for the reference SMR it is smaller and inside the pressure vessel. In addition, the turbine-generator chamber portion of the main cavern is 15 m high × 15 m wide × 40 m long.

This represents a reduction in height by about two-thirds and reduction in length by about one-half, the logic being less chamber space

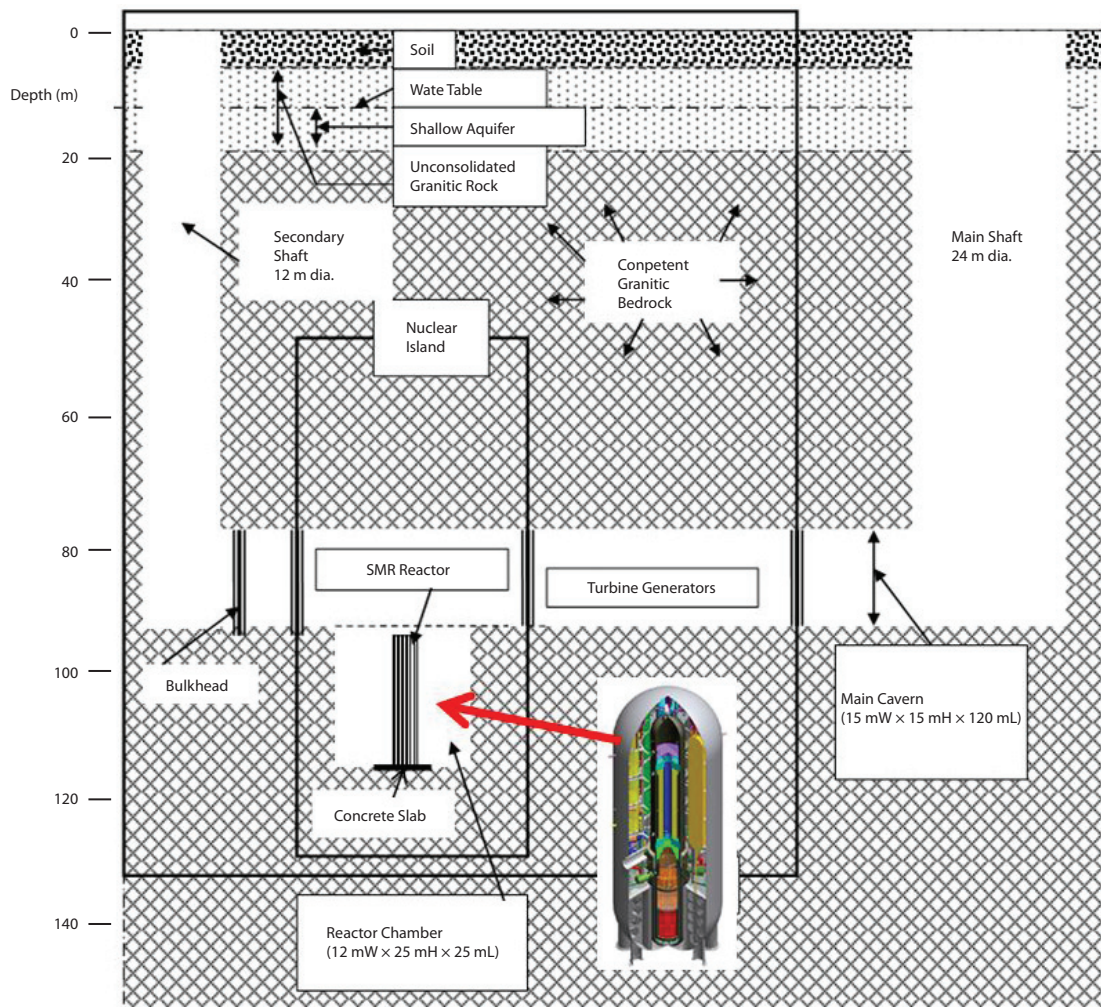


Figure 8: Geometrical base for underground nuclear power plant – SINGLE UNIT, (C.W. Myers and J. M. Mahar, adapted Likar^[9]).

for turbine-generators should be needed for a 100–300 MW SMR, for example, than for a 1 000 MW PWR. The reactor chamber is 12 m wide × 25 m high × 25 m long, and lined with nominal concrete and steel or filled with concrete (not shown) to bring the SMR in intimate contact with the host rock depending on the seismic design requirements. The 25 m length of the reactor chamber, combined with having its long axis parallel to the long axis of the main cavern, provides space to rotate the SMR pressure vessel from its horizontal position during transport through the main cavern to its final vertical position in the reactor chamber. Once in position, the SMR would have an annular space for inspection, maintenance and other uses of 10 m on either side of the pressure vessel, parallel to the long axis of the main cavern. Underground openings for a condenser and spent fuel storage pool are not shown on Figure 8, but to be conservative their excavation costs are included on Table 3. Also, cooling towers are not shown but it can recognize that they might be needed for water-cooled SMRs. The elevation difference between the ground surface and underground condenser will be an important topic relating to cost and engineering consideration. Under the definition the nuclear island encloses safety-class structures, systems and components: the reactor pressure vessel, reactor chamber, bulkheads sealing entrances to the reactor chamber, and the natural (host rock) containment structure.

In the case of bedrock SMR, the nuclear island would include those portions of the host rock surrounding the reactor chamber for which

containment credit is taken. The nuclear island is shown schematically in Figure 8 with lateral boundaries passing through the two bulkheads nearest the reactor chamber. The nuclear island has a lower boundary at 130 m depth, and upper boundary at 50 m depth. Penetrations into the host rock containment structure should be controlled, the same as with a surface containment structure. The nuclear island is shown as a rectangle but in reality its shape would be dependent on site-specific geological, hydrological, and rock mass conditions, and would therefore be expected to have a more irregular shape. Four leak-tight bulkheads are shown.

Two isolate the turbine-generator chamber from the main shaft and from the reactor chamber and two others isolate the 12 m shaft from the reactor chamber. The two bulkheads adjacent to the reactor chamber must provide containment in the event of a reactor accident and are therefore safety class. On Figure 8, the rectangular outline shown as the unit cell encloses the chambers, tunnel, and shaft needed to operate a single underground SMR. Usage of the term follows Giraud^[10] and is analogous to use of unit cell in crystallography, which refers to the way a crystal structure is created by repeating a pattern of atoms. A multiple reactor installation based on the unit cell in Figure 8 can be thought of as created similarly by repeating the unit cell pattern of the underground workings. Note that the unit cell shown in Figure 8 does not include the main shaft but it does include the 12 m diameter shaft. The primary purpose of the main shaft is to provide subsurface access during excavation and for transport of the

Table 3: Preliminary Excavation Cost Estimates

Shafts	Nominal Dimensions (m)	Volume (m ³)	Cost million €
Main Shaft	24 m (dia), 90 m (deep)	/	47.3
Secondary Shaft	12 m (dia), 90 m (deep)	/	15.7
SUB TOTAL			63.0
Main Cavern	$W = 15 \text{ m}, H = 15 \text{ m}, L = 120 \text{ m}$	27 000	2.2
Reactor, Chamber	$W = 12 \text{ m}, H = 25 \text{ m}, L = 25 \text{ m}$	7 500	5.4
Condenser	22 m × 27 m × 30 m	17 800	1.1
Spent Fuel Pool	13.7 m × 24 m × 43 m	14 200	0.9
SUB TOTAL			9.6
TOTAL			72.6

Excavation cost of main shaft, secondary shaft, condenser, and spent fuel pool are from (Mahar et al. 2007, adapted Likar⁽⁹⁾). Unit cost of main cavern excavation is 81.5 €/m³. Unit cost of reactor chamber excavation is 720 €/m³.

reactor pressure vessel and other large equipment. After construction it would be available for other purposes including construction of subsequent SMR installations. In the case of horizontal opening with tunnel or similar horizontal connection, the shaft construction is not necessary.

Single-unit installation-drill and blast - construction procedure

As shown in Table 3, the cost per-reactor for single-unit bedrock SMR installation is approximately € 72.0 million, the price of the main shaft is approximately € 47.3 million, is by far the largest cost component. The 12 m shaft is € 15.7 million and all other excavations total only € 9.0 million. This estimates include ground support and internals in the shafts needed during excavation, but not cost to grout the bedrock if needed, construct the bulkheads, or any of the internals (platforms or stairways, for example) within the reactor chamber (Figure 9).

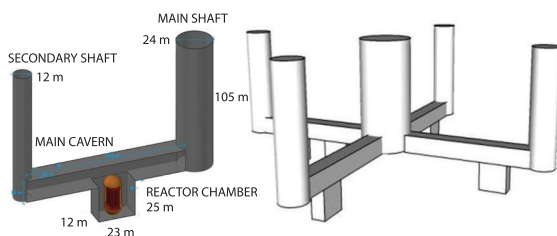


Figure 9: Single and four unit installation, (Giraud^[10], adapted Likar^[9]).

Four-unit installation-drill and blast - construction procedure

The concept for the four-unit installation is to build in series four of the unit cells shown in Figure 9 at the same depth, and have them positioned orthogonally around the main shaft. This allows the € 47.2 million cost of the main shaft to be shared among four SMRs. By doing this the per-reactor cost drops to € 35.4 million for the fourth reactor. It should be possible for the first reactor to be in operation while excavation is underway for the second, and similarly for subsequent reactors. Following the logic described for the staggered build of IRIS reactors, this approach also has the potential to reduce the capital at risk and cash outflow relative to conventional large, light water reactor construction.

Twelve-unit installation - tunnel boring machine construction

The first concept for a twelve-unit facility would be to adapt for bedrock SMRs siting the approach described by Giraud^[10], based on earlier work by Mahar et al.^[11], which uses tunnel boring machine (TBM) technology to construct an underground nuclear park with twelve, scale 1 000 MW, PWR reactors.



Figure 10: Twelve unit installation^[10].

The underground facility has a total length 2 400 m, square-shaped footprint, with three power plants in each of its 600 m long sides. The total excavation cost of the TBM tunnel, secondary access tunnels and all shafts is estimated at € 236 million^[10], or € 19.7 million per reactor location.

Although not in individually excavated chambers, as with the single- and four-unit concepts described above, each reactor and its turbine generator is isolated from all others by airlock/bulkheads, reducing inter-reactor accident and investment risk. A second concept for a twelve-unit facility would be to site multiple SMR reactors together in a common chamber(s). Assuming TBM excavation technology is used as described in the preceding paragraph, and assuming because of more efficient use of space the twelve SMRs could be sited in a facility with an excavated length one-half as long, i.e., 1 200 m long, and assuming the excavation would cost $\approx 60\%$ as much, then the total excavation cost would be € 141.7 million and the per-reactor cost about € 11.8 million. From Figure 11 can see the individual unit cells are located around the perimeter, while access tunnels are located at the upper right and lower left.

Cost advantages for underground nuclear power parks

In addition to nuclear catastrophe in Fukushima today are the enormous investment costs associated with the construction of nuclear power plants has traditionally been the greatest economic limiting factor for the expansion of nuclear power. Nuclear power plants that are planned to be built in the United States have had a wide variety of projected construction costs. Progress Energy recently contracted with Westinghouse to build two AP1000 reactors in Florida at a total cost of € 6.0 billion. With the need for substantial additional transmission infrastructure, plus financing and other fees, Progress expects the entire project to cost approximately € 11.0 billion (U.S. Congress, 1989). This amounts to between 2 755 €/kW and 4 959 €/kW of installed capacity, depending on the elements covered in the costs. Other nuclear power plants applying for combined construction and operating licenses are estimating construction costs as low as 1 967 €/kW (U.S. Congress, 1989). Such wide variation in cost

estimates is in part the result of recent substantial variations in material costs of concrete, steel, and copper. Because of the high capital costs associated with nuclear power plants, it is reasonable for those in the nuclear industry to be skeptical of a plan to complicate the construction process in any way, such as by placing plants underground.

However, it is likely that underground construction could actually be an overall economically advantageous endeavor for power plant owners. Building nuclear power plants underground can bring cost savings for construction in a variety of ways. Various options for the construction of power plants underground can be considered. One of them is cost savings which can be realized in the construction of containment structures. In addition, savings could be realized by reducing the overall volume of the reactor components due to enhanced emergency core cooling capability. Another advantage of underground reactors in rock is that they face far less seismic vulnerability and therefore need not be built with as strict seismic isolation requirements as surface plants. All of these

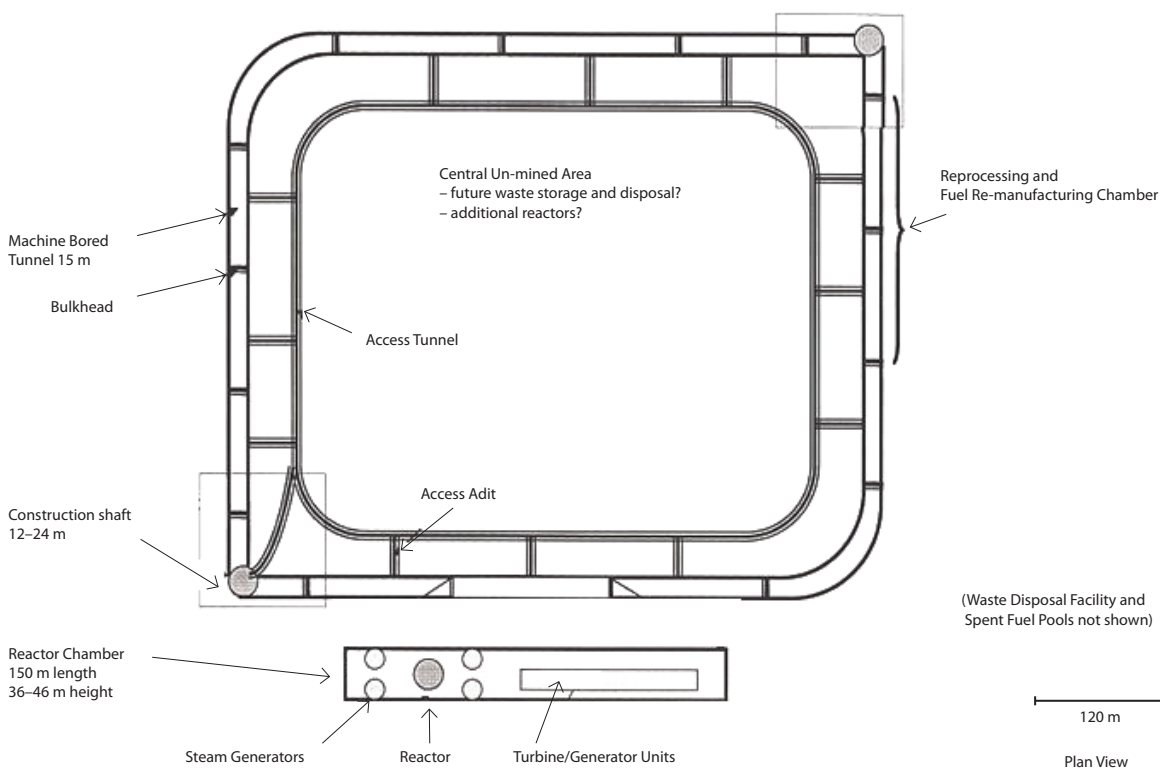


Figure 11: A simplified schematic of an underground nuclear power park^[10].

factors combine to potentially reduce construction costs significantly. Construction cost savings for underground nuclear power plants are highly dependent on the ingenuity involved in designing the plant, enhanced Emergency Core Cooling Capability. This is because the large compartment for storing emergency cooling water within the containment above conventional reactors would not be necessary, as more than adequate water storage would be available above ground should emergency core cooling be needed. From this point of view nuclear power plant building close to existing hydro plant has many advantages, because cooling water is available in big amounts.

Construction of reactors underground allows for a variety of options in placing the various components of the nuclear power plant. The tunneling technology has long existed to excavate a large enough volume of underground space to place reactors as they are currently designed. For example, the AP 1 000 containment building is a cylinder with a height of 83 m and a diameter of 40 m. The ABWR containment building has a height of 30 m and a diameter of 30 m. These recent designs, involving large heights for the containment structures, are the result of the efforts to incorporate passive emergency core cooling capabilities into the designs, using gravity feed for the emergency core water. Such considerations pale in significance when reactors are placed underground because the emergency core cooling water can be placed at the ground surface. Thus, gravity driven water pressure can be provided from water reservoir on the surface which existed for hydro power plant that would be 10 bar or more (for depths of 100 m or more). Such emergency core cooling capacities (virtually unlimited) and large pressure heads warrant complete reconsideration of emergency core cooling passive designs. Thus, while it is possible to excavate a volume of rock comparable to the space for current containment buildings, the abundance of host rock and the greatly enhanced passive core cooling capability offer a number of innovative ways of placing the major components of a nuclear steam supply system. For example, PWRs constructed underground would not need to have the steam generators and the pressure vessel all in the same compart-

ment. By separating components of the system in adjacent compartments a more efficient use of the underground space can be achieved.

Conclusions

Underground structures suffer appreciably less damage than surface structures in situations when subject to earthquake loading. Reported damage decreases with increasing overburden or depth of location. Deep tunnels are safer and less vulnerable to earthquake loading than shallow underground structures.

Most of the damage locations coincide with reactivating existing faults and fracture zones, but these can be identified before and/or during construction whilst conducting adequate investigations. Severe damage and collapse of tunnels from shaking occur only under extreme conditions. Usually damage due to shaking is rare in underground facilities. Where such damage has occurred, the rock is either very poor or subject to very high stresses and the lining has bad quality (i.e. brick or unreinforced liners).

Earthquake experience shows that most damage occurs to the tunnel liner, and such damage is well correlated with its quality of construction. Support measures holding a sufficient ductility would absorb the vibrations from an earthquake and maintain its supportive function despite surface damage such as cracking. No damage or minor damage can be expected in rock tunnels for peak ground acceleration at the ground surface less than about 0.2–0.4 g, depending on type of lining and rock mass conditions.

Existing underground hydropower plants being located in favorable quality rock mass would also constitute suitable bedrock for a SMR sitting in the goal to produce high capacity of electricity at the lowest possible. That possibility is still open to start with activities very soon. In addition such test and demonstration facilities for prototype SMRs should be done to start within the regions without risk of damage from military attack or earthquakes.

Where bedrock conditions would be adequate for sitting SMRs, the solution with underground nuclear power plant is economic and environ-

mental friendly. The main advantage is in using existing transmission grid and transportation infrastructure. Whilst certain benefits related to investigations is present from the results of original hydropower plant and existing workforce expertise in power generation and distribution.

In the safety domain high margins of safety and physical protection against accidents and external threats are achieved by underground citing. Integration of nuclear and hydropower plants has potential benefit in the environmental restoration process.

References

- [1] Myers, C. W. (2011): *Utility of Installing Small Modular Reactors at Underground Hydropower Plants*, Presentation at 1st Annual ANS SMR 2011 Conference October 30 – November 3, 2011, Washington, DC, pp. 18.
- [2] Broch, E. (2006): *Use of rock caverns in urban areas in Norway*, International Tunneling Association [online]. Available on: <<http://www.ita-aites.org/cms/fileadmin/filemounts/general/pdf/ItaAssociation/Organisation/Members/MemberNatons/Egypt/PapersSharm2006/kn05.pdf>>.
- [3] Dowding, C. & Rozen, A. (1978): *Damage of rock tunnel from earthquake shaking*, Journal of Geotechnical Engineering ASCE, Vol. 104: 175–191.
- [4] Hashash, Y. M. A., Hook, J. J., Schmidt, B., Yao, J. I.-C. (2001): *Seismic design and analysis of underground structures*. Tunnelling and Underground Space Technology, 16, 4, pp. 247–293.
- [5] Power M. S., Rosidi D., Kaneshiro J. Y. (1998): *Seismic Vulnerability of Tunnels and Underground Structures Revisited*. 1998. Proc. of North American Tunnelling '98. Newport Beach, CA: Balkema, Rotterdam, The Netherlands, p. 243–250.
- [6] Rocscience, Inc. (2012): *Phase2 – finite element analysis for excavations and slopes* [online]. Available on: <<http://www.rocscience.com>>.
- [7] Rahn, F. J., Adamantiades, A. G., Kenton, J. E. and Braun, C. (1984): *A Guide to Nuclear Power Technology: A Re-source for Decision Making*. John Wiley and Sons, New York.
- [8] Mahar, J. M., Kunze, J. F., Myers, C. W. (2008): *Underground Nuclear Power Parks – Power Plant Design Implications*,|| ICONE 16-48889, Proceedings of the 16th International Conference on Nuclear Engineering, ICONE16, May 11–15, 2008, Orlando, Florida, USA.
- [9] Likar, J. Grov, E. (2012): *The possibility of joint operation hydro and nuclear power plants*, Research report in preparation.
- [10] Giraud, K. M. (2009): *Life Cycle Analysis of an Underground Nuclear Park*,|| M. S. Thesis, Department of Nuclear Engineering, Idaho State University, Pocatello, Idaho, USA.
- [11] Mahar, J. M., Kunze, J. F., Myers, C. W., Loveland, R. (2007): *Advantages of Co-Located Spent Fuel, Reprocessing, Repository and Underground Reactor Facilities*,|| American Nuclear Society, Advanced Nuclear Fuel Cycles and Systems, Boise, Idaho, September 9–13, 2007.

Analysis of risk assessment and law basis for construction of underground structures

Analiza ocene tveganja in pravni okvirji gradnje podzemnih objektov

Mario Mazurek^{1,*}, Peter Grilc², Jakob Likar³

¹Municipality Metlika, Naselje Borisa Kidriča 2, 8330 Metlika, Slovenia

²University of Ljubljana, Faculty of Law, Poljanski nasip 2, 1000 Ljubljana, Slovenia

³University of Ljubljana, Faculty of Natural Sciences and Engineering, Aškerčeva cesta 12, 1000 Ljubljana, Slovenia

*Corresponding author. E-mail: mario.mazurek@siol.net

Abstract

In the construction of underground structures are always present risks due to unexpected ground conditions, the most basic goal is to provide stability in the planning and construction phase. Due to influence of parameters, which are known as random variables, is expedient to develop risk analysis with probabilistic approach, which enable to research the reliability of groups of data from geotechnical investigations and safety against the failure. It is also important to have carefully determined contract relation and obligations between the client and the contractor. In this article there will be represented risk assessment for basic stability reliability of underground structure and general overview of valid legislation in the Republic of Slovenia for the field of structure construction, set of laws, international recommendations and guidelines and law harmonisation at construction of the underground structures and divisions of risk between the subscriber and the contractor.

Key words: underground structures, risk assessment, probability approach, reliability index, construction contract

Izvleček

Pri gradnji podzemnih objektov so vedno tveganja zaradi nepričakovanih hribinskih razmer, najosnovnejši cilj pa je zagotavljanje stabilnosti v fazi načrtovanja in gradnje. Zaradi vpliva parametrov, ki imajo lastnosti naključnih spremenljivk, je smotno izdelati analize tveganja z verjetnostnim načinom, kjer se lahko preveri zanesljivost skupine podatkov iz geotehničnih raziskav ter varnost pred porušitvijo. Pomembno je tudi, da je natančno določeno pogodbeno razmerje ter obveznosti med naročnikom in izvajalcem. V članku bo predstavljena ocena tveganja za osnovno stabilnostno zanesljivost podzemnega objekta in splošen pregled veljavne zakonodaje v Republiki Sloveniji za področje graditve objektov, zakonikov, mednarodnih priporočil in smernic ter pravno usklajevanje pri gradnji podzemnih objektov in delitvi tveganja med naročnikom in izvajalcem.

Ključne besede: podzemni objekti, ocena tveganja, verjetnostni način, indeks zanesljivosti, gradbena pogodba

Introduction

Construction of underground structures is, because of its specificities, placed at the most demanding constructions with present risks due to unexpected ground condition. In spite of most contemporary knowledges and advanced global technology, construction of underground structures is an inimitable process with present risks. Unexpected ground conditions can cause rock mass failure during excavation, invasions of ground water, changes within structure and firmness of the ground, excess deformation and the injury of people and property. It is always the first and basic goal to ensure the stability of the underground structure in the planning and construction phase, stability must be ensured directly during excavation. Ground stability reliability, load-bearing support elements or system ground-support against failure or excess deformations must be adequately verified, evaluated and analyzed. Professional approach also depends on the principle of responsibility, conscientiousness and morality of the clients in the construction, because some risks can be expected but absolutely all risks are can't be expected. Due to the increased level of risk, and a large number of influences, ground and material characteristics, which have by physical laws properties of random variables, it is adequately to create a risk analysis with a probability approach. The statistical methods and tools can check the reliability of the geotechnical surveys data and measurements, reliability and safety against failure of individual structure or the whole system in interaction ground-support. In the construction of underground structures are included a large number of participants from various professional disciplines, including design engineers, engineers of different disciplines, specialists in the field of geotechnical engineering and tunneling, geologists, economic analysts and financial advisors, negotiation experts, lawyers and environmental specialists, supervisors, site managers, government organizations and companies, inspection and advisory services. At all stages, there are a number of risks that need to be continuously assessed and managed. This means that all participants in the project could on a professional basis and

with sufficient information to timely respond and make the right decisions. Therefore, it is also important carefully regulated and defined contractual relationship and obligations between the subscriber and contractor and must be also provided appropriate interpersonal communication and coordination between all participants. Unprofessional conduct, inappropriate decisions, violations of the rights and duties can lead to disagreements, which can even lead to litigation on the courts and establishing legal liability. The first part of this article will present theory and method for assessing the risk of unreliable geotechnical parameters calculating the reliability index and probability against the failure during the planning phase, which is presented by summarizing of examples of several authors. The main advantage of the proposed method is that it is widely available, because all calculations can be performed in the Microsoft Excel program. In the second part of article are general overviews of the legislation in the Republic of Slovenia in the field of construction and construction of underground structures, codes, international recommendations and guidelines and legal harmonization. The significance of the law basis is important in the conclusion of construction contracts and negotiations, and further in the adoption and sharing of the risk between the subscriber and the contractor.

Risks at the construction of underground structures

Risk management means skill which represents making decisions with a certain degree of uncertainty. By the conclusion of the construction contract contractor undertake responsibility to achieve the final result which means to built the structure or other construction work, and he takes over the risk that this result will be finally achieved^[1]. Since the conclusion of the contract until its fulfillment passing a relatively long period in which it can occur a number of business risks. Therefore it is necessary to determine rules before the conclusion of the contract, about which client is involved to negative consequences of the realization of these risks^[1].

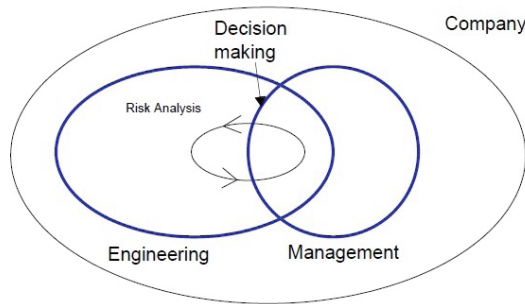


Figure 1: Risk analysis as a part of a risk management process in organization^[2].

Unforeseen events and underground structures stability

Correspondently with second paragraph of 653. part of OZ are (necessary) unforeseen works that which must be done urgently in order to ensure the stability of the structure or to prevent the damage, the main cause of that can be unexpected difficult nature of the ground, unexpected water or some other unexpected event. In the project documents unforeseen work are not provided because they are unpredictable emergency work. Correspondently with OZ contractor may carry out such works without previously acquired subscriber's consent if such works have to be carried out immediately.

Conventional deterministic assessment of the stability of underground structures includes the calculation of the factor of safety and other indicators of stability. Limit state determines calculated boundary of structure, which must never be exceeded. The resistance of the material and the corresponding strength is never possible to identify with completely certainty. Limit state of the structure is divided into:

- ultimate limit state – a partial or complete failure and instability of the structure,
- serviceability limit state – exceeded conditions of the structure applicability which are for example excessive displacements and damage vibration.

Risks management guidelines

Guidelines for the management of risks in the construction of tunnels and underground structures are prescribed by the International Tunnelling and Underground Space

Association (ITA/AITES). The guidelines apply to all participants in the planning and management of risks in the construction of tunnels and underground structures. The guidelines are prescribed to subscribers and consultants, which are implementing risk assessment and taking into consideration the modern methods of risk assessment and describe the phases of risk management, from the initial to the final phase of the project.

Reliability analysis

Deterministic method for risk analysis is made only from the engineering data that are predetermined by the rules, terms and data. The method has no way of determining the probability of the limit values and the actual safety of the structure. Probabilistic method for the risk analysis is made on the mathematical models. The assumption is that all external influences and the strength characteristics of materials or structures are random variables, which are displayed as an appropriate statistical distribution, with a mean value and standard deviation. In this case, it is necessary to perform a series of calculations, in which each parameter systematically changing on the maximum possible interval for determination of the impact on the factor of safety (F) and on the stability sensitivity of each parameter.

In geotechnical engineering factor of safety and stability depends on the random variables and they all represents the strength parameters of the ground. Dependence of the stability are also a support system parameters, such as support pressure, steel or concrete strength. Then it is necessary to properly analyze and assess the distribution of factor of safety (F), reliability index (β) and consequentially probability of failure (P_f). Reliability index (β) provides more information about the reliability of geotechnical designing and geotechnical structures.

Probabilistic assessment of limit states

Project design load capacity is usually designated as R and load that causes a force or load as S .

The boundary that separates the safe and unsafe side or failure is the limit state, defined by the following equation^[3]:

$$G(X) = R - S = 0 \quad (1)$$

The following equation is also called as the performance function $G(X)$, determined by design engineer. Performed must be condition $G(X) \geq 0$ for the safe performance and structure stability. In the equation $X = \text{vector of random variables}$. Mathematically, in case if $R > S$ that means the safe side and failure happens in the case of $R < S$.

Approximation method First-Order Reliability Method (FORM)

The analysis with FORM provides one or more following results^[4]:

- reliability index (β),
- probability of failure (P_f) or probability of a worst case scenario,
- the most likely combination of parameters which are representing the degree of failure,
- sensitivity of the result in any change in the parameter value.

The first step in analyzing the probability of failure using probabilistic methods is the mathematical assumption from the engineer which determines performance function $G(X)$ and impacts which causes unsatisfactory performance or failure. Calculations can be done with adverted FORM method in Microsoft Excel data sheet.

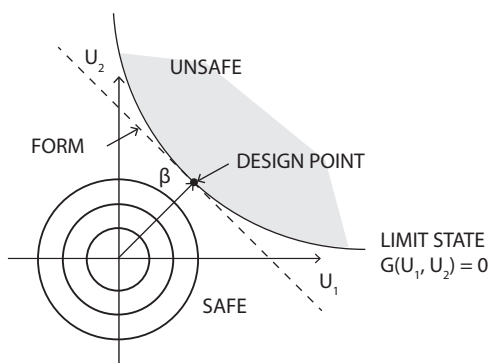


Figure 2: The FORM approximation and definition of and design point^[4].

FORM approximation includes^[4]:

- transformation of main random vector in a standard Gaussian vector,
- determination of the point of maximum of probability density (most likely point of failure or planned point which is (β) point) within the area of failure,
- assessing the probability of failure as $P_f \approx \Phi(-\beta)$ where Φ is the standard Gaussian cumulative distribution function.

In 2003 was by Low represented a method for calculating the reliability index (β). Approach is based on analysis with matrix system^[4]:

$$\beta = \min \sqrt{\left[\frac{X_i - \mu_i}{\sigma_i} \right]^T [R]^{-1} \left[\frac{X_i - \mu_i}{\sigma_i} \right]} \quad (2)$$

In case $\{X : G(X) = 0\}$

Training example with FORM method

Represented example of structure reliability analysis is summarized from authors^[5] and it was calculated in thesis^[6]. Determined is performed function $G(X) = 0$ in case when support pressure $p_i = 0.4$ MPa and under hidrostatic stress field. In the data sheet are shown the mean values μ_i distributed by normal distribution and standard deviations σ_i of random variables which represents the ground parameters from which depends the design stability of underground structure. Inproper combination of represented main geotechnical parameters can cause excess plastic zone of excavated area which could be the main reason for excess radial displacement and structure damage or failure. The values in bottom represented Excel column of x_i^* are initially set on the mean values μ_i . The next step is calculation of design point x_i^* with Excel considering with numerical changing initial values of μ_i under condition $G(X) = 0$. Finally calculated values in column of x_i^* are the most critical values of ground parameters on limit state, which are in this example represented like random variables. Design point x_i^* shows the most critical values of φ , c , p_r , E_{rm} , which represents a combination of parameters of a ultimate limit state. Parameters φ and c , are in this example pro-

posed with correlation coefficient -0.5 . Calculated combination of parameters in column x_i^* ($\varphi = 21.09^\circ$, $c = 0.2075$ MPa, $p_i = 0.3542$ MPa, $E_{rm} = 373$ MPa) are the most sensitive values which are representing the ultimate limit state. Performed function in this case is set as a criterium of plastic zone:

$$G_1(X) = L - \frac{R_{pl}}{R} \quad (3)$$

and second criterium is criterium of underground structure convergence:

$$G_2(X) = \varepsilon_{max} - \frac{u_{rpl}}{R} \quad (4)$$

- L is the maximum ratio by R_{pl} ,
- R_{pl} is radius of plastic zone of underground structure [m],
- R is radius of cross section of underground structure [m],
- ε_{max} is maximum ratio by u_{rpl} ,
- u_{rpl} is total internal radial displacement of underground structure [mm].

Preliminarily proposed ratio for limit state of this example is:

$$L = 2$$

$$\varepsilon_{max} = 2 \%$$

Calculations are based on performed function $G_1(X) = 0$ and assumed Mohr-Coulomb model. For this example are afforded next random variables:

- radius of underground structure or a tunnel (R),
- hidrostatic ground pressure (p_0),
- Poisson ratio (ν),
- cohesion (c),
- friction angle (φ),
- reactive support pressure on the edge of excavation (p_i),
- Young modul of ground (E_{rm}).

Table 1: Structure radius, ground and support pressure parameters

	R/m	p_0/MPa	ν	p_i/MPa
Random variables	2.5	2.5	0.3	0.4

Table 2: Normal distributed ground parameters with calculated design point

Random variables	Dist.	μ_i	St dev σ_i	x_i^*
$\varphi/^\circ$	Norm	21.093	2.045	21.090 5
c/MPa	Norm	0.287	0.038	0.207 47
p_i/MPa	Norm	0.4	0.06	0.354 22
E_{rm}/MPa	Norm	373	48	373

Table 3: Correlation matrix

R			
1	-0.5	0	0
-0.5	1	0	0
0	0	1	0
0	0	0	1

Table 4: Matrix system for calculating the reliability index (β)

R^{-1}			
1.333	0.667	0	0
0.667	1.333	0	0
0	0	1	0
0	0	0	1

$[x_i - m_i]/\sigma_i$	$[[x_i - m_i]/\sigma_i]^T$		
-0.0012	-0.0012	-2.0930	0.7629
-2.0930			
0.7629			
0.0000			

$[R^{-1}][x_i - m_i]/\sigma_i$	$[[x_i - m_i]/\sigma_i]^T [R^{-1}][x_i - m_i]/\sigma_i$
-1.3970	0.0017
-2.7915	
0.7629	
0.0000	

Table 5: Limit state ratios and values of performed functions

L	ε_{max}	$G_1(X)$	$G_2(X)$
2	0.02	0.000 227 82	0.001 594 784

Results of $G_1(X)$ and $G_2(X)$ are values from Excel analysis when $G_1(X)$ and $G_2(X)$ are by numerical calculating approaching to be equivalent to 0. For calculating needed condition $G(x_i^*) = 0$ was used function Solver in Excel.

Table 6: Results of reliability index β and probability of failure P_f

β	$P_f/\%$
1.704	4.415

Training example for three cases of support pressure scenario

Input data and concept for this example was summarized from authors^[7]. Performed function $G(X)$ in this case is set as a criterium of plastic zone, where is assumed equation (3). Analysis is made for circular tunnel under hidrostatic stress field. Method for calculating this results are the same like in a previous example. Following results and diagrams are summarized from^[6]. The objective of following results is to represent the relation between p_i and β and between p_i and P_f .

Table 7: Assumed support pressures

Assumed support pressure	$p_i = 0.0$ MPa
Assumed support pressure	$p_i = 0.3$ MPa
Assumed support pressure	$p_i = 0.8$ MPa

Table 8: Calculated values of β and P_f for different support pressures p_i

p_i /MPa	$G_1(X)$	β	P_f /%
0.0	-0.000 001 0	0.707	23.989
0.3	-0.000 000 6	3.238	0.060
0.8	-0.000 000 9	8.844	0

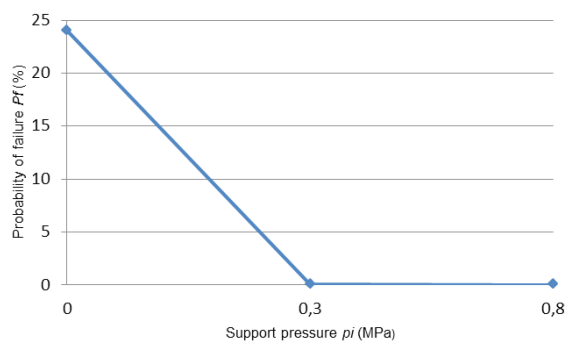


Figure 3: Relation between p_i and β .

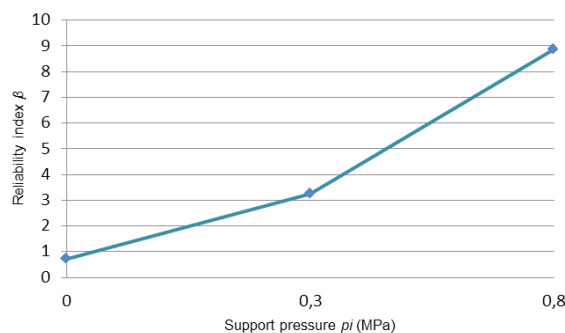


Figure 4: Relation between p_i and P_f .

From diagrams above it is visibly, when p_i increases also reliability index β increases and the probability of failure P_f in this case declines. Diagram functions are linear specially for this case, because only three different points were taken into consideration.

Law basis and construction contract

The definition of the legal obligations in the following sections proceedings within the wider formal sense, especially are exposed regulations relating to the construction of underground structures. Following represented law basis for construction of underground structures are summarized from^[6] where they are closely considered.

Legal rules are divided into:

- basic rights and obligations of the participants, the rules in the case if the participants agree otherwise,
- enforced rules from which the participants can not resign, this rules protects certain fundamental values of contract law.

The basis for the creation of obligations contracted for the construction and construction contract in Republic of Slovenia are Obligacijski zakonik (Code of Obligations; hereinafter OZ), which replaced Zakon o obligacijskih razmerjih (Law of Obligations; hereinafter ZOR) and Zakon o graditvi objektov^[8] (Construction Act; hereinafter ZGO-1) (Ur. l. RS 110/2002)^[9]. In the first phase of the contract proposal shall be reviewed general terms and in the second phase shall be drawn special or tender conditions.

Regulations and legal obligations

Obligacijski zakonik (Code of Obligations)

Obligacijski zakonik in Slovenia determines the relationships of the obligation law and in the field of commercial contract law contains the basic principles and general rules for all obligations. It is a branch of civil law, which governs the legal law relations and as a result means an obligation^[1-10].

FIDIC - General conditions for construction contracts

FIDIC (Federation Internationale des Ingenieurs-Conseils) is a French acronym for the International world alliance of consulting engineers, which has been established in 1913. FIDIC publishes guidelines used by consulting engineers. General provisions includes guidelines, standard forms, contract documents and the contracts between the subscriber and the consultant. In the Slovenian language is in printed form available 10 FIDIC recommendations. "FIDIC contract" means: a contractual agreement, a letter of tender acceptance, tender letter, the general and special conditions, census (specification), drawings (plans), and all other documents (if they are available) which are listed in the "contractual agreement" or in a "a letter of tender acceptance"^[11]. FIDIC general contract conditions are the same for all contracts around the world, but special conditions are always based on the individual contract or on a single specific object^[11].

Posebne gradbene uzance – Ur. l. SFRJ 1. april, št. 18/1977 (Special Usages for Construction)

Posebne gradbene uzance (Special Usages for Construction; hereinafter PGU) takes its source from France, issued by the Privredna komora Jugoslavije (Commerce Chamber of Yugoslavia). In a similar way as an international FIDIC conditions they defines the relationships and other activities in the construction sector and further substantiates the individual concepts that are important in the construction phase. Basically, they are subordinated to the Obligacijski zakonik. The same as the typed legal rules of OZ, the provisions of PGU are also used in the subordinate way, means only if the clients did not otherwise regulate the specific issues with specific and individual provisions of the contract. They should be necessary adapted to the current Slovenian legislation. PGU have been used for many years and if participants agree in that case they are still valid. They are also used in the case law, if there is no other legal norms^[11].

Special cases

In accordance with the 2. term of Obligacijski zakonik participants can arrange their contractual obligation on the otherwise than it is determined in OZ, unless if the specific provision of this legal code (OZ) or of its meaning does not show anything else. In accordance with the 3. term of OZ participants are free to regulate obligations, but they should not edit them in conflict with the constitution, with the mandatory provisions or with the principles of morality.

Construction supervision

Building legislation of the Republic of Slovenia supervisory role in the construction defines the manual Priročnik za nadzor pri gradnji issued by Inženirska zbornica Slovenije (Slovenian Chamber of Engineers). The contractor is obliged to allow to the subscriber the constant control over parts and control over the quantity and quality of the used material^[1].

Slovenian legislation in the field of construction provides the following participants at construction of structures: investor - the subscriber which orders and finances the project and the services, design engineer, superintendent for construction works, and the contractor carrying out the work and builds the structure. In the case of complex structures construction is also present the reviser. Construction supervision has control of tasks and responsibilities to oversee compliance of the construction with the project documentation, approvals and regulations.

Good business practices

Morality do not provide the content of required conduct, but the extreme limits of permissible conduct. The prohibition of conduct that opposes to the morality is protecting the fundamental social values. Conscientiousness and honesty of the participants requires that the conclusions and implementations of the rights and fulfilling their obligations do not only strive to achieve their own interests, but also to the interests of the other party.

Prohibited are dishonorable treatments, and treatments that are contradicted to the morality, and practices that are dishonorable to the interests of the counterparty. For example, in

the German legal system are general restrictive standards of good practice (*gute Sitten*, comparable to the standards of the morality by OZ) and the loyalty and trust (*Treu und Glauben*, comparable with conscientiousness and honesty by OZ). Restrictive standards of the U.S. economic contract law are good faith and the injustice or unfairness (unconscionability). General restrictive standards of autonomous rules are good faith, fair dealing, inconsistent behaviour^[10].

Careful treatment of a good specialist

General contract law also refers to careful treatment. When participants complete their obligations under their occupation, they must deal with a greater degree of careful treatment – careful treatment of a good specialist. Economic activity is a professional activity. The rules of the profession are not the average knowledge, but that means a narrow business area knowledge of the participants. The most important criteria for assessing careful treatment of a good specialist are rules and practices of the profession^[10].

Business practices

Business practice is the conduct that is expected from persons of certain properties between the economic subjects. Their defined elements are^[10]:

- determination of conduct,
- expectedness and
- qualification of subjects to which it relates.

Rules of business practices shall apply in every case. Correspondently with the OZ business practices have a normative nature^[10].

The responsibilities of project participants

The contractor's liability for defects

Construction works contractor which takes the part of the project works, which was submitted by the investor as the subscriber shall be responsible only for the professional and technical mistakes and defects in the project, if the investor was not adverted from contractor, although the contractor as an expert knew or should have known the project mistakes and defects. But the contractor is not responsible as well for economically rashly performance which is proposed in the project^[1].

The contractor of construction works can not figure out the mistakes and errors in static calculations, which were the basis for the preparation of project documentation, resulting in a too small quantity of steel reinforcement which depends from a load capacity which must be ensured for the building structure. Based only on the basis of a of project documentation review this cannot be figured out. But this can be determined when during construction works the consequences are shown – for example, when cracks on the construction are starting to show up^[1].

Responsibility for the object errors, which are caused by deficiencies of the ground

In view of the ground complexity, the terrain must be necessary investigated with the geological and geotechnical studies. Nature of the ground must be taken into consideration by design engineer. The findings of such deficiencies of project documentation exceed the contractor's obligations in connection with the project documentation^[1].

During construction (for example, during excavation pit excavation) circumstances may arise (such as intrusion of groundwater) that even when the contractor (depending on experience and knowledge that contractor has) can wake doubt about it that these (actual) properties of land are properly taken into account in project solutions (such as the depth of the foundation). In this case (and only in this case) is to these shortcomings contractor obliged to warn the subscriber, because otherwise its liability for defective building will not be able to relieve^[1]. Under English law is one of general obligation on the design engineer to review the ground, whether it is appropriate for the construction of the facility by the subscriber needs. Error of project documentation goes so well that they have been used in the design of irregular baseline specifications and load capacity of the ground, or if the latter is based on the false static calculations^[1].

Reduction and exclusion of liability

The contractor shall not be relieved of liability if the error has occurred because the implementation of each part of the work by demand

of the subscriber. However, if it is before the implementation of each part according to subscriber requirements contractor puts his attention to the risk of errors, contractor's liability is reduced, in the circumstances of the each case can also be eliminated^[1].

Construction contract

Construction contract is a work contract between the subscriber and the contractor and must be made in writing shape specially to protect the interests of the participants and evidentiary purposes^[1]. Both clients must be unanimous in all links of the contract. The subscriber does not require from the contractor to use of certain means and method of construction, but the subscriber is interested in the result of this work^[1]. Business relationships in which this task relates primarily to contractual relationships of certain persons – economic subjects, addresses the economic contract law, which is a part of commercial law and in most legal systems recognized the existence of this specific law branch^[10]. At the conclusion of the construction contract occurs bilateral contractual obligation.

The importance of the principle of contract clients conscientiousness and honesty

The principle of conscientiousness and honesty requires that contract client in the exercise of the rights acquired by the conclusion of the contract, and the fulfillment of contractual obligations not only seeks to achieve its own interests, which concluded the contract, but with the right amount and in an appropriate manner is also responsible for the realization and protection of the interests of the other contract client^[1].

In concluding construction contracts under Austrian standards following provisions shall apply:

- ground is the property of the subscriber and also represents a subscriber's risk,
- the contracts are determined and applied in unit prices,
- the means and methods for unchanged ground conditions are contractor's risk.

Special terms in construction contract which are related to the excavation and support system of a tunnel

The subscriber and the contractor mutually agree about the main steps in the progress of the excavation and primary tunnel support. The subscriber puts special attention to ensure the stability of the underground structure and the contractor has to put special attention to safety work and to the workers health. The contractor shall be responsible for technically correct and timely installation of appropriate support elements^[12]. Contractor shall not be entitled to additional payment for better features of built-in material if such be installed, otherwise it is not a mistake, even if such material is not intended to project documentation. However, if the properties of the material are worse than anticipated with the project documentation, there is a mistake and contract unrespecting. The contractor in this case can not be held responsible for mistake^[1].

Conclusions

The advantages of the presented FORM method approach is simple use comparing with other standard mathematical approaches. Level of mathematical computing depends from project pretentiousness and determined limit state function. When structural analysis are computing there is investigated the design point x_i^* which represents the most probably point of structural failure on limit state. There must be performed a condition which means $G(x_i^*) = 0$. Summarized experiences from other authors which were the references for thesis and this article are representing that gained results with this method are almost equivalent to the results from standard mathematical approaches. Design point shows also the sensitivity of the ground parameters, which is very important characteristic of reliability analysis. The analysis with FORM provides the calculation of reliability index (β) and consequentially probability of failure (P_f) which can also show a worst case scenario of underground structures designing.

Slovenian legislation in the field of construction provides the following participants in the construction: investor - the subscriber that orders and finances the project and the services, the design engineer, supervisor which overseeing work, and the contractor carrying out the work and builds. The contractor by signing and conclusion of the contract undertakes responsibility to carry out the necessary work or built underground structure, thereby assumes the risk to be successful and to reach the ultimate goal. The subscriber has the right to executes the professional supervision of the contractor's parts to verify and ensure their proper implementation, in particular concerning the kind, quantity and quality of work, materials and equipment and on schedule. Conscientiousness and honesty of the participants require that the conclusion and implementation of the rights and fulfilling their obligations not only strive to achieve their own interests, but also to the interests of the other contract client. When determining the legal rules is important to consider the enforced rules, which both clients must take into consideration, and the optional basic rules which may clients agree otherwise. Potential risks can be reduced or avoided with next approaches:

- designing in more appropriate location of underground structure or a tunnel road,
- material designing with appropriate mechanical and geometrical characteristics,
- appropriate dimensional designing and reliability analysis,
- professional, conscientious and honest work,
- good communication of all participants in the project,
- supervising, measurements and monitoring,
- protection of surrounding objects, environmental and machines protection,
- with the timely measure in foreseen, unforeseen and critical situations.

References

- [1] Juhart, M., Plavšak, N. (2004): *Obligacijski zakonik (OZ) (posebni del) s komentarjem, 3. knjiga (435. do 703. člen)*. Ljubljana: GV Založba, 1205 p. ISBN 86-7061-349-2.
- [2] Nývlt, O., Prívar, S., Ferkl, R. (2011): Probabilistic risk assessment of highway tunnels. *Tunnelling and Underground Space Technology*, 26, pp. 71-82.
- [3] Zhang, W., Goh, A.T.C. (2012): Reliability assessment on ultimate and serviceability limit states and determination of critical factor of safety for underground rock caverns. *Tunnelling and Underground Space Technology*, 32, pp. 221-230.
- [4] Griffiths, D., V., Fenton, G., A. (2007): *Probabilistic methods in geotechnical engineering*. Udine: CISM. 346 p. ISBN 978-3-211-73365-3.
- [5] Low, B., K., Li, H.-Z. (2010): Reliability analysis of circular tunnel under hydrostatic stress field. *Computers and Geotechnics*, 37, pp. 50-58.
- [6] Mazurek M. (2013): *Analiza ocene tveganja in pravni okvirji gradnje podzemnih objektov*: Magistrsko delo. Ljubljana, 73 p.
- [7] Low, B., K., Lü, Q. (2011): Probabilistic analysis of underground rock excavations using response surface method and SORM. *Computers and Geotechnics*, 38, pp. 1008-1021.
- [8] Breznik, J., Duhovnik, J. (2005): *Zakon o graditvi objektov (ZGO-1) s komentarjem*. Ljubljana: GV Založba. 837 p. ISBN 86-7061-386-7.
- [9] Žemva, Š. (2010): *Gradbene kalkulacije z osnovami operativnega planiranja in obračunom gradnje objektov: priručnik za prakso*. Ljubljana: CPU – Center za poslovno usposabljanje, Gospodarska zbornica Slovenije, 672 p. ISBN 978-961-6666-37-4.
- [10] Kranjc, V. (2006): *Gospodarsko pogodbeno pravo*. Ljubljana: GV Založba, 496 p. ISBN 86-7061-429-4.
- [11] Šajna, A. (2012): *Priročnik za nadzor pri gradnji*. Ljubljana: Inženirska zbornica Slovenije, 62 p. ISBN 978-961-6724-17-3 (pdf).
- [12] Galler, R. (2010): Fair contracts in the field of tunneling. *International NATM Workshop Singapore*.

A review of stratigraphic surfaces generated from multiple electrical sounding and profiling

Prikaz sekvenčnih stratigrafskih površin, pridobljenih z geoelektričnim sondiranjem in profiliranjem

Kamaldeen Omosanya^{1,*}, Akinwale Akinmosin², Jonathan Balogun²

¹Olabisi Onabanjo University, Department of Earth Sciences, Ago-Iwoye, Nigeria

²University of Lagos, Department of Geoscience, Akoka, Nigeria

*Corresponding author. E-mail: kamaloomosanya@yahoo.com

Abstract

In this work, we investigate the accuracy of stratigraphic surfaces derived from multiple electrical sounding and traversing. Eight (8) VES stations with $AB/2$ of > 80 m each and three (3) Wenner profiling of > 120 m each were used for this investigation. The three principal surfaces interpreted include conglomeratic sand (top layer), sandstone (presumably compacted) and clayey sandstone. These rocks are correlated to the Ise Formation of eastern Dahomey Basin. Our result shows that widely-spaced VES are error-prone and may result in misinterpretation of subsurface resistivity and rock boundaries. Smaller spacing between VES stations can effectively detect minute resistivity anomalies. On the other hand, the inversion method used for interpretation of profiling data can influence the final resistivity values. We propose the criteria for generating stratigraphic surfaces to include (a) adequate geological mapping (b) small electrode spacing for profiling (c) closely-spaced VES stations and profiling lines (d) interpolation of thickness and resistivity in multiple direction and (e) the use of drill hole logs to tie VES models.

Key word: stratigraphic surfaces, VES, profiling, Ise

Izvleček

V članku opisujemo natančnost stratigrafskih površin, ki jih konstruiramo z geoelektričnim sondiranjem in profiliranjem. V ta namen smo uporabili podatke osmih točk vertikalnega električnega sondiranja (VES) z $AB/2 > 80$ m s Schlumbergerjevo elektrodno razporeditvijo in podatke treh profilov dolžine > 120 m z Wennerjevo elektrodno razporeditvijo. Iz podatkov geoelektričnega sondiranja in profiliranja smo interpretirali tri osnovne tipe kamnin, ki vključujejo konglomeratni pesek (zgornja plast), peščenjak (pretežno sprijet), zaglinjen peščenjak in preperelo podlago. Ti trije tipi ustrezajo enotam v Isa-formaciji iz Abeokuta skupine vzhodnega Dahomejskega bazena. Naši rezultati kažejo, da ima redka razporeditev VES-točk lahko za posledico napačno določitev električnih upornosti in s tem nepravilno določitev geoloških meja. Z manjšimi razdaljami med sondami lahko učinkovito zaznamo tudi majhne upornostne anomalije. Problem 2D-profiliranja je inverzna metoda modeliranja in kot posledica tega tudi doseg preiskav. Predlagamo nekaj meril za konstruiranje stratigrafskih površin, ki naj vključujejo (a) ustrezno geološko kartiranje, (b) majhne medelektrodne razdalje za profiliranje, (c) gosto razporeditev VES-točk in prečnih profilov, (d) interpolacijo debelin in električnih upornosti v več smereh in (e) uporabo podatkov vrtin, na katere navežemo VES-modele.

Ključne besede: sekvenčne stratigrafske površine, geoelektrično sondiranje, geoelektrično kartiranje, Ise

Introduction

Resistivity geophysical survey is one of the oldest and cheapest method of investigating subsurface electrical property and resistivity variation^[1, 2]. Resistivity method is used to solve a wide variety of groundwater problems which include determination of zones with high yield potential in an aquifer e.g.^[3, 4], leechate and other groundwater contamination e.g.^[5, 6], determination of the boundary between saline and fresh water zones^[7, 8], exploration of geothermal reservoirs^[9, 10], and estimation of hydraulic conductivity and transmissivity of aquifer^[11].

Sounding is one dimensional (1D) in nature providing subsurface information at a single point on the ground e.g.^[12]. Contrastingly, profiling is two dimensional (2D) data providing a cross section beneath the Earth's surface unlike 3D data that image the geology as a volume^[13]. Three dimensional methods are unique in that they provide better resolution and visualization^[14, 15]. Hence, the earth volume can be displayed in depth (cm, m, km) and $x - y$ coordinates system^[16, 17]. Planning 3D surveys could be laborious and expensive, often involving the design of appropriate line geometry for source (current electrode) and receiver (potential electrode) locations. To achieve this, a rectangular grid comprising of a line at least approximately along the line of steepest descent down the structure and another along a contour line on the structure is required *cf.*^[18]. This is the general practice in 3D geophysical surveying *cf.*^[19, 20]. Initial knowledge of the structure from surface or regional geology, satellite imagery, previous geophysical surveys such as gravity and magnetic is crucial for successful survey planning and design^[19, 20].

The practice of generating shallow stratigraphic surfaces from multiple 1D or 2D resistivity data is budding in less developed countries. This is consequent to the sparse availability of equipment and knowledge appropriate to conduct 3D and 4D surveys^[21]. Stratigraphic surfaces obtained through such practices are error prone and may result in misinterpretation of geological features and its associated resources.

The aim of this study is to validate the accuracy of stratigraphic surfaces generated from multiple sounding and profiling, an important piece of information for precise delineation of stratigraphic boundaries and subsurface resources. We hope to provide adequate information that will bridge the gap between constructed stratigraphic surfaces and those generated from real 3D surveys. The paper starts with a general overview of the regional geology. Description of geophysical methods which include electrical sounding and profiling along specific surveys lines follows. In the discussion we reappraise the techniques and their relevance to the current study and eventually provide criteria for generating realistic stratigraphic surfaces.

Regional Geologic Setting and Stratigraphy

The study area is located east of the West African Craton (WAC) (Figure 1). The Dahomey basin constitute part of a system of West African peri-cratonic basin developed during Late Jurassic to Early Cretaceous rifting associated with the opening of the Gulf of Guinea^[22-25]. The crustal separation and thinning was accompanied by an extended period of thermally induced basin subsidence through the Middle - Upper Cretaceous to Tertiary as the South American and the African plates entered a drift phase^[26, 27]. The Ghana Ridge, presumably an offset extension of the Romanche Fracture Zone, and the Benin Hinge Line, a bedrock escarpment which separates the Okitipupa structure from the Niger Delta basin are located on the western and eastern boundaries of the Dahomey basin. The Benin Hinge Line is the continental extension of the Chain Fracture Zone. The onshore part of the basin covers a broad arc-shaped belt profile of ~600 km² in extent. The onshore section attains a maximum width along its N-S axis, ~130 km around the Nigerian - Republic of Benin border. The basin narrows to ~50 km on the eastern side where the bedrock assumes a convex upwards outline with concomitant thinning of sediments. Notably, along the north eastern fringe of the basin where it rims the Okitipupa high is a brand of tar (oil) sands and bitumen seepages^[28]. The eastern Dahomey basin has been investigated specifically for its oil sand resource^[29].

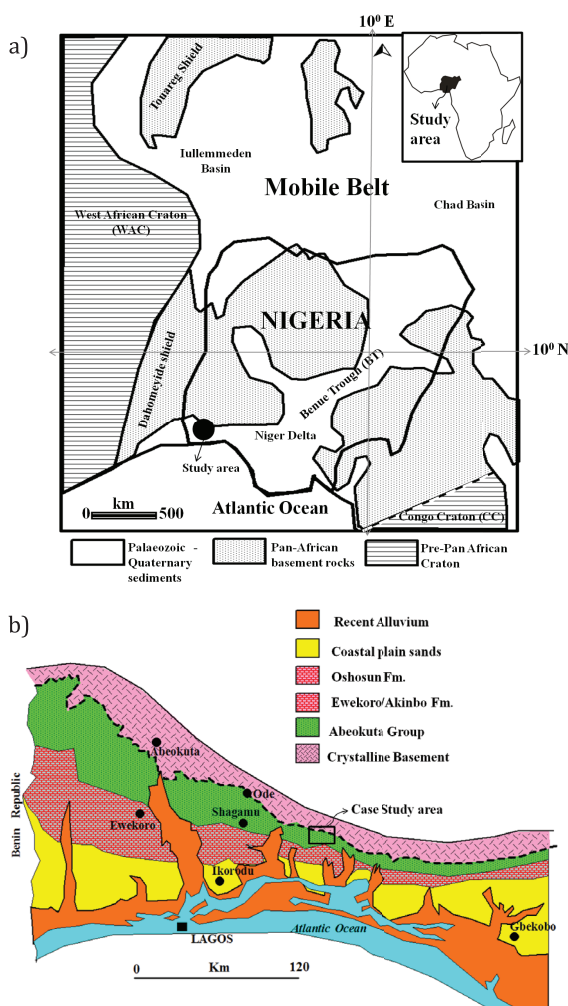


Figure 1: a) Regional geological map of Nigeria in the context of West African and Congo Craton (modified after^[30]). b) Simplified Geological map of the study area and environs. The geological boundary between the crystalline bedrock and sedimentary rock is shown with thick broken line. Further litho and chrono stratigraphic division of the study area is provided in Table 1.

The lithostratigraphic units of the case study area are summarised in Figure 1b and Table 1. The area belongs to the Ise Formation of the Cretaceous Abeokuta group which is the oldest and the thickest group of sediment in the Dahomey basin^[31, 32]. The Abeokuta group is composed of the Ise, Afowo and Araromi Formation. Ise Formation unconformably overlies the bedrock complex of Southwestern Nigeria. This unit consists of conglomerates, grits, coarse to medium grained sands interbedded with kaolinite. The conglomerates are imbricated and composed of ironstones at some localities^[33]. An age range of Neocomian-Albian is assigned to this Formation based on paleontological assemblages^[32].

The Afowo Formation comprises coarse to medium grained sandstone with variable but thick interbedded shale, siltstone and claystone. The sandy facies are tar-bearing while the shales are organic-rich^[34]. Using palynological assemblage, a Turonian age is assigned to the Lower part of this Formation, while the upper part ranges into Maastrichian. The youngest Cretaceous Formation in the group is Araromi Formation which is composed of fine-medium grained sandstone, shales, siltstone with interbedded limestone, marl and lignite.^[32] assigned a Maastrichian to Palaeocene age to this formation based on faunal content.

The Abeokuta group is overlain by the Imo group (Ewekoro and Akinbo Formation^[31, 33, 35, 36], the Oshosun Formation^[31, 33], Coastal plain sands and recent alluvium^[31].

Table 1: The stratigraphic units of eastern Dahomey basin

Jones and Hockey (1964) ^[31]		Omatsola and Adegoke (1981) ^[32]		Agagu (1985) ^[36]		
	Age	Formation	Age	Formation	Age	Formation
Quaternary	Recent	Alluvium			Recent	Alluvium
Tertiary	Pleistocene-Oligocene	Coastal Plain Sand	Pleistocene-Oligocene	Coastal Plain Sand	Pleistocene-Oligocene	Coastal Plain Sand
	Eocene	Ilaro	Eocene	Ilaro	Eocene	Ilaro
	Palaeocene	Ewekoro	Palaeocene	Oshosun Akinbo Fm	Palaeocene	Oshosun Akinbo Ewekoro
Cretaceous	Late Senonian	Abeokuta	Maastrichtian-Neocomian	Araromi Afowo Ise	Maastrichtian-Neocomian	Araromi Afowo Ise
Precambrian Crystalline Bedrock Rocks						

Methods

Resistivity surveys including three (3) profiling lines and eight (8) vertical electrical sounding (VES) were done over an area of $\sim 56\,400\text{ m}^2$. The sounding involves application of artificial electrical field method where electrode spacing is increased along traverse lines to obtain subsurface information at a given location (the survey layout is shown in Figure 3). The greatest limitation of electrical resistivity sounding method is that it does account greatly for lateral changes in the subsurface resistivity^[1]. For a more accurate result of the subsurface model, a two dimensional (2D) model where the resistivity changes in vertical and horizontal direction along the survey line was incorporated with the vertical electrical sounding. In this case, it was assumed that resistivity does not change in the direction perpendicular to the survey line. This method also finds its usefulness in the area of moderately complex geology^[13]. The ohmmeter resistivity meter used for the research measures resistance based on Ohm's law for current (I), voltage (V) and resistance (R) (Figure 2).

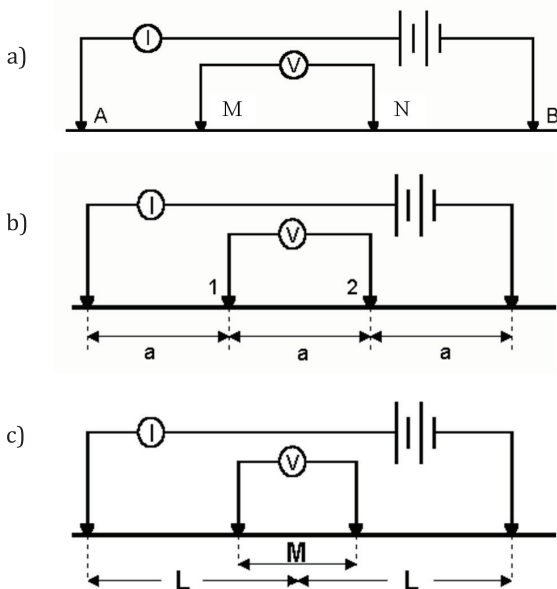


Figure 2: a) General electrode configuration for electrical geophysical method; b) Wenner array configuration, c) Schlumberger array configuration.

Sounding

The VES uses the principle of wider current electrode separation offers deeper current penetration and depth probe e.g.^[8, 37]. Hence, apparent resistivity values observed at larger separations are governed by the resistivity of deeper layers^[38, 2]. Current was injected into the earth through two electrodes (A and B) and the resulting voltage differences were measured at two potential electrodes (M and N). Hence, an apparent resistivity (ρ_a) values at each separation can be calculated using the general relation, $\rho_a = KV/I = KR$ ^[39]. Electrode configuration of $AB \geq 5 MN$ was maintained except with the initial values of current and potential electrodes spacing of $AB/2 = 1.0\text{ m}$ and $MN/2 = 0.25\text{ m}$. The electrode layout for the sounding is shown in Figure 2c.

K is the array geometric factor and is defined as $K = \pi/2l (L^2 - l^2)$, where L is $AB/2$, l is $MN/2$; current (I) and voltage (V) values, and the geometric factor (K) depends on the arrangement of the four electrodes. For this study, Schlumberger array was used for the sounding. The resistivity measurement for each $AB/2$ and corresponding $MN/2$ separations are shown below:
 $AB/2 = 1, 2, 3, 4, 6, 6, 9, 12, 15, 15, 20, 25, 32, 40, 40, 50, 65, 80, 100$ and
 $MN/2 = 0.25, 0.25, 0.25, 0.25, 0.25, 0.5, 0.5, 0.5, 0.5, 1, 1, 1, 1, 1, 2.5, 2.5, 2.5, 2.5, 2.5$.

The apparent resistivities (ρ_a) were plotted against the electrode spacing ($AB/2$) in order to obtain a resistivity-depth model for iteration on the WINRESIST software. The best iterations were obtained at RMS error of $< 5\%$. The depth, thickness and resistivity of the geoelectric layers were estimated and used to build 2D and 3D resistivity tomogram for the area.

Profiling

The profiling involve constant separation technique (CST) using the Wenner electrode configuration. Three (3) profile lines $\sim 120\text{ m}$ long were chosen along the less rugged portion of the survey area (Figure 3). Subsequently, the profiles lines were separated $\sim 20\text{ m}$ in the N – S direction to give better resolution of the subsurface resistivity variation. A current of 5 mA was introduced into the ground and the mean resistivity value

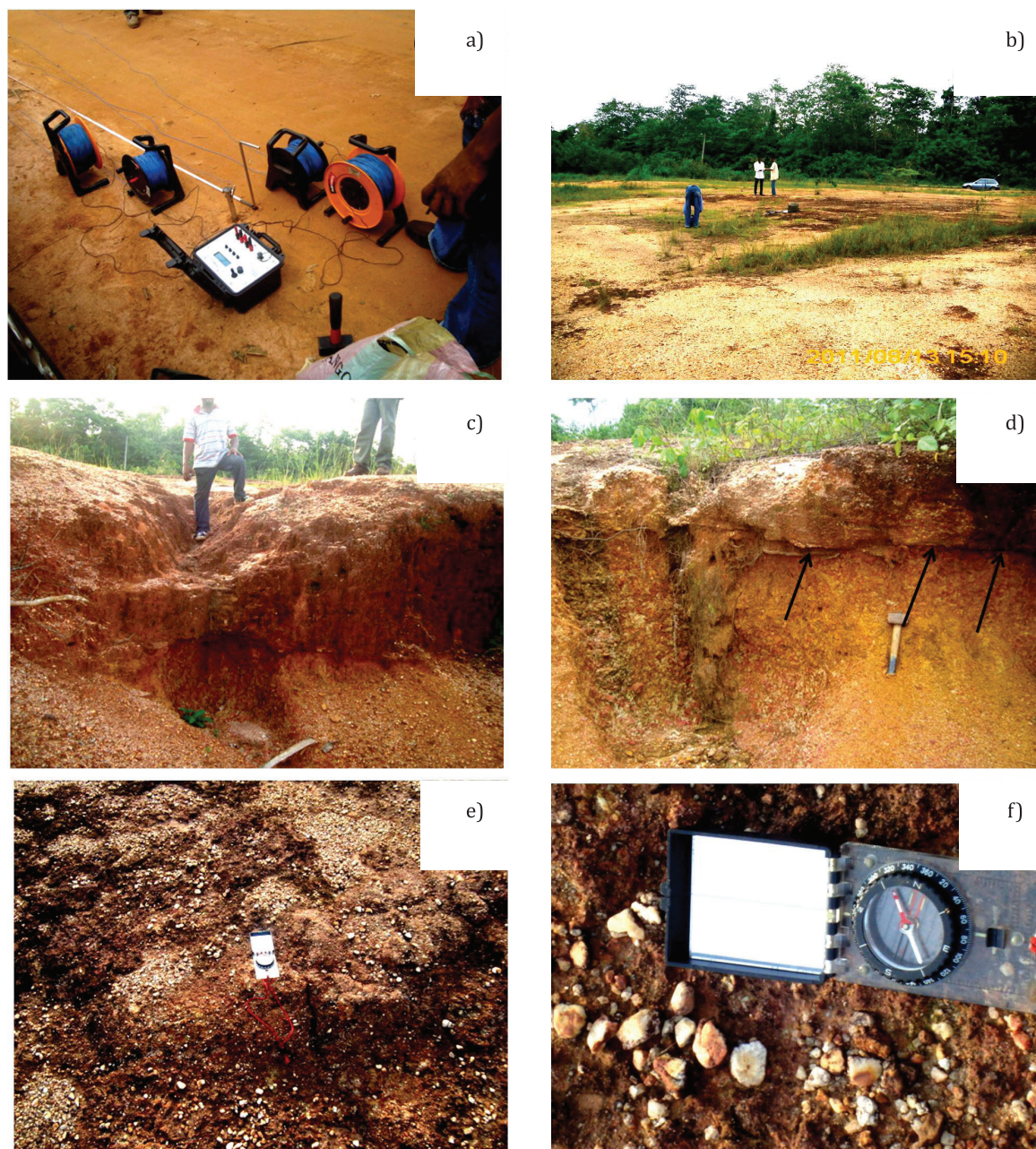


Figure 3: a) The survey layout for the electrodes; b) The survey area where both profiling and sounding were carried out. The topography is nearly horizontal and the rocks are characterised by angle of dip of $< 1^\circ$; c) cross section through the subcrop; d)–e) Outcrop of conglomeratic sandstone, the bedding plane between the conglomeratic sands and sandstone is nearly horizontal; f) Clasts of sandstone found in the conglomeratic sandstone are sub-rounded to very well-rounded.

over four cycles was obtained. As the distance between the current electrodes was progressively increased, the position of the potential electrode remained unchanged until the voltages were too small to be measured. The electrode spacing between adjacent electrode was assigned “ a ”. Hence, for a system with 20 electrodes, there are $(20 - (1 \times 3))$, $(20 - (2 \times 3))$, $(20 - (3 \times 3))$, $(20 - (4 \times 3))$ possible measurements for “ $1a$ ”, “ $2a$ ”, “ $3a$ ”, “ $4a$ ”

respectively and so on. This implies that, as the electrode spacing increases, the number of measurement decreases.

The first procedure was to carry out all the possible measurements for the Wenner array with electrodes spacing of “ $1a$ ”. For the first measurement, electrodes 1 to 4 were as A, M, B and N respectively. The positions of these electrodes were changed according to increasing number of elec-

trode spacing for “1a”. The same technique was repeated for “2a”, “3a”, “4a”, “5a” and “6a” spacing. The profiling was done with the practical assumption that depths of (3, 6, 9, 12, 15 and 18) m were being investigated (depth is ~ 0.6 of electrode spacing). The electrode layout for Wenner is shown in Figure 2b.

Resistivity values derived from the survey were converted to apparent resistivities using the geometric factor for Wenner; the data were processed on Excel spreadsheet and RES2DINV ver 3.55 software. Smooth and robust inversions were done to compare results and detect sedimentary boundaries. The inversion pro-

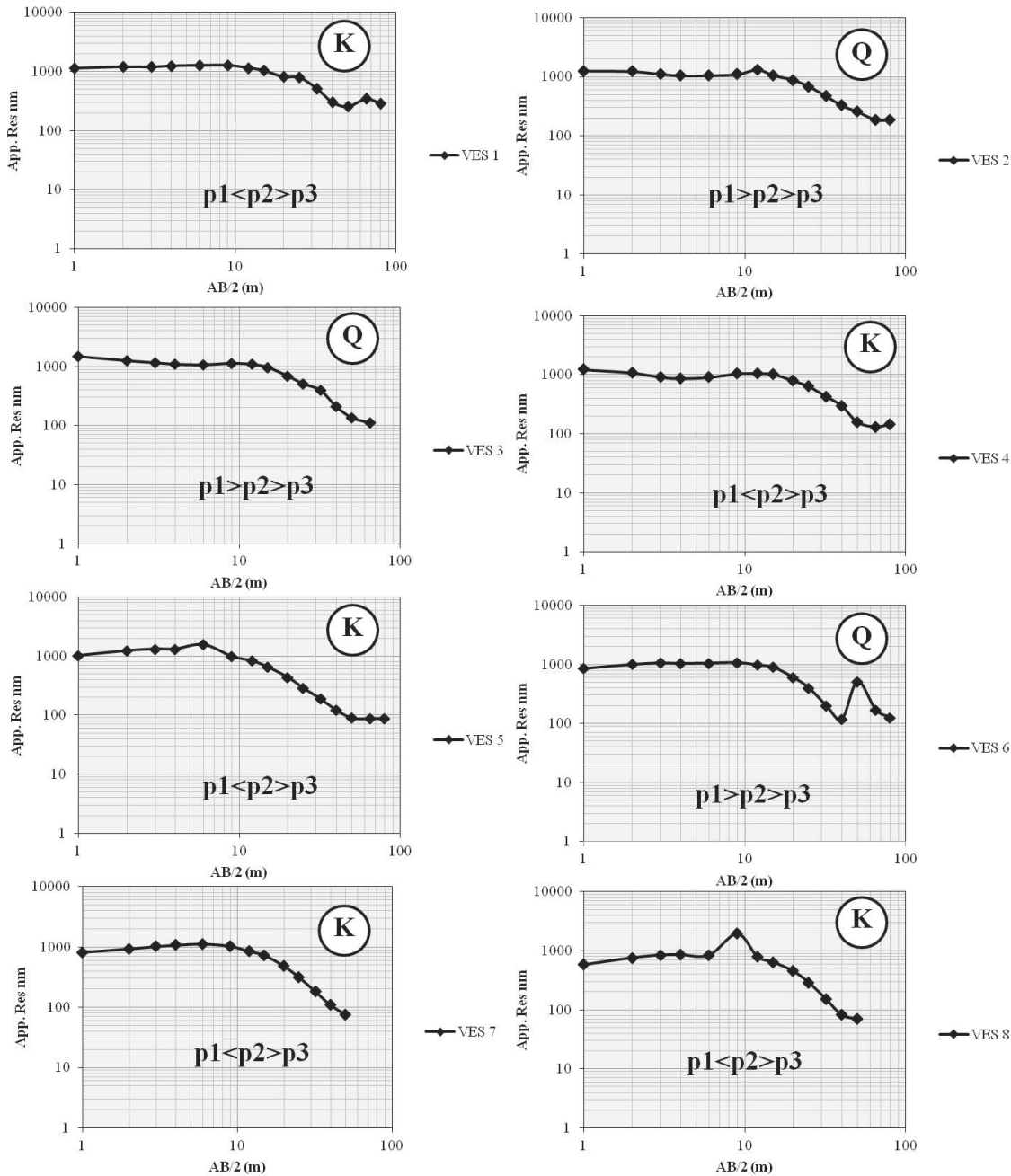


Figure 4: The resistivity plot for the VES stations were done from direct field measurements. The AB/2 versus apparent resistivity shows that the subsurface is multi-layered and composed of three rock types characterised as K- and Q-type curves.

cess is iterative, and useful for creating resistivity models of the subsurface^[38, 14]. A starting model was chosen based on a-priori information from ground truth or averaged geophysical measurements; apparent resistivity data was modelled according to the survey geometry. The calculated data were compared with the field measurements and the model updated to accommodate the difference between the observed and estimated results. This procedure was repeated until the derived data matched the actual readings to within an interpreter defined level of error^[40]. The consequence of the inversion process is a better estimate of depth

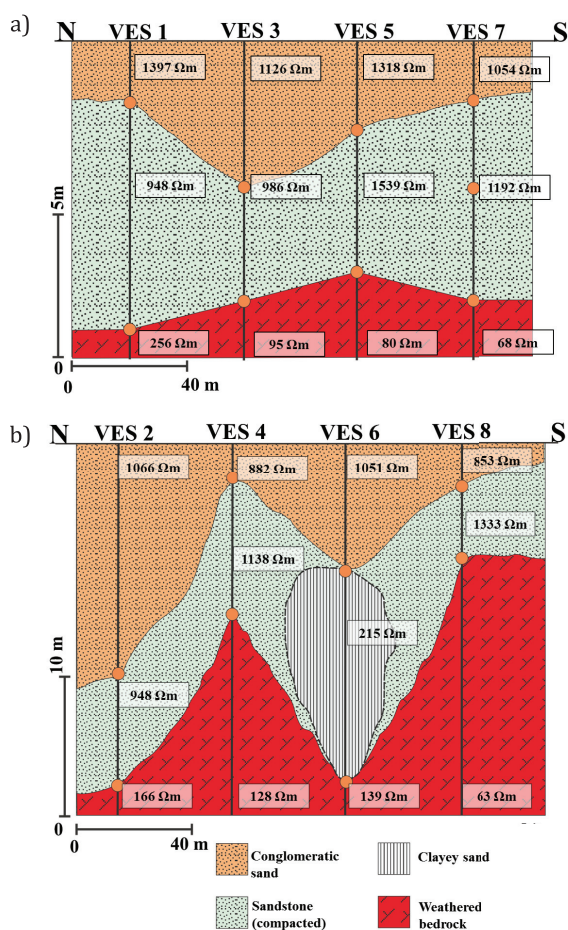


Figure 5: Cross section through the study area. Thicknesses and resistivities of the geoelectrical section were interpolated from multiple VES models which include a) VES 1, 3, 5, & 7 and b) VES 2, 4, 6, & 8. The sections revealed exaggerated angle of dip and strata geometries for the three rock types. The weathered bedrock is characterised by comparatively low apparent resistivity suggestive of high clay content.

for cross section plots, which turns resistivity pseudo sections into reliable approximations of the subsurface variation.

Interpolation resistivity and thickness of the layers

Estimated thickness and resistivity of three principal rock types were interpolated across the position of the VES stations and the profile lines to generate cross sections and 3D tomogram (Figures 5 and 6). The x and y direction include longitude and latitude of the stations and positions at every 20 m along each of the traverse, z -value is the thickness of the layers estimated. The stratigraphic thickness (isopach) maps were produced on Surfer 8 (Figures 6 and 8).

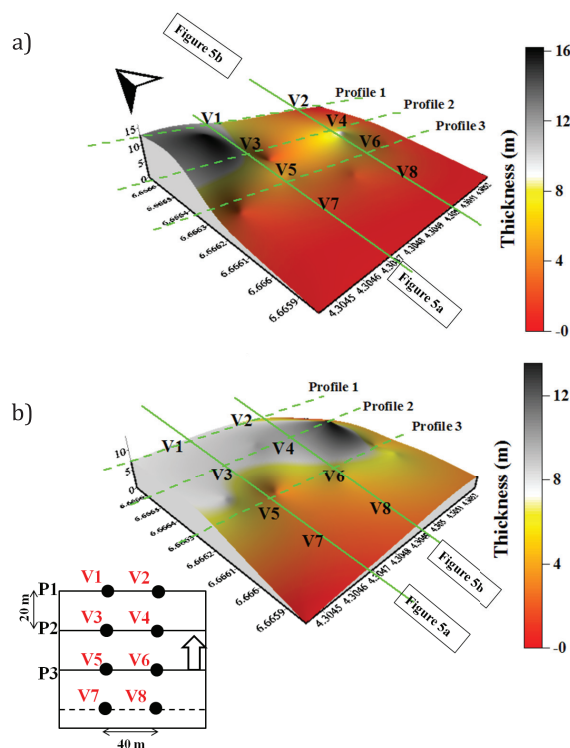


Figure 6: Isopach map for a) conglomeratic sand b) sandstone. The highest thicknesses are recorded in the NW region of the study area corroborating the result of Figure 8. The isopach maps were produced by interpolating the thicknesses of both rock types across the VES stations. N.B: The numbered circles correspond to the position of VES 1 to 8. Inset: The survey layout.

Results

In the following section the result from the survey is presented in phases such as the vertical electrical sounding, 2D models, and stratigraphic surfaces/3D models. These sections are followed by a discussion on the accuracy of the geological boundaries obtained from both results.

Geo-electric layers from Vertical Electrical Sounding

The plots of apparent resistivity against electrode spacing $AB/2$ are indicative of 3-layered stratigraphy. The curves are K and Q curves (Figure 4). The four (4) lithology units include conglomeratic sand (topmost stratum at all VES station), sandstone (presumably compacted), clayey sandstone and weathered bedrock. These units have resistivity values of 853–1 397 Ω m, 948–1 539 Ω m, 215 Ω m and 63–256 Ω m and thickness of 2–16 m, 4–14 m, 14 m and infinity respectively (Figure 5 and Table 2). The inferred weathered bedrock occurs at depth of ~8 m to ~24 m at all the VES stations. The clayey sand was detected beneath VES 6 only and apparently represents a different sandstone facies from the compacted sandstone and sandstone found at other VES points (Figure 5 and Table 2).

Electrical Reflection Coefficient

In order to validate resistivity anisotropy across layers and boundary condition of the interpreted intervals, an estimate of the electrode reflection coefficient, k was calculated along the interfaces of the different rock types using equation 1

$$k = \left(\frac{\rho_1 - \rho_2}{\rho_1 + \rho_2} \right) \quad (1)$$

k is electrical reflection coefficient

ρ_1 = apparent resistivity of the first layer

ρ_2 = apparent resistivity of the second layer

The k between conglomeratic sand and sandstone is -0.1 across VES point 4, 5, and 7. Across VES 2 and 3 k between those two lithological

Table 2: Parameters determined from the VES points

VES No	No of Layers	Depth	Thickness	Resistivity	Lithology
1	3	0-2	2	1 397	Conglomeratic Sand
		2-10	8	948	Sandstone
		10-∞		256	Weathered Bedrock
2	3	0-16	16	1 066	Conglomeratic Sand
		16-24	8	948	Sandstone
		24-∞		166	Weathered Bedrock
3	3	0-5	5	1 126	Conglomeratic Sand
		5-9	4	986	Sandstone
		9-∞		95	Weathered Bedrock
4	3	0-2	2	882	Conglomeratic Sand
		2-12	10	1 138	Sandstone
		12-∞		128	Weathered Bedrock
5	3	0-3	3	1 318	Conglomeratic Sand
		3-8	5	1 539	Sandstone
		8-∞		80	Weathered Bedrock
6	3	0-9	9	1 051	Conglomeratic Sand
		9-23	14	215	Clayey Sand
		23-∞		139	Weathered Bedrock
7	3	0-2	2	1 054	Conglomeratic Sand
		2-9	7	1 192	Sandstone
		9-∞		68	Weathered Bedrock
8	3	0-3	3	853	Conglomeratic Sand
		3-8	5	1 333	Sandstone
		8-∞		63	Weathered Bedrock

units is 0.1, and for VES 1 and 8 k is 0.2 and -0.2 accordingly (Table 3). This suggests that the coefficient is relatively consistent across some of the VES points. However, at VES 6, the k value between the conglomeratic sand and clayey sand is 0.7, suggesting a high degree of dissimilarity between these lithology types. Furthermore, the k value between the weathered bedrock and sandstone at VES points 1, 2, 3, 4, 5, 7 and 8 ranges from 0.7 to 0.9 (Table 3).

Table 3: Electrical reflection coefficient across the interpreted interfaces

VES No	Res. Point	Resistivity	Lithology	Electrical reflection coefficient
1	p1	1 397	Conglomeratic Sand	0.2
	p2	948	Sandstone	0.6
	p3	256	Weathered Bedrock	
2	p1	1 066	Conglomeratic Sand	0.1
	p2	948	Sandstone	0.7
	p3	166	Weathered Bedrock	
3	p1	1 126	Conglomeratic Sand	0.1
	p2	986	Sandstone	0.8
	p3	95	Weathered Bedrock	
4	p1	882	Conglomeratic Sand	-0.1
	p2	1 138	Sandstone	0.8
	p3	128	Weathered Bedrock	
5	p1	1 318	Conglomeratic Sand	-0.1
	p2	1 539	Sandstone	0.9
	p3	80	Weathered Bedrock	
6	p1	1 051	Conglomeratic Sand	0.7
	p2	215	Clayey Sand	0.2
	p3	139	Weathered Bedrock	
7	p1	1 054	Conglomeratic Sand	-0.1
	p2	1 192	Sandstone	0.9
	p3	68	Weathered Bedrock	
8	p1	853	Conglomeratic Sand	-0.2
	p2	1 333	Sandstone	0.9
	p3	63	Weathered Bedrock	

In contrast, there is a strong similarity between the clayey sand and weathered bedrock at VES 6. This is evidenced by k value of 0.2 (Table 3). Overall, a high k suggests dissimilarity between rock types while a very low value implies homogeneity of rock types.

Resistivity cross section from 2D profiling

The apparent resistivity values for the profiling are described from the smooth inverted pseudo section. Profile 1 revealed three rock types which include conglomeratic sands with resistivity value of 386–1 065 Ω m, compacted ferruginised sandstone of > 1 065 Ω m, and weathered bedrock of < 386 Ω m (Figure 7). Contrastingly, the robust pseudo section shows dominance of com-

packed ferruginised sandstone having resistivity values of > 1 249 Ω m from the surface to depth of ~12 m. Other rock types include conglomeratic sands and weathered bedrock with resistivity value of 354–1 249 Ω m and < 354 Ω m respectively (Figure 7). Both pseudo sections show that the conglomeratic sands are sandwiched within the compacted ferruginised sandstone on the eastern side of profile 1. Equally, profile 2 shows a similar succession of rock types but with resistivity value of > 852 Ω m, 337–852 Ω m, and < 337 Ω m. At the uppermost and central section of profile 2, the conglomeratic sands are interbedded within the compacted ferruginised sandstone (Figure 7). However, the conglomeratic sands are predominant at the western to central uppermost section of profile 3, occurring to depth of ~12 m and ~5 m on the smooth and robust pseudo section respectively (Figure 8). To the eastern uppermost part, the compacted ferruginised sandstone occurs to depth of < 9 m. The resistivities of the rock types include > 1 019 Ω m, 277–1 019 Ω m and < 277 Ω m for compacted ferruginised sandstone, conglomeratic sands and weathered bedrock respectively.

Average resistivities for the three principal rock types are 150–1 000 Ω m, > 1 019 Ω m and < 400 Ω m (Figure 7). Field observation shows that weathered bedrock is composed of weathered clasts of feldspar apparently related to either porphyritic granite or porphyroblastic gneiss protolith. The degree of weathering is intense and the rock equivocally resembles a mudstone (Figure 3).

Stratigraphic surfaces from multiple VES and profiling

The isopach map in Figure 6 shows that conglomeratic sand is the thickest NW of the profile lines and thins to SW and SE. An anomalous high thickness of conglomeratic sand was identified ENE of the study area. Similarly, the sandstone is the thickest NE of the traverses where it is manifested expressed as a dome compared to thickness values in the surrounding (Figure 6). The thickness of sandstone in the NE is smaller than in the NW. The lowest thickness of the sandstone layer is recorded SW of profile lines (Figure 6).

The cross sections produced from VES data shows that conglomeratic sand is the thickest beneath VES 2 and relatively constant across VES 1, 5, & 7 which concur with the thickness trend observed in Figure 5. Furthermore, Figure 6 revealed similar variation in thickness for the sandstone layer when compared with Figure 8. The highest thickness of the sandstone beneath VES 6 is attributed with the presence of the clayey sand (Figure 5). It is important to note that profile line 3 crosses VES 5 and VES 6; both soundings are located at 40 m and 80 m mark of the profile line respectively. The three layers interpreted from the 2D profile are conglomeratic sand, sandstone and weathered bedrock with resistivity value of $> 792 \Omega m$, $396-792 \Omega m$ and $< 396 \Omega m$, their thicknesses being $\sim 9 m$, $\sim 4 m$ and infinity respectively. Two

layers were interpreted under VES 6: they include the conglomeratic sand and the sandstone with resistivity value of $> 792 \Omega m$ and $560 \Omega m$ respectively. When compared with the result from the VES points, the overlap between resistivities and depth values exist (see Figures 5, 6 and 8).

Discussion

The main purpose of resistivity surveys is to determine either the variation of resistivity with depth or estimate the lateral variations in resistivity associated with the presence of economic deposits, pollutants or tectonic structures^[41-43]. The former reflect horizontal stratification of earth materials involving meas-

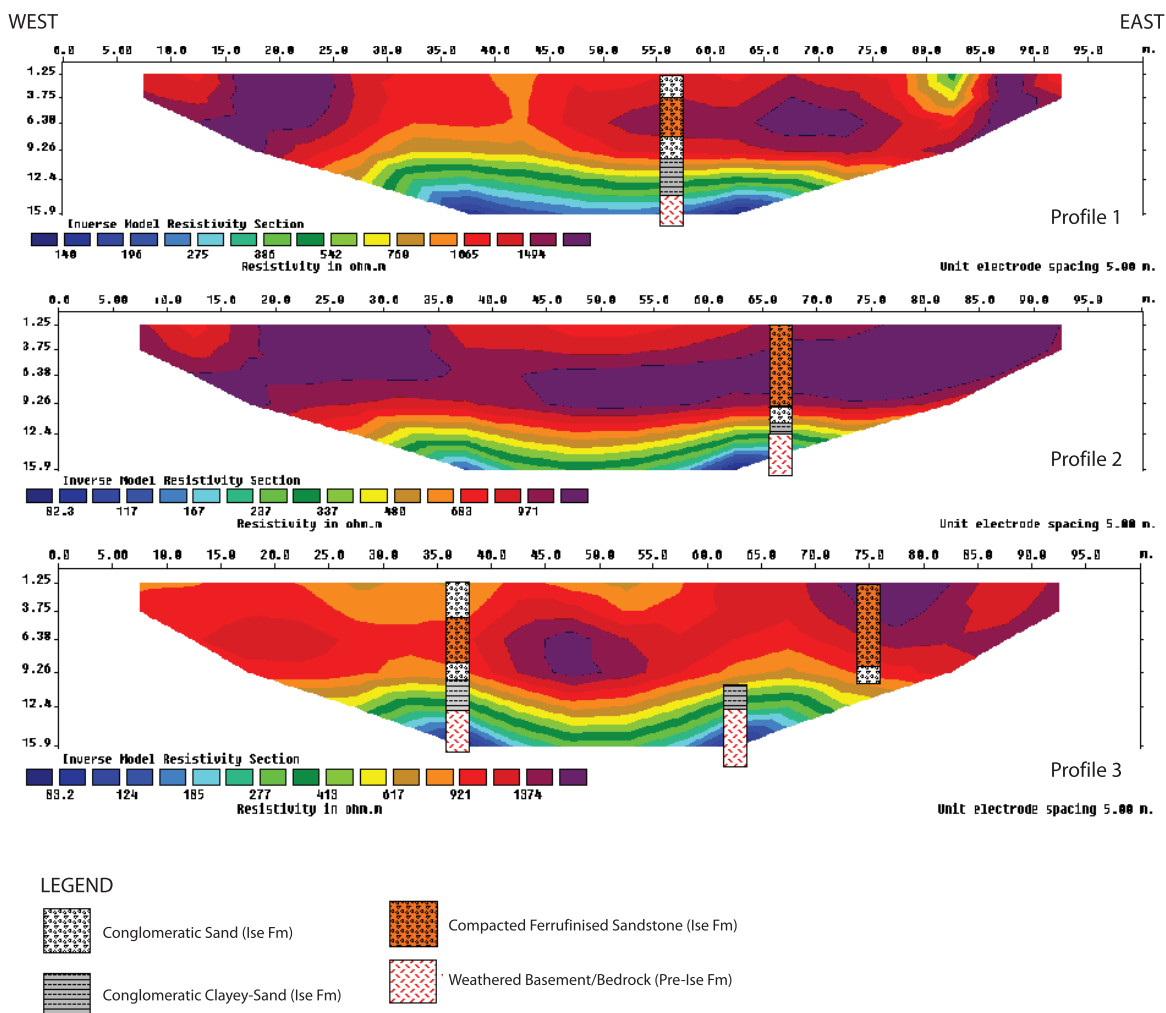


Figure 7: The smooth inverted resistivity pseudo section along Profile 1, 2 and 3 from North to South. The principal lithology types include the conglomeratic sands, compacted ferruginised sandstone and the weathered bedrock with resistivity values of $150-1\ 000 \Omega m$, $>1\ 019 \Omega m$ and less than $400 \Omega m$ respectively.

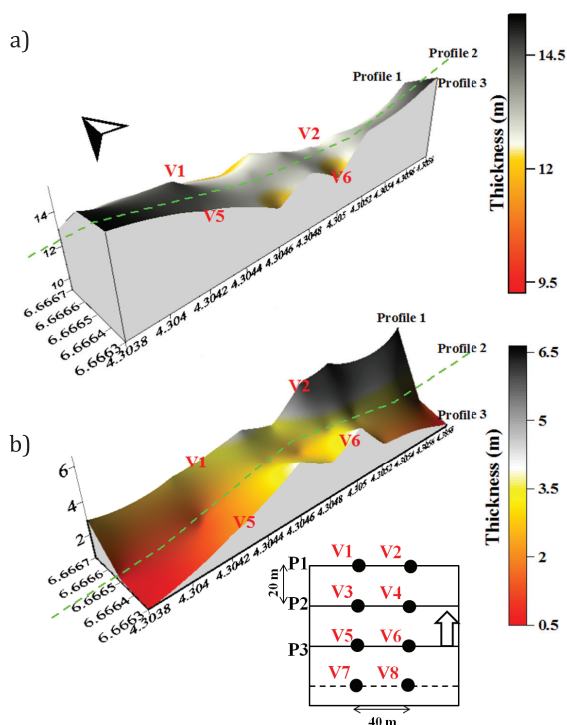


Figure 8: a) Isopach map and cross section of the Ise Formation b) Cross section through the weathered bedrock/basement. These figures are produced from interpolation of the 2D pseudo sections in Figure 7. The position of profile lines is from the north of Fig. 6 to the E-W broken line. N.B: The Ise Formation is sensu the conglomeratic sands and compacted ferruginised sandstone. The isopach map displays the thickness of the Ise to the top of the weathered basement, while the topography for the basal unit was estimated from the difference of the thickness of Ise Formation from the total depth shown on stratigraphic sections. Inset: The survey layout.

urements of apparent resistivity at a single location with systematically varied electrode spacing. This procedure is called vertical electrical sounding (VES), or vertical profiling^[44]. Surveys of lateral variations can be made at spot or along definite lines of traverse, a procedure called horizontal profiling or constant separation traversing (CST)^[38, 40]. The greatest limitation of sounding is that it does not adequately account for horizontal variation in subsurface resistivity. Profiling or 2D models are more accurate but suffer the set back of limited depth of investigation. During profiling, the resistivity variation in both vertical and horizontal direction is modelled effectively especially for shallow depths. Therefore, using sounding and profiling to produce stratigraphic surfaces entail viewing the geology from different perspective yet with the goal of prodding similar result.

Array configuration and parameters are considerably dependent on the objective of the survey, available time and topography of the site^[39]. To get the best subsurface information requires a well constrained survey with appropriate electrode configuration. This invariably affects data processing and the quality of interpretation model. The number of measurement is proportionate to electrode spacing and length of the survey traverse^[38]. Schlumberger array allows the highest number of electrode spacing and survey length possible. Not only this, Schlumberger array provides for high signal-to-noise ratios, good resolution of horizontal layers, and good depth sensitivity^[45]. An initial distance from the center of the array to either of the current electrodes is spacing s . Consequently, errors in apparent resistivity are within 2 % to 3 % if the distance between the potential electrodes does not exceed $2s/5$ ^[46]. Potential electrode spacing is dependent on the minimum value of s . However, Wenner array is suited to smallest number of measurement but greater lateral resolution. In rugged topography, Wenner configuration electrode spacing is ineffective^[40, 12].

Specifically, Wenner profiling in this study used initial a spacing of 5 m while the sounding were done starting with s value of 1 m for current electrodes. Hence, the maximum a spacing of 40 m can only yield depth of ~ 24 m while maximum current electrode spacing of 80 m can yield depth of < 40 m. It implies the depth of investigation is not consistent across both survey. To remove the ambiguity in depth requires running several VES prior the profiling. The exercise would provide a guide for the best electrode spacing needed for the 2D profiling. The resolution of the traverse line is governed by the fineness of the grid derived from initial VES parameter^[39]. Therefore, combined vertical and horizontal methods may be used. If available drill hole logs at the sounding station can be used to effectively tie the lithology to their resistivity values.

Processing for both techniques is straight forward. Most resistivity meter are designed to measure resistance, the apparent resistivity value is derived from the product of the resistance with the appropriate geometric factor for the electrode configuration used. The caution during acquisition is to effectively monitor how

the potential diminishes with increasing current spacing. This will reduce error associated with underestimation of the geology during processing and interpretation of results. Again, this is dependent on the shrewdness of the geophysicist and his experience to increase the current appropriately. Of importance is the interval or cycles over which the resistance value is averaged. Averaging the resistance value in a cycle of 4 has proved very effective^[21,47].

The interpretation of sounding starts with plotting field measured apparent resistivity against electrode spacing in a diagram. The plot is a curve which is used to define initial geoelectrical model such as resistivities and thicknesses for each individual layer. Before the model could be defined, the plot is matched with standard master curves to obtain the best fit of layer parameters^[38, 1, 2]. The initial model obtained is subsequently run over different commercial

software and iterated at the least possible error. This procedure benefits greatly from the knowledge of local geology and the experience of the geophysicist. The greatest shortcoming of the direct interpretation pertains to electrical anisotropy at different depth and strata^[1, 2]. Often the final geoelectrical sections are interpolated over several soundings to obtain cross section or a volume of the geology. For profiling, apparent resistivity values are plotted and contoured on maps or plotted as profiles. On the resistivity pseudo section, areas of anomalous values or patterns can be identified. 2D profiling integrates technique of 1D sounding along a survey line (i.e. 2D plane). The result is a contoured image, which displays the distribution of apparent resistivity values. In order to convert the apparent resistivity data to true resistivity, the data are inverted using either robust or smooth inversion, most often^[48, 14].

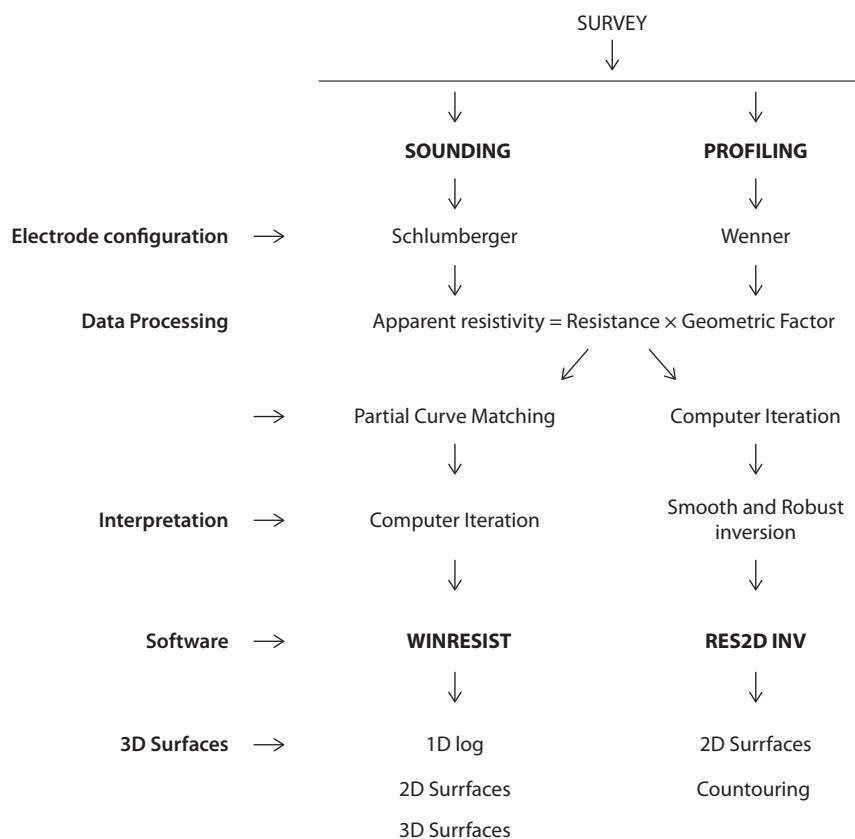


Figure 9: Flowchart for comparing geoelectrical techniques of sounding and profiling as used in this work. Differences in results are related to the data processing technique and to acquisition parameters especially the direction of survey line and electrode spacing.

Furthermore, stratigraphic surfaces were produced by interpolating thickness and resistivity in a grid of 40 m × 40 m in the N-S and E-W direction. This resulted in an overestimation of the geometry of the sections especially the angle of dip and strata geometry. Figure 5 shows that the Ise Formation is characterised by angle of dip > 1° which contradicts the observation made on the field. The actual dips of the Ise strata are < 1° as shown in Figure 3d. In addition, the clayey sand is shown as a lens within the compacted sandstone (Figure 5). These features were not picked by the profiles/resistivity pseudo sections. However, the location of the ferruginised sandstones lobes and lenses were adequately resolved despite the 2D section being oriented in N-S direction in contrast to E-W direction of the profiling lines. The surfaces interpolated from the profiling are rather closely spaced compared with the VES. Hence, the stratigraphic surface obtained from the profiling has better resolution and estimation of the stratigraphic geometry. The overlap between smooth and robust inverted pseudo sections shows that the geometry of the strata was effectively mapped. Robust inversion is useful for mapping complex geology and lap geometries^[48]. Therefore, interpolation of geoelectrical section can be a fruitful exercise where the lateral continuity of strata is not geologically variable.

In order to reduce interpretation errors associated with electrical anisotropy, it is useful to estimate the electrical coefficient (Equation 1, Table 3). For the VES section, it provides hints on resistivity heterogeneity in the downhole direction. As it is often the case with VES, resistivity is higher perpendicular to layering e.g. bedding, foliation, lamination etc. rather than along layering^[14]. In this work, electrical coefficients signify the presence of multi-layer geoelectrical section. High absolute k values are associated with very dissimilar lithology type. Hence, the k values from the VES corroborate the interpretation of the resistivity pseudo sections. However, determining the electrical coefficient over the profiles could be laborious.

Conclusion

In the absence of 3D equipments and methods for resistivity investigation in developing countries, this study has provided guideline for generating stratigraphic surfaces from available data acquired by multiple electrical sounding and profiling. In this work we showed that stratigraphic surfaces interpolated from the 1D and 2D data are reasonably similar in terms of thicknesses and resistivities of the layers. The maximum thickness of the Ise Formation estimated from both techniques is > 16 m. Resistivity values range from 900–1 300 Ω m. In addition, both techniques pointed to the presence of highly weathered clayey bedrock. However, the differences in results from both techniques are correlated to acquisition parameters such as the electrode spacing, distance between traverses and VES locations. Interpolation of VES data is very useful in an environment where the geology is simple and characterised by less variability. A combination of VES and CST array, such as a multi-level dipole-dipole array, can overcome the limitations associated with the both techniques. To generate effective stratigraphic surfaces, interpolation of resistivity and thickness along variable azimuth is required. Drill hole logs and advanced geological mapping could enhance the results obtained from these methods and consequently the representation of surfaces generated from them. Hence, the criteria for generating stratigraphic surfaces using sounding and profiling data should include advanced geological mapping, small electrode spacing, azimuthal interpolation combining both vertical and horizontal methods and adequate information from drill hole logging. A general comparison of both techniques is given in Figure 9.

Acknowledgement

We acknowledge comments and opinions of the anonymous reviewers. The understanding and support of Maryam, Aisha and Hawa during the preparation of the manuscript is remarkable.

References

- [1] Kearey, P., Brooks, M., Hill, I. (2002): *An introduction to geophysical exploration*. Wiley- Blackwell.
- [2] Telford, W., Geldart, L., Sheriff, R., Keys, D. (1976): *Applied geophysics*. Cambridge University Press.
- [3] Sainato, C., Galindo, G., Pomposiello, C., Malleville, H., de Abelleyra, D., Losinno, B. (2003): Electrical conductivity and depth of groundwater at the Pergamino zone (Buenos Aires Province, Argentina) through vertical electrical soundings and geostatistical analysis. *J. South Am. Earth Sci.*, 16, pp. 177–186.
- [4] Shaaban, F. F. (2001): Vertical electrical soundings for groundwater investigation in Northwestern Egypt: a case study in a coastal area. *J. Afr. Earth Sci.*, 33, pp. 673–686.
- [5] Ariyo, S. O., Omosanya, K. O., Oshinloye, B. A. (2013): Electrical resistivity imaging of contaminant zone at Sotubo dumpsite along Sagamu-Ikorodu Road, Southwestern Nigeria. *Afr. J. Environ. Sci. Technol.*, 7, pp. 312–320.
- [6] Reyes-López, J. A., Ramírez-Hernández, J., Lázaro-Mancilla, O., Carreón-Diazconti, C., Garrido, M. M. L. (2008): Assessment of groundwater contamination by landfill leachate: A case in México. *Waste Manag.*, 28, pp. 33–39.
- [7] Adeoti, L., Alile, O., Uchegbulam, O. (2009): Geophysical investigation of saline water intrusion into freshwater aquifers: A case study of oniru, Lagos State. *Sci. Res. Essays*, 5, pp. 248–259.
- [8] Sikandar, P., Bakhsh, A., Ali, T. (2010): Vertical electrical sounding (VES) resistivity survey technique to explore low salinity groundwater for tubewell installation in Chaj Doab. *J. Agric. Resour.*, 48, pp. 547–566.
- [9] Cid-Fernandez, J., Araujo, P. (2007): VES characterization of a geothermal area in the NW of Spain. *EIEAF Che* 6, pp. 2173–217.
- [10] El-Qady, G. (2006): Exploration of a geothermal reservoir using geoelectrical resistivity inversion: Case study at Hammam Mousa, Sinai, Egypt. *J. Geophys. Eng.*, 3, pp. 114–121.
- [11] Mazác, O., Cislérova, M., Vogel, T. (1988): Application of geophysical methods in describing spatial variability of saturated hydraulic conductivity in the zone of aeration. *J. Hydrol.*, 103, pp. 117–126.
- [12] Ojelabi, E., Badmus, B., Salau, A. (2002): Comparative Analysis of Wenner and Schlumberger Methods of Geoelectric Sounding in subsurface delineation and groundwater exploration-a case study. *J. Geol. Soc India*, 60, pp. 623–628.
- [13] Griffiths, D., Barker, R. (1993): Two dimensional resistivity imaging and modeling in areas of complex geology. *J. Appl. Geophys.*, pp. 211–226.
- [14] Loke, M. H. (2000a): Electrical imaging surveys for environmental and engineering studies: A Practical Guide to 2D and 3D Surveys., 2004, pp. 61. Available on: <www.terrajp.co.jp/lokenote.pdf>.
- [15] Loke, M. H. (2000b): *Topographic modelling in electrical imaging inversion* in: Proceedings 62nd Meeting of the European Association of Exploration Geoscientists, Glasgow, Scotland. pp. 1–4.
- [16] Collela, A., Lapenna, V., Rizzo, E. (2004): High-resolution imaging of the High Agri Valley Basin (Southern Italy) with electrical resistivity tomography. *Tectonophysics*, 386, pp. 29–40.
- [17] Steeples, D. (2001): Engineering and environmental geophysics at the millennium. *Geophysics*, 66, pp. 31–35.
- [18] Stone, D., 1994. *Designing Seismic Surveys in Two and Three Dimensions* in: SEG, 244. (* Edited by Charles A. Meeder). Society of Exploration Geophysicists, Tulsa, Oklahoma.
- [19] Vermeer, G. J. (2000): *3-D Seismic Survey Design*. Society of Exploration Geophysicists, Tulsa, Oklahoma.
- [20] Weimer, P., Davis, T. (1996): *Applications of 3-D Seismic Data to Exploration and Production*, SEG, 270. Society of Exploration Geophysicists, Tulsa, Oklahoma.
- [21] Akinmosin, A. A., Omosanya, K. O., Ikhane, P. R., Mosuro, G. O., Adetoso, A. O. (2012): Electrical Resistivity Imaging (ERI) of basin fills in some parts of Eastern Dahomey. *Int. Res. J. Geol. Min.*, 2(7), pp. 174–185.
- [22] Burke, K. C., Dessauvagie, T. F., Whiteman, A. (1971): The opening of the Gulf of Guinea and Geological History of the Benue Depression and Niger Delta. *Nat. Phys. Sci.*, 233, pp. 51–55.
- [23] Kingston, D., Dishroon, C., Williams, P. (1983): Global Basin Classification System. *AAPG Bull.*, 67, pp. 2175–2193.
- [24] Klemme, H. (1975): *Geothermal Gradients, Heat-flow and Hydrocarbon Recovery.*, in: A.G. Fischer and S. Judson (eds), *Petroleum and Global Tectonics*. Princeton Univ. Press, Princeton, New Jersey, pp. 251–304.
- [25] Whiteman, A. (1982): *Nigeria: Its Petroleum Geology, Resources and Potential*. Graham and Trontman, London.
- [26] Mpanda, S. (1997): Geological development of east African coastal basin of Tanzania. *Acta Univ. Stockh.* 45, pp. 121.

- [27] Storey, B. C. (1995): The role of mantle plumes in continental break-up, case history from Gondwanaland and nature. *Nature*, 377, pp. 301–308.
- [28] Ekweozor, C., Nwachukwu, J. (1989): The origin of Tar sands in southwestern Nigeria. *NAPE Bull.*, 4, pp. 82–84.
- [29] Akinmosin, A., Omosanya, K., Ariyo, S., Folorunsho, A., Aiyeola, S. (2011): Structural control for bitumen seepages in imeri, southwestern Nigeria. *International Journal of Basic and Applied Sciences*, 11, 1, pp. 93–103.
- [30] Woakes M, Ajibade C. A, Rahaman, M. A. (1987): Some metallogenic features of the Nigerian Basement, *Jour. of Africa Science*, 5 pp. 655–664.
- [31] Jones, H., Hockey, R. D. (1964): The Geology of Part of Southwestern Nigeria. *Geol Surv Nig Bull*, 3.
- [32] Omatsola, M., Adegoke, O. (1981): Tectonic evolution and Cretaceous stratigraphy of the Dahomey Basin. *J. Min. Geol.*, 18, pp. 130–137.
- [33] Nton, M. (2001): Aspect of Rock Evaluation Studies of the Maastrichtian-Eocene Sediments. *J. Min. Geol.*, 13, pp. 33–39.
- [34] Enu, E. (1990): Aspect of Rock Evaluation Studies of the Maastrichtian-Eocene Sediments. *J. Min. Geol.*, 40, pp. 29–40.
- [35] Nton, M., Elueze, A. (2005): Composition Characteristics and Industrial Assessment of Sedimentary Clay bodies in part of Eastern Dahomey basin, Southwestern Nigeria. *J. Min. Geol.*, 4, pp. 175–184.
- [36] Agagu, O. K. (1985): *A geological guide to bituminous sediments in Southwestern Nigeria*. Unpubl. Report, Department of Geology, University of Ibadan.
- [37] Vouillamoz, J. M., Chatenoux, B., Mathieu, F., Baltasat, J. M., Legchenko, A. (2007): Efficiency of joint use of MRS and VES to characterize coastal aquifer in Myanmar. *J. Appl. Geophys.*, 61, pp. 142–154.
- [38] Cardimona, S. (2002): *Electrical resistivity techniques for subsurface investigation*. Dep. Geophys. Univ. Mo. Rolla-Mo.
- [39] Loke, M. H., Chambers, J. E., Rucker, D. F., Kuras, O., Wilkinson, P. B. (2013): Recent developments in the direct-current geoelectrical imaging method. *J. Appl. Geophys.*, 95, pp. 135–156.
- [40] Dahlin, T., Loke, M. H. (1998): Resolution of 2D Wenner resistivity imaging as assessed by numerical modelling. *J. Appl. Geophys.*, 38, pp. 237–249.
- [41] Dhakate, R., Singh, V. S., Negi, B. C., Chandra, S., Rao, V. A. (2008): Geomorphological and geophysical approach for locating favorable groundwater zones in granitic terrain, Andhra Pradesh, India. *J. Environ. Manage.*, 88, pp. 1373–1383.
- [42] Hussein, M. T., Awad, H. S. (2006): Delineation of groundwater zones using lithology and electric tomography in the Khartoum basin, central Sudan. *Comptes Rendus Geosci.*, 338, pp. 1213–1218.
- [43] Nguyen, F., Garambois, S., Jongmans, D., Pirard, E., Loke, MH. (2005): Image processing of 2D resistivity data for imaging faults. *J. Appl. Geophys.*, 57, pp. 260–277.
- [44] Ward, S. (1990): Resistivity and induced polarization methods, in: *Geotechnical and Environmental Geophysics*. Society of Exploration Geophysicists.
- [45] Jha, M. K., Kumar, S., Chowdhury, A. (2008): Vertical electrical sounding survey and resistivity inversion using genetic algorithm optimization technique. *J. Hydrol.*, 359, pp. 71–87.
- [46] Van Nostrand, Robert, G., Cook, K. (1966): *Interpretation of resistivity data*. U. S. Govt. Print. Off.
- [47] Omosanya, K., Mosuro, G., Azeez, L. (2012): Combination of geological mapping and geophysical surveys for surface-subsurface structures imaging in Mini-Campus and Methodist Ago-Iwoye NE Areas, Southwestern Nigeria. *J. Geol. Min. Res.*, 4, pp. 105–117.
- [48] Loke, M. H., Barker, R. (1996): Rapid least-squares inversion of apparent resistivity stratigraphic sections by a quasi-Newton method. *Geophys. Prospect.*, 44, pp. 131–152.

In memoriam

Jakob Mostar

prof. dr. Primož Mrvar, doc. Jurij Smole, ak. kipar

Po daljši bolezni nas je nepričakovano in veliko prezgodaj zapustil prijatelj, zvesti stanovski brat, livar in metalurg Jakob Mostar, rojen 29. 4. 1975 v Ljubljani.

Jakob prihaja iz livarske družine Mostar, ki slovi po več kot stoletni tradiciji livarstva. Osnovno šolo in srednjo strojno šolo je obiskoval v Ljubljani, kjer je že zanetil iskro ljubezni do livarstva. Diplomiral je leta 2001 na Univerzi v Ljubljani, Naravoslovnotehniški fakulteti, Oddelku za materiale in metalurgijo, Katedri za livarstvo, pod mentorstvom prof. dr. Milana Trbižana. Tema diplomskega dela je bila Merjenje aktivnosti kisika in termična analiza taline za indefinitne valje, ki jo je končal z odliko. Ko sem na dopustu prejel klic, da je dragi in spoštovani Jakob preminil, me je globoko potrlo in prizadelo. V mislih se mi je zavrtilo vse najino iskreno in plodno sodelovanje. Delila sva ljubezen do livarstva in metalurgije, pa tudi, ko sva se bolje spoznala, ugotovila, da imava zelo podobne poglede na življenje in slovenstvo. Lahko rečem, da je Jakob bil in je v naših srcih izjemen človek v pristnem pomenu te besede, saj je dajal pomoč in podporo mnogim, kot se spominjam še iz časa študija. Bil je najboljši študent generacije, inovator in delu predan človek.

Jakobova livarna, ki jo je z veliko predanostjo in ljubeznijo do metalurgije postavil kot naslednik družinske tradicije, nam je dala veliko bronastih in aluminijastih izdelkov, zlasti je bil ponosen na nove oblike zvonov, ki so akustično in estetsko izjemno dovršeni. Tudi ulivanje umetnin, plaket in reliefov je bil zanj poseben izziv, ki se mu je rad posvečal, saj je s širjenjem svoje livarne želel uvesti tehniko ulivanja z iztaljivimi modeli (precizijsko litje). Sredi velikega zagona, ko je že prenovil prostore, zgradil nagibno talilno peč in z velikimi koraki stopal skozi življenje, nas je presenetil s svojim odhodom.

V svojem življenju je vzorno skrbel za starše, predano nadaljeval podjetje Livarstvo Mostar, se proslavil z zahtevnimi ulitki, bil športnik in predvsem kolegialen, inovativen ter delaven metalurg. Kar je mogoče še najpomembnejše: njegov blagi temperament in živ duh, s katerim si je odkrival nova obzorja in nas razveseljeval v človeškem in strokovnem smislu, sta ga zapisala v naša srca in zelo ga bomo pogrešali.

Težko razumemo njegov prehod h gospodarju življenja, saj je bil Jakob še poln načrtov in idej. Prepričani smo, da je našel svoj mir in je skupaj s predniki. Tukaj nam ostajajo spomini nanj in njegova dela, ki krasijo Slovenijo in svet: njegovi zvonovi, plakete, skulpture ter tehnični ulitki iz bakrovih in aluminijevih zlitin.

Jakob, srečno in na svidenje nad zvezdami!



Jakob Mostar

Instructions to Authors

Navodila avtorjem

RMZ – MATERIALS & GEOENVIRONMENT (RMZ – Materiali in geokolje) is a periodical publication with four issues per year (established in 1952 and renamed to RMZ – M&G in 1998). The main topics are Mining and Geotechnology, Metallurgy and Materials, Geology and Geoenvironment.

RMZ – M&G publishes original scientific articles, review papers, preliminary notes and professional papers in English. Only professional papers will exceptionally be published in Slovene. In addition, evaluations of other publications (books, monographs, etc.), in memoriam, presentation of a scientific or a professional event, short communications, professional remarks and reviews published in RMZ – M&G can be written in English or Slovene. These contributions should be short and clear.

Authors are responsible for the originality of the presented data, ideas and conclusions, as well as for the correct citation of the data adopted from other sources. The publication in RMZ – M&G obligates the authors not to publish the article anywhere else in the same form.

RMZ – MATERIALS AND GEOENVIRONMENT (RMZ – Materiali in geokolje), kratica RMZ – M&G je revija (ustanovljena kot zbornik 1952 in preimenovana v revijo RMZ – M&G 1998), ki izhaja vsako leto v štirih zvezkih. V reviji objavljamo prispevke s področja rudarstva, geotehnologije, materialov, metalurgije, geologije in geokolja.

RMZ – M&G objavlja izvirne znanstvene, pregledne in strokovne članke ter predhodne objave samo v angleškem jeziku. Strokovni članki so lahko izjemoma napisani v slovenskem jeziku. Kot dodatek so zaželeni recenzije drugih publikacij (knjig, monografij ...), nekrologi In memoriam, predstavitev znanstvenih in strokovnih dogodkov, kratke objave in strokovne replike na članke, objavljene v RMZ – M&G v slovenskem ali angleškem jeziku. Prispevki naj bodo kratki in jasni.

Avtorji so odgovorni za izvirnost podatkov, idej in sklepov v predloženem prispevku oziroma za pravilno citiranje privzetih podatkov. Z objavo v RMZ – M&G se tudi obvežejo, da ne bodo nikjer drugje objavili enakega prispevka.

Specification of the Contributions

Optimal number of pages is 7 to 15; longer articles should be discussed with the Editor-in-Chief prior to submission. All contributions should be written using the ISO 80000.

- Original scientific papers represent unpublished results of original research.
- Review papers summarize previously published scientific, research and/or expertise articles on a new scientific level and can contain other cited sources which are not mainly the result of the author(s).
- Preliminary notes represent preliminary research findings, which should be published rapidly (up to 7 pages).
- Professional papers are the result of technological research achievements, application research results and information on achievements in practice and industry.

Vrste prispevkov

Optimalno število strani je 7–15, za daljše članke je potrebno soglasje glavnega urednika. Vsi prispevki naj bodo napisani v skladu z ISO 80000.

- Izvirni znanstveni članki opisujejo še neobjavljene rezultate lastnih raziskav.
- Pregledni članki povzemajo že objavljene znanstvene, raziskovalne ali strokovne dosežke na novem znanstvenem nivoju in lahko vsebujejo tudi druge (citirane) vire, ki niso večinsko rezultat dela avtorjev.
- Predhodna objava povzema izsledke raziskave, ki je v teku in zahteva hitro objavo obsega do sedem (7) strani.
- Strokovni članki vsebujejo rezultate tehnoloških dosežkov, razvojnih projektov in druge informacije iz prakse in industrije.

- Publication notes contain the author's opinion on newly published books, monographs, textbooks, etc. (up to 2 pages). A figure of the cover page is expected, as well as a short citation of basic data.
- In memoriam (up to 2 pages), a photo is expected.
- Discussion of papers (Comments) where only professional disagreements of the articles published in previous issues of RMZ – M&G can be discussed. Normally the source author(s) reply to the remarks in the same issue.
- Event notes in which descriptions of a scientific or a professional event are given (up to 2 pages).
- Recenzije publikacij zajemajo ocene novih knjig, monografij, učbenikov, razstav ... (do dve (2) strani; zaželena slika naslovnice in kratka navedba osnovnih podatkov).
- In memoriam obsega do dve (2) strani, zaželena je slika.
- Strokovne pripombe na objavljene članke ne smejo presežati ene (1) strani in opozarjajo izključno na strokovne nedoslednosti objavljenih člankov v prejšnjih številkah RMZ – M&G. Praviloma že v isti številki avtorji prvotnega članka napišejo odgovor na pripombe.
- Poljudni članki, ki povzemajo znanstvene in strokovne dogodke zavzemajo do dve (2) strani.

Review Process

All manuscripts will be supervised shall undergo a review process. The reviewers evaluate the manuscripts and can ask the authors to change particular segments, and propose to the Editor-in-Chief the acceptability of the submitted articles. Authors are requested to identify three reviewers and may also exclude specific individuals from reviewing their manuscript. The Editor-in-Chief has the right to choose other reviewers. The name of the reviewer remains anonymous. The technical corrections will also be done and the authors can be asked to correct the missing items. The final decision on the publication of the manuscript is made by the Editor-in-Chief.

Form of the Manuscript

The contribution should be submitted via e-mail as well as on a USB flash drive or CD.

The original file of the Template is available on RMZ – Materials and Geoenvironment Home page address: www.rmz-mg.com.

The contribution should be submitted in Microsoft Word. The electronic version should be simple, without complex formatting, hyphenation, and underlining. For highlighting, only bold and italic types should be used.

Composition of the Manuscript

Title

The title of the article should be precise, informative and not longer than 100 characters. The author should also indicate the short version of the title. The title should be written in English as well as in Slovene.

Recenzentski postopek

Vsi prispevki bodo predloženi v recenzijo. Recenzent oceni primernost prispevka za objavo in lahko predlaga kot pogoj za objavo dopolnilo k prispevku. Recenzenta izbere uredništvo med strokovnjaki, ki so dejavni na sorodnih področjih, kot jih obravnava prispevek. Avtorji morajo predlagati tri recenzente. Pravico imajo predlagati ime recenzenta, za katerega ne želijo, da bi recenziral njihov prispevek. Uredništvo si pridržuje pravico, da izbere druge recenzente. Recenzent ostane anonimni. Prispevki bodo tudi tehnično ocenjeni in avtorji so dolžni popraviti pomanjkljivosti. Končno odločitev za objavo da glavni urednik.

Oblika prispevka

Prispevek lahko posredujete preko e-pošte ter na USB mediju ali CD-ju.

Predloga za pisanje članka se nahaja na spletni strani: www.rmz-mg.com.

Besedilo naj bo podano v urejevalniku besedil Word. Digitalni zapis naj bo povsem enostaven, brez zapletenega oblikovanja, deljenja besed, podčrtavanja. Avtor naj označi le krepko in kurzivno poudarjanje.

Zgradba prispevka

Naslov

Naslov članka naj bo natančen in informativen in naj ne presega 100 znakov. Avtor naj navede tudi skrajšan naslov članka. Naslov članka je podan v angleškem in slovenskem jeziku.

Information on the Authors

Information on the authors should include the first and last name of the authors, the address of the institution and the e-mail address of the leading author.

Abstract

The abstract presenting the purpose of the article and the main results and conclusions should contain no more than 180 words. It should be written in Slovene and English.

Key words

A list of up to 5 key words (3 to 5) that will be useful for indexing or searching. They should be written in Slovene and English.

Introduction**Materials and methods****Results and discussion****Conclusions****Acknowledgements****References**

The sources should be cited in the same order as they appear in the article. They should be numbered with numbers in square brackets. Sources should be cited according to the SIST ISO 690:1996 standards.

Monograph:

[1] Trček, B. (2001): *Solute transport monitoring in the unsaturated zone of the karst aquifer by natural tracers*. Ph. D. Thesis. Ljubljana: University of Ljubljana 2001; 125 p.

Journal article:

[2] Higashitani, K., Iseri, H., Okuhara, K., Hatade, S. (1995): Magnetic Effects on Zeta Potential and Diffusivity of Nonmagnetic Particles. *Journal of Colloid and Interface Science*, 172, pp. 383–388.

Electronic source:

CASREACT – Chemical reactions database [online]. Chemical Abstracts Service, 2000, renewed 2/15/2000 [cited 2/25/2000]. Available on: <<http://www.cas.org/casreact.html>>.

Podatki o avtorjih

Podatki o avtorjih naj vsebujejo imena in priimke avtorjev, naslov pripadajoče inštitucije ter elektronski naslov vodilnega avtorja.

Izvleček

Izvleček namena članka ter ključnih rezultatov z ugotovitvami naj obsega največ 180 besed. Izvleček je podan v angleškem in slovenskem jeziku.

Ključne besede

Seznam največ 5 ključnih besed (3–5) za pomoč pri indeksiranju ali iskanju. Ključne besede so podane v angleškem in slovenskem jeziku.

Uvod**Materiali in metode****Rezultati in razprava****Sklepi****Zahvala****Viri**

Uporabljane literaturne vire navajajte po vrstnem redu, kot se pojavljajo v prispevku. Označite jih s številkami v oglatem oklepaju. Literatura naj se navaja v skladu s standardom SIST ISO 690:1996.

Monografija:

[1] Trček, B. (2001): *Solute transport monitoring in the unsaturated zone of the karst aquifer by natural tracers*. doktorska disertacija. Ljubljana: Univerza v Ljubljani 2001; 125 str.

Članek v reviji:

[2] Higashitani, K., Iseri, H., Okuhara, K., Hatade, S. (1995): Magnetic Effects on Zeta Potential and Diffusivity of Nonmagnetic Particles. *Journal of Colloid and Interface Science*, 172, str. 383–388.

Spletna stran:

CASREACT – Chemical reactions database [online]. Chemical Abstracts Service, 2000, obnovljeno 15. 2. 2000 [citirano 25. 2. 2000]. Dostopno na svetovnem spletu: <<http://www.cas.org/casreact.html>>.

Scientific articles, review papers, preliminary notes and professional papers are published in English. Only professional papers will exceptionally be published in Slovene.

Annexes

Annexes are images, spreadsheets, tables, and mathematical and chemical formulas.

Annexes should be included in the text at the appropriate place, and they should also be submitted as a separate document, i.e. separated from the text in the article.

Annexes should be originals, made in an electronic form (Microsoft Excel, Adobe Illustrator, Inkscape, AutoCad, etc.) and in .eps, .tif or .jpg format with a resolution of at least 300 dpi.

The width of the annex should be at least 152 mm. They should be named the same as in the article (Figure 1, Table 1).

The text in the annexes should be written in typeface Arial Regular (6 pt).

The title of the image (also schemes, charts and graphs) should be indicated in the description of the image.

When formatting spreadsheets and tables in text editors, tabs, and not spaces, should be used to separate columns. Each formula should have its number written in round brackets on its right side.

References of the annexes in the text should be as follows: "Figure 1..." and not "as shown below:". This is due to the fact that for technical reasons the annex cannot always be placed at the exact specific place in the article.

Manuscript Submission

Contributions should be sent to the following e-mail address: rmz-mg@ntf.uni-lj.si.

In case of submission on CD or USB flash drive, contributions can be sent by registered mail to the address of the editorial board:

RMZ – Materials and Geoenvironment, Aškerčeva 12, 1000 Ljubljana, Slovenia.

The contributions can also be handed in at the reception of the Faculty of Natural Sciences and Engineering (ground floor), Aškerčeva 12, 1000 Ljubljana, Slovenia with the heading "for RMZ – M&G".

Znanstveni, pregledni in strokovni članki ter predhodne objave se objavijo v angleškem jeziku. Izjemoma se strokovni članek objavi v slovenskem jeziku.

Priloge

K prilogam prištevamo slikovno gradivo, preglednice in tabele ter matematične in kemijske formule.

Priloge naj bodo vključene v besedilu, kjer se jim odredi okvirno mesto. Hkrati jih je potrebno priložiti tudi kot samostojno datoteko, ločeno od besedila v članku.

Priloge morajo biti izvirne, narejene v računalniški obliki (Microsoft Excel, Adobe Illustrator, Inkscape, AutoCad ...) in shranjene kot .eps, .tif ali .jpg v ločljivosti vsaj 300 dpi. Širina priloge naj bo najmanj 152 mm. Datoteke je potrebno poimenovati, tako kot so poimenovane v besedilu (Slika 1, Preglednica 1).

Za besedilo v prilogi naj bo uporabljena pisava Arial navadna različica (6 pt).

Naslov slikovnega gradiva, sem prištevamo tudi sheme, grafikone in diagrame, naj bo podan v opisu slike.

Pri urejevanju preglednic/tabel, v urejevalniku besedila, se za ločevanje stolpcev uporabijo tabulatorji in ne presledki.

Vsaka formula naj ima zaporedno številko zapisano v okroglem oklepaju na desni strani.

V besedilu se je potrebno sklicevati na prilogo na način: „Slika 1 ...“, in ne „...“ kot je spodaj prikazano:“ saj zaradi tehničnih razlogov priloge ni vedno mogoče postaviti na točno določeno mesto v članku.

Oddaja članka

Prispevke lahko pošljete po elektronski pošti na naslov rmz-mg@ntf.uni-lj.si.

V primeru oddaje prispevka na CD- ali USB-mediju le-te pošljite priporočeno na naslov uredništva:

RMZ – Materials and Geoenvironment, Aškerčeva 12, 1000 Ljubljana, Slovenija

ali jih oddajte na:

recepции Naravoslovnotehniške fakultete (pritličje), Aškerčeva 12, 1000 Ljubljana, Slovenija s pripisom „za RMZ – M&G“.

The electronic medium should clearly be marked with the name of the leading author, the beginning of the title and the date of the submission to the Editorial Office of RMZ – M&G.

Information on RMZ – M&G

- Editor-in-Chief
Assoc. Prof. Dr. Peter Fajfar
Telephone: +386 1 200 04 51
E-mail address: peter.fajfar@omm.ntf.uni-lj.si

- Secretary
Ines Langerholc, Bachelor in Business Administration
Telephone: +386 1 470 46 08
E-mail address: ines.langerholc@omm.ntf.uni-lj.si

These instructions are valid from July 2013.

Elektronski mediji morajo biti jasno označeni z imenom vsaj prvega avtorja, začetkom naslova in datumom izročitve uredništvu RMZ – M&G.

Informacije o RMZ – M&G

- urednik
izr. prof. dr. Peter Fajfar
Telefon: +386 1 200 04 51
E-poštni naslov: peter.fajfar@omm.ntf.uni-lj.si

- tajnica
Ines Langerholc, dipl. poslov. adm.
Telefon: +386 1 470 46 08
E-poštni naslov: ines.langerholc@omm.ntf.uni-lj.si

Navodila veljajo od julija 2013.

TRAJNO PREDNAPETO GEOTEHNIČNO SIDRO RAFAEL TPGS 10



- 1 Končna protikorozijska zaščita je dosežena z uporabo kupolastega zaščitnega pokrova iz umetne mase, ki je UV obstojen, odporen na mehanske poškodbe ter nespremenljiv av območjih megle ob soljenih cestah in obmorskih vremenskih razmerah. Namestitev kupole je enostavna, saj ni potrebe po vrtanju dodatnih lukenj za pritrdilna sredstva. Zaščitni pokrov je sive barve, ki se sklada z betonsko konstrukcijo.
- 2 Dvojno varnostno tesnjenje sidrne glave, z dodatnim drenažnim odtokom, ščiti glavo sidra pred pronicanjem zaledne vode. Tesnila so rezultat razvoja podjetja Rafael ter zagotavljajo visoko raven tesnjenja okroglih in elipsastih zaščitnih cevi sidra.
- 3 V sidrih uporabljamo kakovostna visoko vredna jeklena pramena: nominalni premer $\varnothing = 15,7 \text{ mm}$ (0,62"), nominalna površina prečnega prereza 150 mm^2 , kakovost jekla (meja plastičnosti $f_{p0,1k} = 1670 \text{ N/mm}^2$, natezna trdnost $f_{pk} = 1860 \text{ N/mm}^2$).
- 4 Rebrasta cev za geotehnična sidra Rafael je lasten razvoj podjetja. Spiralna navojnica, z večjo razliko med korenom in temenom, zagotavlja boljšo odpornost na upogibanje pri različnih temperaturah okolice ter boljši odpor injekcijske mase na rebra in s tem večjo nosilnost sidra v vrtni.
- 5 Jeklene sestavne dele sidra vstavljamo v pripravljene utore, kar zagotavlja središčno postavitev sidra in s tem enakomeren prenos sile na zaledno konstrukcijo.
- 6 Sidro Rafael z enojnim sistemom napenjanja je enostavno in zagotavlja visoko kakovost napenjanja, skladno z Evropskim tehničnim soglasjem ETA - 08/0002, avstrijskega partnerskega podjetja VBT GmbH.
- 7 V skladu s pridobljenim Slovenskim tehničnim soglasjem lahko običajno protikorozijsko zaščito s sivim kupolastim pokrovom, zapolnjenim z vročim vazelinom, zaščitimo tudi s prozornim zaščitnim pokrovom in prozornim protikorozijskim gelom, ki nudi velik napredek pri enostavni manipulaciji, kontroli in vizualnem izgledu.

Proizvodi podjetja Rafael so izdelani v skladu z veljavno regulativo Republike Slovenije – Zakon o gradbenih proizvodih. S svojo hitro odzivnostjo na želje in potrebe naročnikov zagotavljamo kratke dobavne roke sider, v primerih načrtovanja daljšega skladiščenja, pa, z namenom zaščite in preprečevanja oksidacije golih jeklenih pramen v veznem delu, notranjost sidra zaščitimo z inertnim plinom.

Slovenčeva 93
SI 1000 Ljubljana

tel.: +386 (1) 560 36 00

fax: +386 (1) 534 16 80

www.irgo.si



Inženirska geologija

Hidrogeologija

Geomehanika

Projektiranje

Tehnologije za okolje

Svetovanje in nadzor





ISSN 1408-7073